SUSTEN

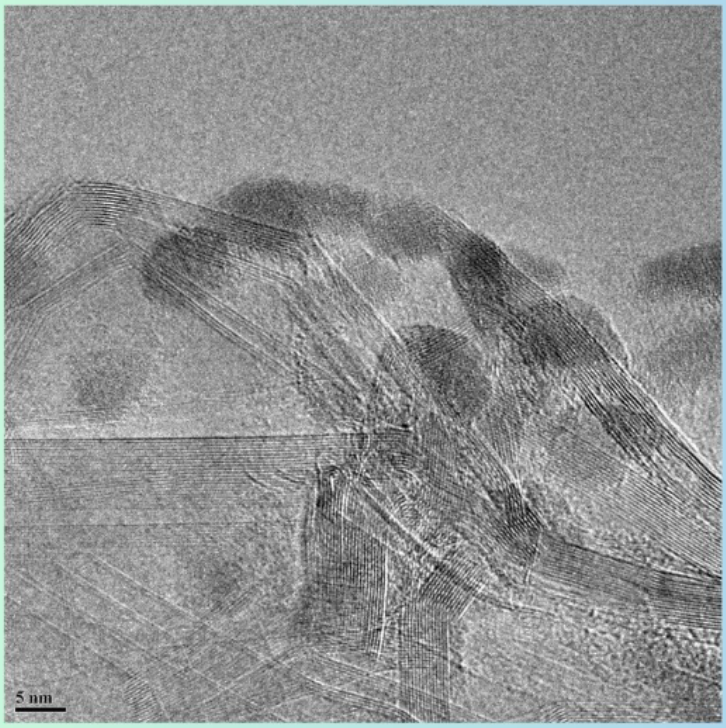

SUSTAINABLE ENGINEERING

Volume 1, Issue 1

UMS
UNIVERSITI MALAYSIA SABAH

Journal of Sustainable Engineering

Editorial Committee

https://jurcon.ums.edu.my/ojums/index.php/SE
EISSN: 3083-8231

CONTENTS

https://jurcon.ums.edu.my/ojums/index.php/SE
EISSN: 3083-8231

Sustainable Engineering

Article
Volume 1, Issue 1, 2024
https://doi.org/10.51200/susten.v1i1.5144

Oil Extraction from Rice Bran Using Conventional and Bio-based Solvents

S M Anisuzzaman[1,2,*], Vivian Michelle Yih[2]
[1]Energy and Materials Research Group, Universiti Malaysia Sabah, UMS Road, 88400, Kota Kinabalu, Sabah, Malaysia
[2]Chemical Engineering Program, Faculty of Engineering, Universiti Malaysia Sabah, UMS Road, 88400, Kota Kinabalu, Sabah, Malaysia
[*]Correspondence: anis_zaman@ums.edu.my; *Scopus Author ID 55444058500
Received: 14 June 2024, Accepted: 16 July 2024

Abstract: Rice bran is the outer layer of the rice grain, rich in essential nutrients and bioactive compounds. It is a valuable by-product used for various purposes, including extracting rice bran oil (RBO) known for its health benefits. This study focused on extracting oil from the nutritious rice bran using conventional solvent (n-hexane) and bio-based solvent (iso-propanol) for comparison under diverse conditions. The RBO yields were analysed at different temperatures of 40°C, 50°C, and 60°C, with bran-to-solvent ratios of 1:3, 1:5, and 1:7, and extraction times of 2, 4, and 6 hours. The highest yields were 12.4% for n-hexane at 60°C, 1:7 ratio, and 6 hours, and 9.76% for iso-propanol at 60°C, 1:7 ratio, and 4 hours. The extracted oil underwent comprehensive physical analysis, including density, acid value, free fatty acid, and iodine value test. The physical analysis revealed density values of 0.867 g/mL for n-hexane and 0.866 g/mL for iso-propanol. Acid values were 21.48 mg KOH/g (n-hexane) and 26.90 mg KOH/g (iso-propanol). Free fatty acid percentages were 10.74% (n-hexane) and 13.45% (iso-propanol). Iodine values were 65.48 mg (n-hexane) and 60.40 mg (iso-propanol). The collected data were analysed using response surface methodology (RSM) to optimize the extraction condition, predicting the highest yield at 60°C, with a bran-to-oil ratio of 1:5 parts solvent, and an extraction time of 6 hours. Statistical analysis confirmed the significance of the optimization model ($p < 0.05$). Overall, this study provided valuable insights, advancing more efficient and effective RBO production methods.

Keywords: rice bran; extraction; n-hexane; iso-propanol

1. Introduction

Paddy produces 73.5% white rice, 3.5% broken rice, 15% husk, and 8% rice bran when it is milled [1]. In recent years, rice bran has been studied for its potential biological functions, which include antioxidant and anti-inflammatory effects, cancer prevention, coronary heart disease prevention, and cholesterol reduction [2, 3]. Furthermore, rice bran contains 18%-22% oil, as well as a variety of bio-active phytochemicals such as oryzanol, phytosterol, tocotrienol, squalene, polycosanol, phytic acid, ferulic acid, and inositol hexaphosphate [4]. Rice bran oil (RBO) has grown in popularity as a nutritious component and is now a lucrative by-product of the rice processing industry [5, 6].

An important by-product of the rice milling industry, RBO may be produced from rice bran using a variety of methods. Solvent extraction is one of the popular techniques, which involves dissolving the oil from the rice bran using a solvent [7, 8]. n-hexane is the popular solvent utilized due to its ability to remove oil from rice bran. For RBO extraction, other methods exist, including enzymatic techniques, supercritical fluid extraction, ultrasound-assisted extraction (UAE), and

microwave-assisted extraction [8-18]. The choice of solvent, temperature, pressure, duration, and the ratio of rice bran to solvent are the factors that affect the extraction of RBO. To get the most oil out of the extraction process, these characteristics must be carefully taken into account and adjusted [19-21].

RBO is a highly valued vegetable oil due to its numerous health benefits and diverse industrial applications. It is extracted from the bran layer of rice kernels, which contains a significant amount of oil. However, the oil content in rice bran is relatively low, making it challenging to extract efficiently. Hence, several extraction techniques have been developed to overcome this challenge. Table 1 provides a summary of different extraction techniques used to extract RBO.

The choice of solvent is a crucial factor in solvent extraction. Factors such as selectivity, solubility, safety, and cost should be taken into account when choosing a solvent. Different solvents have varying degrees of oil extraction effectiveness, environmental impact, and renewability. According to reports, various solvents can produce distinct natural molecules from a particular substance, resulting in variances in the extract's composition [5, 13, 23]. n-hexane is one of the most often utilised solvents in RBO extraction [12, 13, 23]. Although extremely efficient in removing the oil from rice bran, this solvent is hazardous and combustible, necessitating specific handling and disposal. n-hexane is a volatile organic compound (VOC), which raises environmental issues due to its propensity to contaminate the air and impair human health. On the other hand, iso-propanol has also been utilised as a solvent in RBO extraction [9]. Since it is safer for the environment and less harmful than n-hexane, iso-propanol has been proven to be more effective in extracting RBO [9, 20]. Moreover, n-hexane exhibits a lower boiling point in comparison to iso-propanol, rendering it more volatile and potentially more perilous in extraction procedures. RBO extraction has also been done using ethanol and has the benefit of being able to extract additional substances from the rice bran, such as phytosterols and antioxidants [24, 25].

Nonpolar solvents can also be used to reduce the extraction of polar substances such as polysaccharides and improve extraction efficiency [26, 27]. Therefore, based on the comparative study, iso-propanol, which is a "green" alternative solvent, and n-hexane, which is a traditional solvent, were selected for further study to investigate their impact on RBO yield. A solvent extraction technique was carried out to extract the RBO as it was the most widely used method due to the reason of its technology availability and the variety of advantages that can provide such as the ability to facilitate effective oil recovery [5, 9, 13]. Through the utilization of organic solvents, solvent extraction efficiently releases and concentrates oil components from the intricate structure of rice bran, optimizing the yield and the utilization of resources. Moreover, the technique's remarkable versatility extends to accommodating various types of oil, making it particularly suitable for the investigation of solvents such as n-hexane and iso-propanol which allows it to encompass the comprehensive array of oil constituents found within rice bran. This study also focuses on optimizing the parameters such as temperature, ratio, and extraction time that affect the RBO yield via response surface methodology (RSM). The application of RSM helps to predict the ideal condition to obtain maximum yield (%) and identify the performance of n-hexane and iso-propanol solvent on extracting the RBO [23, 26]. In this study, RSM was used to optimize extraction parameters such as extraction temperature ($X1$), solvent-bran ratio ($X2$), and extraction time ($X3$). The selection of these criteria was made to gather comprehensive data regarding the extraction process and to encompass a broad spectrum of scenarios. This study also

utilised a three-factor, three-level Box-Behnken design (BBD) to determine the optimal Soxhlet conditions for extracting oil from RBO.

Table 1. Summary of extraction technique for RBO production.

Technique	Theory/Concept	Advantages	Disadvantages	References
Solvent extraction	Extraction of oil from rice bran by dissolving the rice bran in the organic solvent such as hexane and iso-propanol.	Low energy consumption Effective oil recovery Versatile in accommodating various solvents	Toxicity of solvent (n-hexane) Required high purity of solvents to be used Costly	[5,9,13]
Supercritical fluid extraction (SFE)	Oil extraction based on the temperature and Pressure manipulation, uses Supercritical fluid (usually S-CO_2) as the extraction solvent.	Faster and more efficient extraction Environmentally friendly	Requires specialized equipment and is more expensive to implement when compared to other methods Complex process	[9,22]
Mechanical pressing (Cold pressing)	Extracting oil from rice bran using mechanical force. It is a physical process that does not involve the use of chemicals or high temperatures.	Environmentally friendly Simple and straightforward Does not required heat or solvent	High labour intensity High residual oil rate High cost and power consumption Easy to cause protein denaturation. Lower oil yield extracted compared to other methods/techniques	[9,10]
Enzyme assisted aqueous extraction (EAAE)	Extracting oil from rice bran using enzymes such as Cellulose, α-amylase and pectinase to break down the oil and make it more accessible for extraction.	Good quality of oil No chemical pollution Low energy consumption Good retention of protein, polysaccharide and other components	Easy to cause protein denaturation. Enzymes used in the process can be expensive. Time-consuming process Shorter shelf life	[11,14, 15]
Ultrasound assisted extraction (UAE)	Used ultrasonic waves to agitate the rice bran and oil, causing the oil to become more accessible for extraction.	Reduce extraction time, energy and solvent to be consumed. Environmentally process	Requires specialized equipment (high Cost) Large amount of labour	[9,12,16]
Microwave assisted extraction (MAE)	Uses microwave energy to increase the efficiency of the extraction process. The process involves the use of microwaves to heat the rice bran and oil, causing the oil to become more accessible for extraction.	High yield and Purity Reduce time and solvent consumption	The need for special equipment Low selectivity Unavoidable reaction in high temperature	[7,17,18,20]

2. Materials and methods

2.1. Raw material

Fresh rice bran was obtained from a local rice mill located in Kota Belud district, Sabah, Malaysia. The bran had been passed through a 30-mesh sieve (700 mm aperture size) to remove the paddy kernels, broken grains, hull fragments, and unwanted foreign materials. After sieving, the rice bran was immediately stabilized before storage to prevent enzymatic rancidity. The rice bran was heat-dried using a dry oven for 10 minutes at 115^{o}C and weighed.

2.2. Apparatus and chemicals

In this study, Soxhlet extractor was used for RBO extraction, Rotavapor model R-215 was utilized for the separation of solvent and oil after extraction for purification purposes. n-hexane with ≥ 99.9 % purity and iso-propanol with ≥ 99.9 % supplied by Sigma Aldrich.

2.3. Oil extraction

The RBO extraction process using both n-hexane and iso-propanol as solvent was carried out by using Soxhlet apparatus The extraction process was done at 40, 50, and 60^{o}C, and bran to solvent ratio at 1:3, 1:5, 1:7 w/v for 2, 4, and 6 hours. A sample of 50 g of rice bran was placed into the thimble and covered with gauze at the top layer and the solvent, solvent was filled in the round-bottomed flask. The extract with the solvent was separated by a rotary evaporator which was filtered using filter paper [4, 28].

2.4. Determination of oil yield

After the extractions, all the samples were filtered twice using Whatman filter paper to separate the oil from the used rice bran. The separated rice bran oil yield was weighed, and the yield was calculated as per 50 g of rice bran basis using the Equation (1):

$$RBO\ yield, (w/w) = \frac{WRBO(g)}{WRB(g)} \times 100 \quad (1)$$

where $WRBO(g)$ is the weight of RBO extracted from the experiment and $WRB(g)$ is the weight of the rice bran before the oil extraction.

2.5. Characterization of extracted oil

Physical characteristics of oil samples derived from the Soxhlet extraction were assessed. Free fatty acid percentage (FFA), oil density, iodine value, and acid value were chosen. These oil qualities were chosen based on other investigations in the same field. It is essential to comprehend these qualities since they affect the stability, shelf life, and suitability of the oil for diverse applications. All oil attributes were tested twice during oil analysis.

2.6. Determination of free fatty acid (FFA)

The acid value (AV) and free fatty acid percentage (FFA, %) of both oil samples were determined following the procedures used by Asmare and Gabbiye [29]. The AV was calculated first, and the FFA content in the RBO was then calculated using the Equation (2):

$$FFA, \% = AV/2 \quad (2)$$

25 mL of a 1:1 combination of diethyl ether and ethanol was added to 5 g of oil in a 250 mL conical flask and mixed thoroughly to determine the AV in accordance. The solution was titrated with 0.1 N KOH after adding 5 drops of phenolphthalein indicator, and the titration's end point was confirmed after constant shaking (change from colourless to pink). During the titration, the amount

of 0.1 N KOH (V) consumed was noted. Equation (3) was used to compute the sample's total acidity, expressed as mg KOH/g.

$$AV = \frac{56.1 \times N \times V}{WRBO} \quad (3)$$

where N is the normality of KOH used, V is the volume (mL) of ethanolic KOH, and $WRBO$ is the weight (g) of RBO sample.

2.7. Determination of oil density

A 50 mL volumetric flask was used in the technique to measure the density of the oil samples, and it was completely dried before use to prevent contamination. The reading was then reset to zero and a dry flask was put on a sensitive electronic balance. Using a pipette, the extracted rice bran oil sample was then added to the flask. By dividing the weight by the volume, the density of the oil was estimated. After repeating the procedure, the average value was calculated. The densities of the oil samples were calculated at room temperature. The density of RBO was calculated using the Equation (4):

$$Density\ of\ RBO\ (w/v) = \frac{WRBO(g)}{VRBO(mL)} \quad (4)$$

where $WRBO(g)$ is the weight of the oil sample and $VRBO$ is the volume (mL) of the oil sample. It is important to note that the density of the oil will vary depending on the temperature, so it is usually measured at a specific temperature, usually at 20°C. The density of oil samples can vary depending on the oil extraction method, the variety of rice used, and the growing conditions.

2.8. Determination of iodine value

A weight of 0.25 g of the oil sample was weighed and transferred to a 250 mL flask, along with 20 mL of chloroform, to dissolve the oil sample. The mixture was then pipetted with the 20 mL Wijs reagent's iodine monochloride solution. The flask was sealed and kept in the dark for one hour, with occasional shaking. After an hour, the liquid was taken out of the dark and 50 mL of distilled water and 10 mL of a 15% potassium iodide solution were added. Once the cork was securely fastened to the flask, the mixture was thoroughly shaken. After the iodine was released, sodium thiosulfate (0.1 N solution of $Na_2S_2O_3.5H_2O$) was added, and the mixture was gently agitated until the yellow colour lightened. After that, 5 drops of 1% starch indicator were added to the mixture, and the titration was continued until the blue tint disappeared [30]. Equation (5) was used to calculate the IV of the oil sample.

$$IV = \frac{Vb - Vs}{W} \times 12.69 \times N \quad (5)$$

where Vb is the volume (mL) of sodium thiosulfate used for the blank, Vs is the volume (mL) of sodium thiosulfate used for the sample, and N is the normality of sodium thiosulfate, and W is the mass of the sample used (g).

2.9. Optimization using response surface methodology (RSM)

RSM was used to optimize the extraction conditions for a particular product utilising three process parameters which are the extraction temperature, extraction time, and bran to solvent ratio. The extraction time, temperature, and bran to solvent ratio were all restricted to being between 2 and 6 hours, 40°C to 60°C, and 1:3 to 1:7, respectively. These parameters were selected to collect thorough information on the extraction process and to cover a wide range of situations. The best conditions for the RBO extraction process can be determined by examining the connection between these process variables and the response variable, which improves process effectiveness. An overview of the coded values for the process parameters is shown in Table 2.

Table 2. Coded values of process parameters and corresponding responses.

Symbol	Parameter	Units	Level -1	Level 0	Level 1
X1	Extraction temperature	°C	40	50	60
X2	Bran to solvent ratio	-	1:3	1:5	1:7
X3	Extraction time	hour	2	4	6
Y	Response (yield of RBO)	%	Y1	Y2	Y3

3. Results and discussion

3.1. Effect of extraction temperature to RBO yield

Figure 1 illustrates the experimental outcomes of the RBO yield for both n-hexane and iso-propanol solvents. The extraction process maintained constant rice bran to oil ratio of 1:5 and an extraction time of 4 for the study.

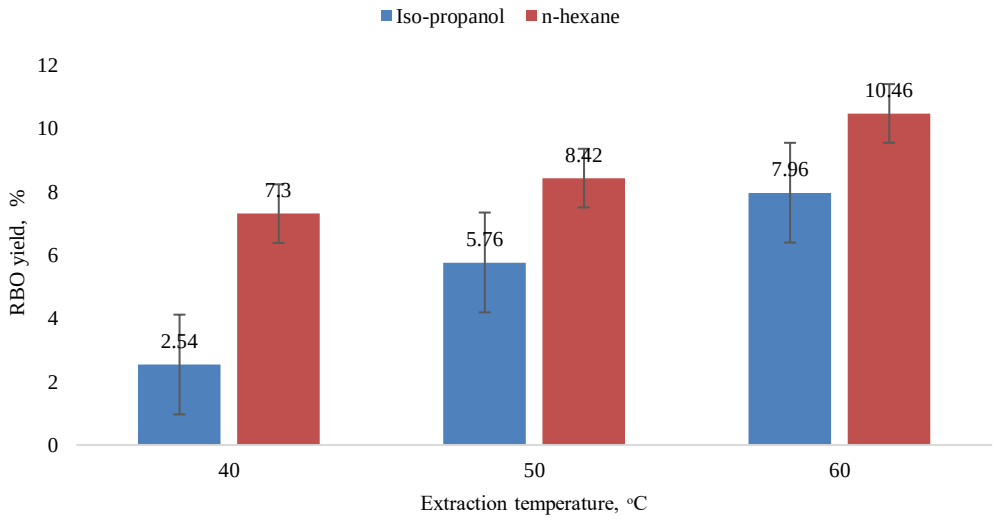

Figure 1. Effect of extraction temperature to RBO yield for n-hexane and iso-propanol.

Based on Figure 1, both solvents used showed an increase in yield of RBO when the extraction temperature increased. At 40°C, iso-propanol produced 2.54% RBO, but n-hexane produced 7.30% RBO. When the extraction temperature was raised to 60°C, the RBO yields increased significantly to 7.96% and 10.46% for iso-propanol and n-hexane, respectively. Djaeni et al. [12] evaluated the extraction process at various temperatures (40, 50, and 60°C) and observed the

maximum yield at 60ºC with a 1:5 ratio, which is consistent with the findings. In addition to that, Pimpa et al. [4] also discovered that 60ºC has produced a better yield than lower temperatures. The increase in yield with temperature could be attributed to increased oil ingredient solubility and diffusion rates, allowing for a more efficient extraction process. Higher temperatures also have promoted faster mass transfer rates and decreased solvent viscosity which makes it easier to extract oil from rice bran. However, the yield achieved from n-hexane solvent exceeds that of iso-propanol. This disparity can be attributed to the varied solubility properties of the two solvents. Because of its higher lipid solubility, n-hexane is frequently utilised in oil extraction procedures. Iso-propanol, on the other hand, has lower lipid solubility and hence produces a lesser amount of RBO. Moreover, the difference in boiling points between iso-propanol and n-hexane can influence the extraction process. The temperatures utilised in this study were lower than the boiling points of both solvents, to ensure stability and prevent evaporation. Thus, n-hexane which has a lower boiling point will facilitate a faster evaporation rate and improves the mass transfer of oil components from rice bran, resulting in a more effective extraction process, whereas iso-propanol's higher boiling point may have contributed to its low oil yield when compared to n-hexane at all tested temperatures [26].

3.2. Effect of rice bran and solvent ratio to oil yield

Figure 2 illustrates the effect of the solid-liquid ratio for both n-hexane and iso-propanol solvents on the RBO yield, while considering a constant extraction temperature of 60°C and an extraction time of 4 hours.

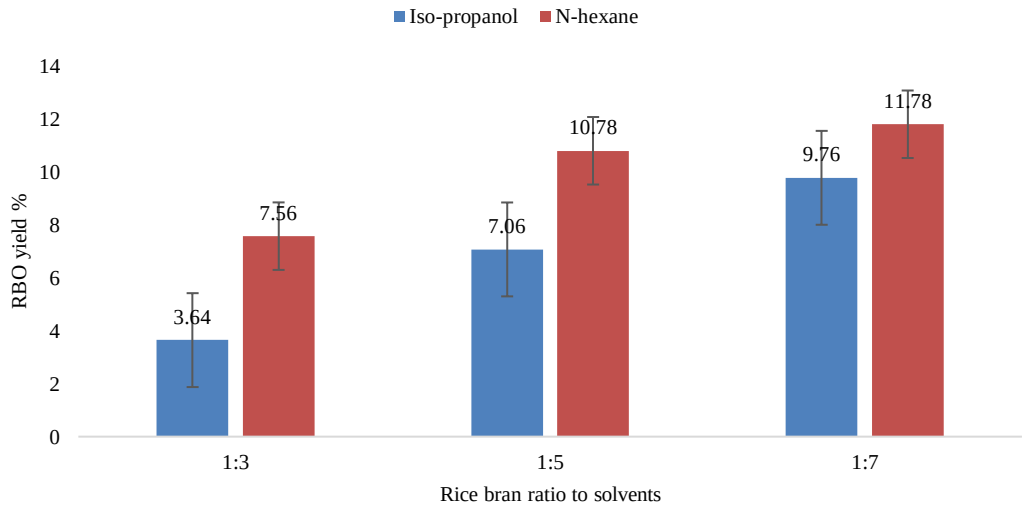

Figure 2. Effect of rice bran and solvent ratio to RBO yield for iso-propanol and n-hexane.

Based on Figure 2, the RBO yield increases as the solid-liquid ratio increases for both iso-propanol and n-hexane solvents. Iso-propanol yielded 3.64% at a ratio of 1:3, ascended to 7.06% at a ratio of 1:5, and increased further to 9.76% at a ratio of 1:7. Similarly, the RBO yield for n-hexane increased from 7.56% at a ratio of 1:3 to 10.78% at a ratio of 1:5 and 11.78% at a ratio of 1:7. This condition is caused by an oil concentration difference between the surface of the rice bran and the solvent. As the solid-liquid ratio increases, more solvent comes into contact with the rice bran,

resulting in a larger concentration gradient. This enhanced concentration gradient encourages oil diffusion and extraction from rice bran, resulting in higher RBO yields [12]. According to Suryati et al. [31], which extracted 50 g of rice bran and used a 250 mL n-hexane solvent (ratio 1:5) resulted in a yield of 13.5%. On the contrary, Nasir et al. [32] carried out an experiment with 50 g of rice bran and 350 mL of the solvent resulted in a yield of 18.34%. The present study shows a similar trend of increasing yield, but with lower yield obtained probably due to extraction method and different rice bran samples. Furthermore, it is notable that greater extraction of RBO was obtained by n-hexane compared to iso-propanol which can be explained due to n-hexane's non-polar nature, which efficiently interacts with the non-polar lipids in RBO. Iso-propanol's polar nature makes it less effective in extracting these non-polar lipids. The chemical composition of RBO and the selectivity of n-hexane contribute to its superior extraction performance.

3.3. Effect extraction time to oil yield

Figure 3 illustrates the experimental outcomes of the RBO yield under different extraction time sfor both n-hexane and iso-propanol solvents. The extraction process maintained constant rice bran to oil ratio of 1:5 and an extraction time of 60°C for the study.

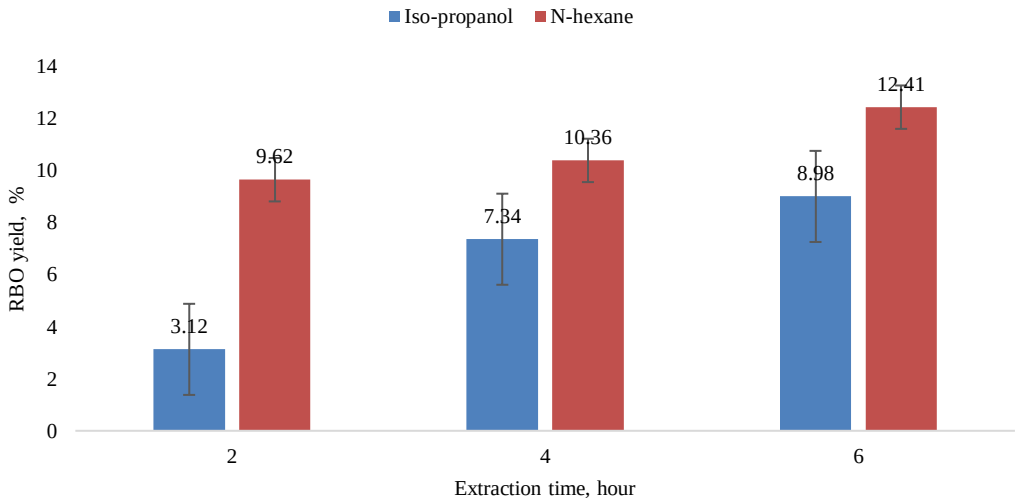

Figure 3. Effect of extraction time to RBO yield for iso-propanol and n-hexane.

From Figure 3, it can be observed that the RBO yield increased with longer extraction times for both iso-propanol and n-hexane solvents. For iso-propanol, the RBO yield was 3.12% at an extraction time of 2 hours, which increased to 7.34% at 4 hours and further increased to 8.98% at 6 hours. Similarly, for n-hexane, the RBO yield increased from 9.62% at 2 hours to 10.36% at 4 hours and reached 12.41% at 6 hours. The oil yield of 12.41% obtained in the present study agrees with past studies which obtained 13.5% of oil yield within 7 hours of extraction time [31]. This can be attributed to the extended duration allowing for a more complete extraction of oil constituents. The relationship between extraction time and RBO yield can be explained by the diffusion process during extraction. Longer extraction times provide more time for the solvent to penetrate the rice bran and dissolve the oil components. This allows for a more efficient extraction, leading to higher RBO yields.

3.4. Characterization of extracted RBO

The highest yields achieved were 12.4% for n-hexane at 60°C, 1:7 ratio, and 6 hours, and 9.76% for iso-propanol at 60°C, 1:7 ratio, and 4 hours. These two RBO samples were chosen to analyse the physical attributes of the oil. Density measurements yielded valuable insights into mass-volume relationships, serving as a cornerstone for accurate measurements within diverse processes. On the other hand, the AV assessment provided insights into acidity levels, directly influencing both shelf life and flavour quality, whereas FFA % contributed to understanding oil purity and overall quality. Concurrently, the IV assumption played an instrumental role in evaluating unsaturation levels, thereby impacting oxidation potential, nutritional considerations, and inherent stability during subsequent storage and culinary applications. Table 3 shows the findings of the physical examination for both samples of RBO.

Table 3. Physical analysis result of RBO sample.

Properties	n-hexane	Iso-propanol
Density, g/mL	0.867	0.866
AV, mg KOH/g	21.48	26.90
FFA, %	10.74	13.45
IV, mg I2/g	65.48	60.40

According to Table 3, the density values for n-hexane and iso-propanol-extracted oils are comparable, differing by just 0.866 g/mL and 0.867 g/mL, respectively which are also quite similar to the density stated in the literature [32,33]. The slight density change implies that the extraction solvents have little to no impact on the total mass and volume of the oils. The iso-propanol-extracted oil displays greater values for the AV and FFA % than the n-hexane-extracted oil. The AV for iso-propanol is 26.90 mg KOH/g, whereas the value for n-hexane is 21.48 mg KOH/g, showing a slightly higher level of acidity in between [34]. Iso-propanol and n-hexane both have FFA% of 13.45% and 10.74%, respectively. Each sample shows a higher amount of AV and FFA% compared to the literature where the FFA% of crude RBO is around 1-2% [33]. The differing extraction processes and the interaction of iso-propanol with the oil's constituents, which enhanced acidity, may be accountable for the higher AV and FFA % in the extracted oil. Iodine values for both oils, 60.40 mg I2/g sample for iso-propanol and 65.48 mg I2/g for n-hexane, are lower than expected. The properties of both n-hexane and iso-propanol-extracted oils are generally within the acceptable range, the slight differences observed between the two solvents may be attributed to their different extraction mechanisms.

3.5. Statistical analysis and optimization

The study focused on three factors which are extraction temperature ($X1$), solvent-bran ratio ($X2$), and extraction time ($X3$), and their respective impacts on the yield of RBO (Y). The design of experiments (DOE) constructed to plan the experimental run with the desired range of each factor and their respective levels are shown in Table 4.

According to Ahmad et al. [35], process optimization involves estimation of coefficients, prediction of responses and checking acceptability of the developed model. The linear model was suggested for the rice bran oil extraction and the resulted linear model in terms of coded variables is as follows, Equation (6):

$$R = 4.9367 + 1.97X1 + 3.06X2 + 2.93X3 \quad (6)$$

where, R denotes the outcome, which in this case is the % of the yield of RBO, and $X1$, $X2$, and $X3$ are the coded variables, which are related to the process variables temperature, solvent-bran ratio, and extraction time, respectively. The coefficients of 1.97, 3.06, and 2.93 in the model equation, respectively, show the influence of each process variable on the response. The correlation coefficient of 1.97 for $X1$ indicates that a one-unit increase in the coded value of temperature $X1$causes a 1.97-unit increase in the percentage yield of RBO (R), providing the other variables of $X2$ and $X3$ are held constant. Similarly, the effects of the solvent-bran ratio and extraction duration on the response are shown by the coefficients of $X2$ and $X3$ for the 3.06 and 2.93, respectively.

Table 4. Design of experiment for three independent variables and experimental results.

Run	Extraction temperature, $X1$		Solid to solvent ratio, $X2$		Extraction time, $X3$		RBO yield, Y	Predicted RBO yield
	Coded value	Actual value	Coded value	Actual value	Coded value	Actual value		
1	-1	40	0	1:5	0	4	2.54	2.96
2	0	50	0	1:5	0	4	5.76	4.93
3	1	60	0	1:5	0	4	7.96	6.89
4	1	60	-1	1:3	0	4	3.64	3.84
5	1	60	0	1:5	0	4	7.06	6.89
6	1	60	1	1:7	0	4	9.76	9.96
7	1	60	0	1:5	-1	2	3.12	3.97
8	1	60	0	1:5	0	4	7.34	6.89
9	1	60	0	1:5	1	6	8.98	9.83

3.6. Model fitting and summary statistics

Experiments based on the recommended optimal medium parameters were used to validate the mathematical model created using the RSM approach. In order to evaluate the effectiveness and precision of the model, a statistical t-test was also carried out utilizing a number of statistical measures, such as the coefficient of determination (R^2), adjusted R^2, and root mean square error (RMSE). Table 5 and 6 display the summary of fit statistics and the ANOVA.

Table 5. Summary of fit statistics.

Statistics	Values
Mean of response	6.24
R^2	0.9323
Adjusted R^2	0.8917
RMSE	0.8640
Observations	9

RMSE value shows 0.8640 which indicates a strong prediction accuracy of the linear model. R^2 value shows that the linear model accounts for about 93.23% of the response's variability.

Additionally, Table 6 ANOVA findings demonstrate that the model component is significant with a p-value of 0.0024, which is less than 0.05, further demonstrating the linear model's suitability for explaining the variation in the response variable. The linear model appears to be a reasonable and appropriate description of the response surface in the investigated extraction process, which indicates that the model is fit to the study. This is supported by the provided fit statistics and the close match between the anticipated and actual RBO yields. This study was also supported by Ahmad et al. [35] who found comparable results using a linear model for the parametric optimization of rice bran, demonstrating the significance of the model terms.

Table 6. Analysis of variance (ANOVA) for regression model.

Source	Sum of square	DF	Mean square	F value	P value	Remarks
Model	51.4206	3	17.1402	22.9577	0.0024	significant
$X1$	15.5236	1	15.5236	20.7924	0.0061	significant
$X2$	18.7272	1	18.7272	25.0833	0.0041	significant
$X3$	17.1698	1	17.1698	22.9973	0.0049	significant
Residual	3.7330	5	0.7466			
Lack of fit	3.3087	3	1.1029	5.1911	0.1655	Not significant
Pure error	0.4243	2	0.2121			
Cor. total	55.1536	8				

Table 6 shows that all three variables have a statistically significant effect on the variability of the response variable, or RBO yield. The model shows a strong capacity to describe the observed variation in the response with a sum of squares (SS) of 51.4206 and 3 degrees of freedom (DF). The mean square (MS) value for the model is 17.1402, and the related F-value and p-value are 22.9577 and 0.0024, respectively. The low p-value indicates that the model's inclusion of the three factors significantly contributes to explaining the response variability, further supported by the relatively high F-value. Each component has a significant impact on the RBO yield. The SS for extraction temperature ($X1$) is 15.5236, the F-value is 20.7924, and the p-value is 0.0061. Similarly, the SS for rice bran to solvent ratio ($X2$) is 18.7272, the F-value is 25.0833, and the p-value is 0.0041. With an SS of 17.1698, an F-value of 22.9973, and a p-value of 0.0049, extraction time ($X3$) is likewise significant. The importance of these variables shows that variations in extraction temperature, rice bran-to-solvent ratio, and extraction time have a significant effect on the RBO yield. The study also contains residual, lack of fit and pure error components. With a value of 3.733 and 5 degrees of freedom (DF), the residual SS represents the model's unexplained variance or error. The SS for lack of fit, which measures the difference between the model and the observed data points, is 3.3087 with 3 degrees of freedom (DF). Notably, the lack of fit is not statistically significant (p-value is 0.1655), showing that the model fits the data satisfactorily. The pure error SS is 0.4243, with two degrees of freedom (DF) indicating variance between replicates.

3.7. Interpretation of the 3D response surface plots

The model's 3D response surface plots from Figures 4 (a-c) depicts the investigation of the interaction effects of the process variables.

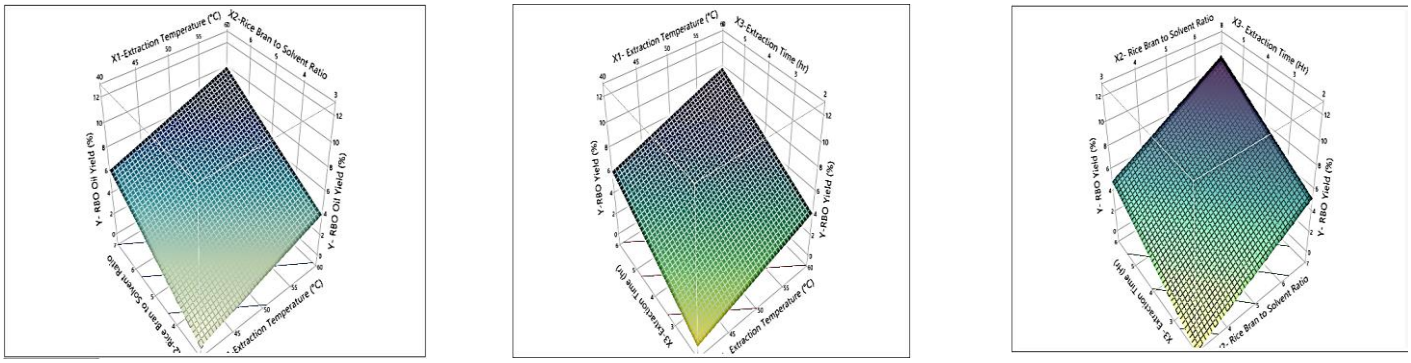

(a) **(b)** **(c)**

Figure 4. 3D Surface Plot of response with respect to (**a**) extraction temperature ($X1$) with solvent–bran ratio ($X2$) (**b**) extraction temperature ($X1$) with extraction time ($X3$) (**c**) bran solvent ratio ($X2$) with extraction time ($X3$).

The effect of temperature ($X1$) and rice bran to solvent ratio ($X2$) on RBO production percentage is depicted in Figure 4(a). Temperature is clearly a highly crucial component influencing oil recovery. The percentage of oil output increases with increasing temperature and decreasing ratio of rice bran to solvent. This is due to the increased solubility of oil in the solvent at higher temperatures, which results in a higher percentage of oil extracted. Wang et al. [26], reported similar findings. Figure 4(b) depicts the 3D surface plot for the interaction of extraction temperature ($X1$) and extraction time ($X3$) on the percentage oil yield from the extraction process, respectively. The results reveal that as the extraction time increases with increasing temperature, so does the proportion of oil extracted from rice bran. The influence of extraction time on the response value (oil yield) is significant; however, the rise is less sharp than that of temperature increment. This suggests that the solvent-bran ratio can affect the amount of oil extracted, with larger ratios offering a more accessible surface area for oil extraction. The interaction impact of solvent-bran ratio ($X2$) and extraction duration ($X3$) on oil yield is depicted in Figure 4(c). As the solvent-bran ratio grows with increasing extraction time, so does the percentage yield of rice bran oil. This shows that the solvent-bran ratio ($X2$), rather than the extraction duration ($X3$), is a critical parameter with a greater impact on the percentage of oil recovery from rice bran. Higher solvent-bran ratios offer a larger volume of solvent to interact with the rice bran, resulting in enhanced extraction efficiency. Increasing the extraction period also allows for more extensive contact between the solvent and the bran, which aids in oil extraction. As a result, the response variable, which is the oil yield, increases with the interaction of solvent-bran ratio and extraction time.

3.8. Interpretation of optimum condition

Based on Figure 5, the maximum value of the response function with the highest desirability of 0.954 has been achieved by using a set of process variables that have been identified with the help of numerical optimization techniques. The objective of this optimization was to maximize the response function, which is the % of yield of RBO, within the specified lower and higher boundaries of 2.54% and 9.83%, respectively. The ideal values for the process variables were found to be at 60°C, 1:5, and 6 hours, respectively.

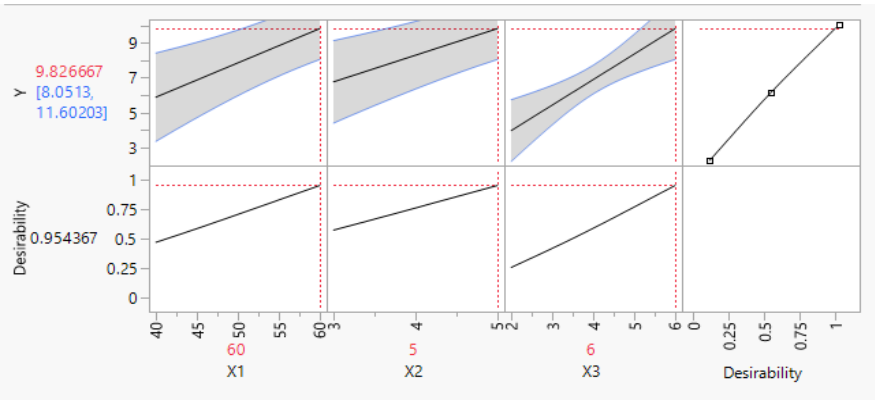

Figure 5. Optimum condition to obtained maximum desirability.

These findings show how well the numerical optimization technique works in identifying the best process variables for a high percentage of RBO yield. The comparison between predicted and actual yield are shown in Table 7.

Table 7. Predicted and actual comparison.

Properties	Experimental condition, X			Response, Y
	Extraction temperature	Rice bran to solvent ratio	Extraction time, hr	RBO yield, %
Predicted	60	1:5	6	9.83
Actual	60	1:5	6	8.98
		Error, %		8.65%

The difference between the expected and actual RBO yields resulted in an 8.65% inaccuracy which is considered significant in this context [36, 37]. These differences can be ascribed to a variety of variables, including experimental uncertainties, sample variations, and potential errors throughout the analytical process.

4. Conclusions

The study successfully evaluated the performance of n-hexane and iso-propanol solvents for RBO extraction, with both showing promising results. Both solvents were tested for their ability to extract oil from rice bran samples and were shown to be successful in extracting rice bran oil, with only minor differences in yields. Temperature, solvent-bran ratio, and extraction time were found to significantly influence oil yield, with higher temperatures leading to increased yields. The study revealed that increasing the temperature from the starting circumstances considerably increased the oil output. Changing the solvent-bran ratio and increasing the extraction time had a similar positive connection with enhanced oil yield. Physical analyses provided insights into the quality of the extracted oil. To achieve higher oil extraction, the final goal was optimized by utilizing the most appropriate solvent, iso-propanol. A linear model was created and tested for optimization. According to ANOVA, temperature, together with the solvent-bran ratio and extraction time, are the key variables that can affect the percentage of oil extracted from rice bran. The expected result indicates that the maximum oil yield that may be obtained under extraction circumstances of 60°C, 6 hours, and a ratio of 1:5 is 9.83% (w/w). It is important to note that this study is only for

experimental purposes and not for any commercial or consumption item and usage of the oil for cooking based on this experiment methodology is not advisable.

Conflict of interest

The authors declare no competing interests.

References

1. Pandey, R.; Shrivastava, S.L. Comparative evaluation of rice bran oil obtained with two-step microwave assisted extraction and conventional solvent extraction. *J. Food Eng.* **2018**, *218*, 106-114, https://doi.org/10.1016/j.jfoodeng.2017.09.009
2. Punia, S; Kumar, M.; Siroha, A.K.; Purewal, S.S. Rice bran oil: Emerging trends in extraction, health benefit, and its industrial application. *Rice Sci.* **2021**, *28(3)*, 217-232, https://doi.org/10.1016/j.rsci.2021.04.002
3. Nayik, G.A.; Majid, I.; Gull, A.; Muzaffar, K. Rice bran oil, the future edible oil of India: A mini review. *J. Rice Res.* **2015**, *3*, 151.
4. Pimpa, B.; Thongraung, C.; Sutthirak, P. Effect of solvents and extraction conditions on the properties of crude rice bran oil. *Walailak J. Sci. Technol.* **2021**, *18(17)*, 1-7, https://doi.org/10.48048/WJST.2021.9611
5. Garofalo, S.F.; Tommasi, T.; Fino D. A short review of green extraction technologies for rice bran oil. *Biomass Conv. Bioref.* **2021**, *211*, 569-587, https://doi.org/10.1007/s13399-020-00846-3
6. Ghosh, M. Review on recent trends in rice bran oil processing. *J. Am. Oil Chem. Soc.* **2007**, *84*, 315-324, https://doi.org/10.1007/s11746-007-1047-3
7. Pandey, R.; Shrivastava, S.L. Comparative evaluation of rice bran oil obtained with two-step microwave assisted extraction and conventional solvent extraction. *J. Food Eng.* **2018**, *218*, 106-114, https://doi.org/10.1016/j.jfoodeng.2017.09.009
8. Oliveira, R.; Oliveira, V.; Aracava, K.K.; Rodrigues, C. Effects of the extraction conditions on the yield and composition of rice bran oil extracted with ethanol – A response surface approach. *Food Bioprod. Proces.* **2012**, *90*(1), 22-31. https://doi.org/10.1016/j.fbp.2011.01.004
9. Garofalo, F. S.; Demichelis, F.; Mancini, G.; Tommasi, T.; Fino, D. Conventional and ultrasound-assisted extraction of rice bran oil with isopropanol as solvent, *Sustain. Chem. Pharm.* **2022**, *29*, 100741, https://doi.org/10.1016/j.scp.2022.100741
10. Dun, Q.; Yao, L.; Deng, Z.; Li, H.; Li, J.; Fan, Y.; Zhang, B. Effects of hot and cold-pressed processes on volatile compounds of peanut oil and corresponding analysis of characteristic flavor components. *LWT* **2019**, *112*, 107648, https://doi.org/10.1016/j.lwt.2018.11.084
11. Xu, D.; Hao, J.; Wang, Z.; Liang, D.; Wang, J.; Ma, Y.; Zhang, M. Physicochemical properties, fatty acid compositions, bioactive compounds, antioxidant activity and thermal behavior of rice bran oil obtained with aqueous enzymatic extraction. *LWT* **2021**, *149*, 111817, https://doi.org/10.1016/j.lwt.2021.111817
12. Djaeni, M.; Listyadevi, Y. L., The Ultrasound-Assisted extraction of rice bran oil with n-hexane as a solvent. *J.Phys. Conf. Ser.* **2019**, *1295(1)*, 012027, https://doi.org/10.1088/1742-6596/1295/1/012027
13. Zhang, Q.W.; Lin, L.G.; Ye, W.C. Techniques for extraction and isolation of natural products: A comprehensive review. *Chin Med.* 2018, *13*, 20, https://doi.org/10.1186/s13020-018-0177-x
14. Sengupta, R.; Bhattacharyya, D.K. Enzymatic extraction of mustard seed and rice bran. *J. Am. Oil. Chem. Soc.* **1996**, *73(6)*, 687-692. https://doi.org/10.1007/BF02517941
15. Hanmoungjai, P.; Pyle, D.L.; Niranjan, K. Enzymatic process for extracting oil and protein from rice bran. *J. Am. Oil. Chem. Soc.* **2001**, *78(8)*, 817-821, https://doi.org/10.1007/s11746-001-0348-2
16. Lehri, D.; Kumari, N.; Singh, R.P. Ultrasound-assisted production and characterization of rice bran lecithin-based nanoemulsions. *J. Dispers. Sci. Technol.* **2020**, *42(9)*, 1368-1375, https://doi.org/10.1080/01932691.2020.1764368
17. Herawati, N.; Gaffar, M.A.F.; Wahyudin, E. Microwave-Assisted Extraction and Identification of γ-Oryzanol from Rice Bran (*Oryza sativa* L. cv *ciliwung*). *Pharmacogn. J.* **2021**, *13(5)*, 1242-1247, https://doi.org/10.5530/pj.2021.13.157
18. Kumar, P.; Yadav, D.; Kumar, P.; Panesar, P.S.; Bunkar, D.S.; Mishra, D.; Chopra, H.K. Comparative study on conventional, ultrasonication and microwave assisted extraction of γ-oryzanol from rice bran. *J. Food Sci. Technol.* **2016**, *53(4)*, 2047-2053, https://doi: 10.1007/s13197-016-2175-2

19. Masud, F.; Fajar; Bangngalino, H.; Indriati, S.; Todingbua, A.; Suhardi, Sayuti, M. Model development to enhance the solvent extraction of rice bran oil. *OCL* **2019**, *26*, 16, https://doi.org/10.1051/ocl/2019009.
20. Shukla, H.S.; Pratap, A. Comparative studies between conventional and microwave assisted extraction for rice bran oil. *J. Oleo. Sci*, **2017**, *66(9)*, 973-979, https://doi.org/10.5650/jos.ess17067
21. Soares, J.F.; Prá, V.D.; Barrales, F.M.; Santos, P. D.; Kuhn, R.C.; Rezende, C.A.; Martinez, J.; Mazutti, M.A. Extraction of rice bran oil using supercritical CO_2 combined with ultrasound. *Braz. J. Chem. Eng.* **2018**, *35(2)*, 785-794, https://doi.org/10.1590/0104-6632.20180352s20160447
22. Juchen, P.T.; Araujo, M.N.; Hamerski, F.; Corazza, M.L.; Voll F.A.P. Extraction of parboiled rice bran oil with supercritical CO_2 and ethanol as co-solvent: Kinetics and characterization. *Ind. Crops Prod*. **2019**, *139*, 111506 https://doi.org/10.1016/j.indcrop.2019.111506
23. Xu, G.; Liang, C.; Huang, P.; Liu, Q.; Xu, Y.; Ding, C.; Li, T. Optimization of rice lipid production from ultrasound-assisted extraction by response surface methodology. *J. Cereal Sci*, **2016**, *70*, 23-28. https://doi.org/10.1016/j.jcs.2016.05.007
24. Phan, V.M.; Tran, H.C.; Sombatpraiwan, S. Rice bran oil extraction with mixtures of ethanol and hexane. *Songklanakarin J. Sci. Technol*. **2021**, *43(3)*, 630-637.
25. Javed, F.; Ahmad, S.W.; Rehman, A.; Zafar, A.S.; Malik. S.R. Recovery of rice bran oil using solid- -liquid extraction technique. *J. Food Process Eng.* **2014**, *38(4)*, 357-362, https://doi.org/10.1111/jfpe.12166
26. Wang, Z.; Li, S.; Zhang, M. Yang, H.; Li, G.; Ren, X.; Liang, S. Optimization of oil extraction from rice bran with mixed solvent using response surface methodology. *Foods* **2022**, *11(23)*, 3849, https://doi.org/10.3390/foods11233849
27. Comerlatto, A.; Voll, F.A.; Daga, A.L.; Fontana, É., Mass transfer in soybean oil extraction using ethanol/isopropyl alcohol mixtures. *Int. J. Heat Mass Transfer* **2021**, *165*, 120630, https://doi.org/10.1016/j.ijheatmasstransfer.2020.120630
28. Handayani, S.; Fajriah, S., Rice Bran Oil Extraction as Trioxolane Raw Material. *Simetrikal J.Eng. Technol.* **2020**. *2(1)*, 13-19, https://doi.org/10.32734/jet.v2i1.3063
29. Asmare M, Gabbiye N. Synthesis and characterization of biodiesel from castor bean as alternative fuel for diesel engine. *Am. J. Energy Eng*. **2014**, *2(1)*, 1-15. https://doi.org/10.11648/j.ajee.20140201.11
30. Amabye, T.G.; Bezabh, A. M. Physicochemical characterization and phytochemical screening of *Jatropha curcasL.* seed oil cultivated in Tigray Ethiopia. *Adv. Biochem.* **2015**, *3(3)*, 35-39. https://doi.org/10.11648/j.ab.20150303.11
31. Suryati, S.; Ismail, A.; Afriyanti, A. Proses pembuatan minyak dedak padi (rice bran oil) menggunakan metode ekstraksi. *J. Teknol. Kimia*, **2015**, *4(1)*, 37-45.
32. Nasir; Subriyer; Fitriyanti, Kamila, Hilma Ekstraksi dedak padi menjadi minyak mentah dedak padi (crude rice bran oil) dengan pelarut n-hexan dan ethanol. *J. Rekayasa Sriwijaya*, **2009**, *18(1)*, 37-44.
33. Orthoefer, F. T. Rice bran oil detection. *Bailey's Ind. Oil Fat. Prod.* 6th Edn. , 1996, 393-409. https://doi.org/10.1002/047167849X.bio015.pub2
34. Mumtaz, M.W.; Adnan, A.; Anwar, F.; Mukhtar, H.; Raza, M. A.; Ahmad, F.; Rashid, U. Response surface methodology: An emphatic tool for optimized biodiesel production using rice bran and sunflower oils. *Energies* **2012**, *5(9)*, 3307-3328, https://doi.org/10.3390/en5093307
35. Ahmad, S.W.; Javed, F.; Ahmad, S.; Akram, M.; Rehman, A. Parametric optimization of rice bran oil extraction using response surface methodology. *Pol. J. Chem. Technol.* **2016**, *18(3)*, 103-109, https://doi.org/10.1515/pjct-2016-0055
36. Mahmood, T.; Ali, R.; Naeem, A.; Hamayun, M.; Aslam, M. Potential of used Camellia sinensis leaves as precursor for activated carbon preparation by chemical activation with H_3PO_4; optimization using response surface methodology. *Process Saf. Environ. Prot.* **2017**, *109*, 548-563, https://doi.org/10.1016/j.psep.2017.04.024
37. Chen, Y.D.; Chen, W.Q.; Huang, B.; Huang, M.J. Process optimization of $K_2C_2O_4$-activated carbon from kenaf core using Box–Behnken design. *Chem. Eng. Res. Des.* **2013**, *91(9)*, 1783-1789, https://doi.org/10.1016/j.cherd.2013.02.024

Sustainable Engineering

Article
Volume 1, Issue 1, 2024
https://doi.org/10.51200/susten.v1i1.5262

Evaluation of Linear Elastic Dynamic Analysis Behavior on RC Buildings in Sabah Subjected to Moderate PGA

Noor Sheena Herayani Harith [1,*], Samnursidah Samir [1], Min Fui Tom Ngui [1,2]

[1]Faculty of Engineering, Universiti Malaysia Sabah, 88400 Kota Kinabalu, Sabah, Malaysia
[2]Eramaju Synergy Sdn Bhd, Lido Plaza, Kota Kinabalu, Sabah, 88300 Malaysia
*Correspondence: sheena@ums.edu.my *Scopus Author ID 57195451970
Received: 15 July 2024, Accepted: 09 Aug 2024

Abstract: Seismic performance of existing buildings in Southeast Sabah needs further examination, as there has been limited research. It is significant to explore the buildings respond to linear elastic dynamic analysis, especially considering that most reinforced concrete (RC) buildings insufficient earthquake-resistant technology. The current study aims to establish the correlation between peak ground acceleration (PGA) and the performance point of buildings under moderate PGA of 0.12g, 0.14g, and 0.16g, and then to assess the expected performance level of three RC buildings. The selection of three buildings within a 10 km radius from the active faults area. The buildings undergo an analytical method that necessitates the utilization of computational techniques to determine their capacity curve, demand curve, and performance point through the application of pushover analysis under the different of PGA. The performance point of buildings is determined by the intersection between capacity and demand curves, indicating Life Safety (LS) in inelastic range. This study critically evaluates the performance point of buildings that indicates inelastic displacement of the roof according to the intersection between capacity and demand curves under the various PGA.

Keywords: Performance point; RC buildings; Acceleration

1. Introduction

Southeast Sabah is characterised as an area with moderate seismicity region, as determined by Mansor et al. [1] through the macrozonation map. This analysis is based on two-thirds of the values from a 2,475-year average return period that corresponds to ground motions having a 2% probability of exceedance in 50 years. Seismic activities with most of the thrust faults and strike-slip faults have been found in Southeast Sabah, where there are numerous fault scarps, damaged roads, mud volcanoes, and hot springs [2]. Figure 1 shows numerous linear features typically spanning 20 to 40 km in length, in the Lahad Datu and Tawau region. These linear features are mostly linked to earthquakes due to thrust faults indicated by the red line and strike-slip faults in the purple line.

The risk of seismic is a quantification of the potential adverse consequences of an earthquake occurring at a particular site due to ground motion expressed through peak ground acceleration (PGA). It represents the highest ground acceleration recorded during an earthquake, typically expressed as a fraction of Earth's gravitational acceleration (g) and the seismic hazard map for Sabah region has been provided by Minerals and Geoscience Department of Malaysia (JMG) [3]. According to Tongkul [4] and Harith et al. [5], it was

determined that the Lahad Datu region of southeast Sabah has the highest PGA value with its maximum value of 0.16g as shown in Figure 2.

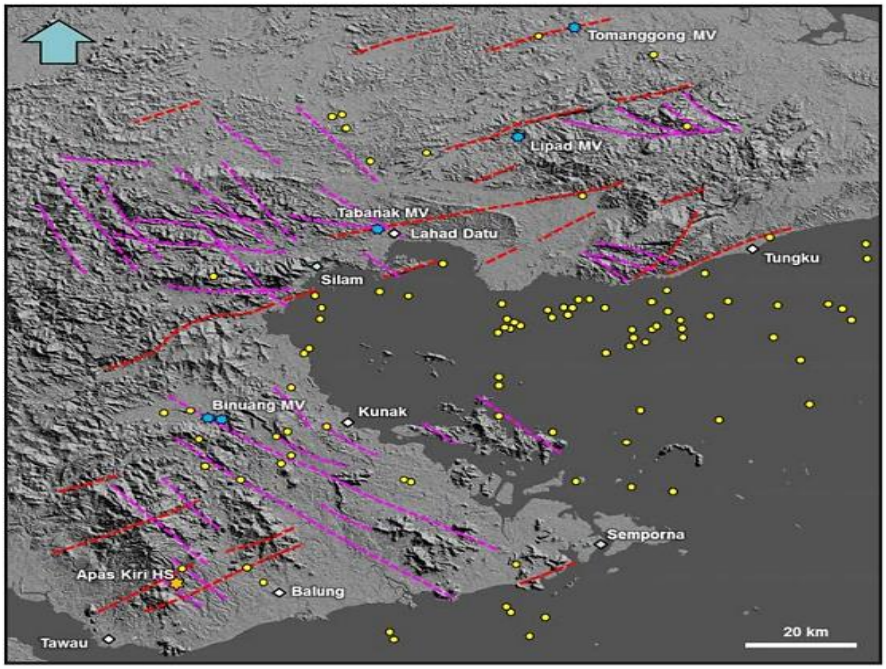

Figure 1. Thrust faults and strike-slip faults in Southeast Sabah [1].

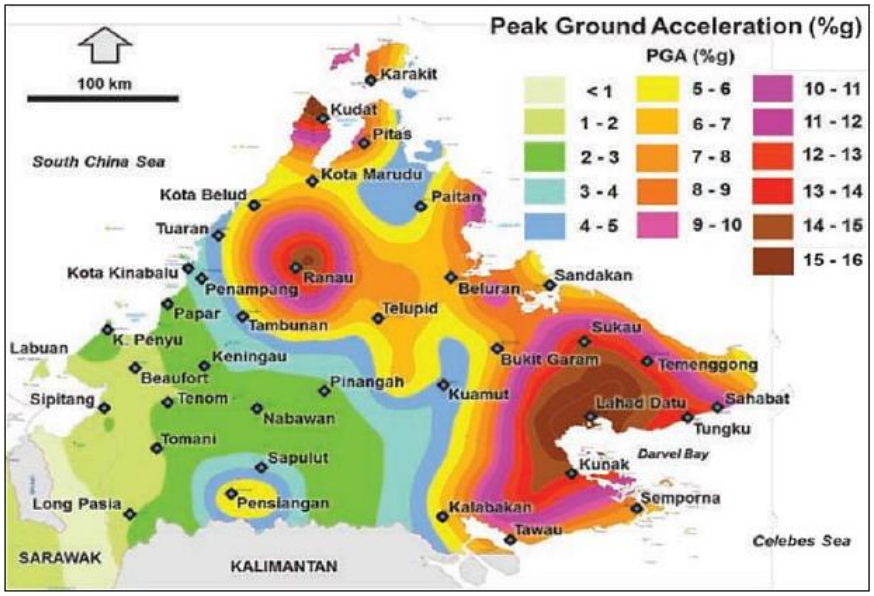

Figure 2. Seismic hazard map [3].

Again Tongkul [6] also stated that most of the earthquakes in this region have a magnitude of less than 5.0 Mw, apart from two earthquakes with a magnitude 6.0 Mw and above, such as the 1976 Lahad Datu earthquake (6.2 Mw) and 1923 Lahad Datu earthquake (6.3 Mw). The Lahad Datu earthquake in July 1976 caused significant property damage to Lahad Datu police complex, low-cost houses, Fire Department flat and Telecom building [6]. The damage that appeared during the event as shown in Figure 3 on the beam and ceiling at Fire Department flat and Telecom buildings. The variances in each building's seismic vulnerability and the observed damage dispersion in earthquake-affected structures are linked

to the features of seismic vibrations that are influenced by source characteristics and geological site conditions [7].

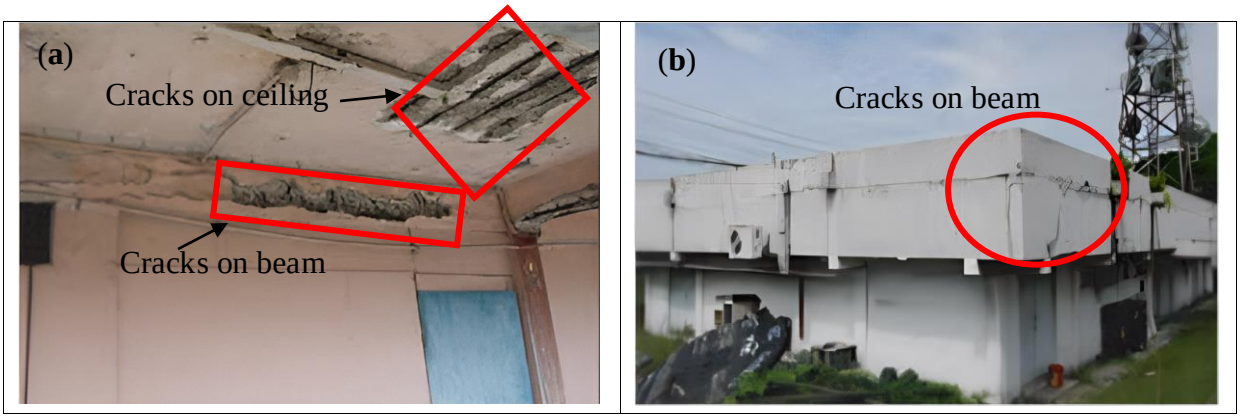

Figure 3. Cracks appeared on RC buildings in Lahad Datu as in (**a**) Fire Department Flat building and (**b**) Telekom building (modified from Tongkul [6]).

For this reason, it is very important to conduct an adequate assessment of this vulnerability, particularly using linear elastic dynamic analysis [8]. Pushover analysis is a straightforward technique for the prediction of non-linear behavior of the structure under seismic loads for the structures [9]. An intersection of the two estimated quantities consisting of seismic demand and seismic capacity, is one of the methods that are used to establish the performance-based analysis. In general, structure in pushover analysis is subjected to a lateral load that monotonically increases and roughly represents the relative inertia forces produced at the centers of masses for each story.

The performance point analysis is the generation of demand and capacity curves, which facilitate performance evaluation based on spectral displacement (Sd) and spectral acceleration (Sa). As defined by Douglas et al. [10], Sd represents the maximum displacement or movement response of a structure to seismic ground motion at a specific frequency. It signifies the expected amount of structural movement, in terms of displacement, at a particular frequency during an earthquake. A higher spectral displacement at a specific frequency suggests that the structure may experience more significant movements and deformations at that frequency. Furthermore, Sa measures the maximum acceleration response of a structure to seismic ground motion at a specific frequency, quantifying how rapidly and forcefully the ground shakes at that frequency during an earthquake.

Therefore, the seismic performance evaluation of buildings needs to be expanded in Southeast Sabah, as this region has seen limited research compared to Northeast Sabah, where numerous studies have been conducted following the 2015 earthquake in Ranau. This is especially necessary because most of the reinforced concrete (RC) buildings in the study area do not adhere to earthquake-resistant design practices using Eurocode 8 (EC8) Part 1 National Annex (NA) in accordance with MS EN1998-1:2015 [11]. This current study attempts to establish the correlation between PGA and the performance point of buildings under moderate PGA of 0.12g, 0.14g, and 0.16g of RC buildings. These three values are used in this study due to the maximum recorded PGA from the seismic station record is 0.12g

(from the 2015 Ranau event). In contrast, the 0.16g is the highest PGA value from the analysis of seismic hazard assessment as studied in MS EN1998-1:2015 [11].

2. Methodology

The study focused on existing buildings, namely Building 1, Building 2, and Building 3 situated in Southeast Sabah. The focus is to study the seismic performance of a multi-story RC building using linear elastic dynamic analysis. The selection of three buildings was selected based on the location that is within a 10 km radius of the active faults. The building is located at the western end of the Lahad Datu Airport, near Kg. Tabanak faults whereas this fault has been identified by the study of Tongkul [2]. The analysis of the anticipated building performance level is conducted under various earthquake loads, specifically PGA of 0.12g, 0.14g, and 0.16g. This approach was motivated by the release of the initial seismic hazard map which identified the Lahad Datu area as a high-hazard zone with PGA values ranging from 0.12g to 0.16g [12]. The analysis procedure in this study contains three distinct phases as illustrated in Figure 4.

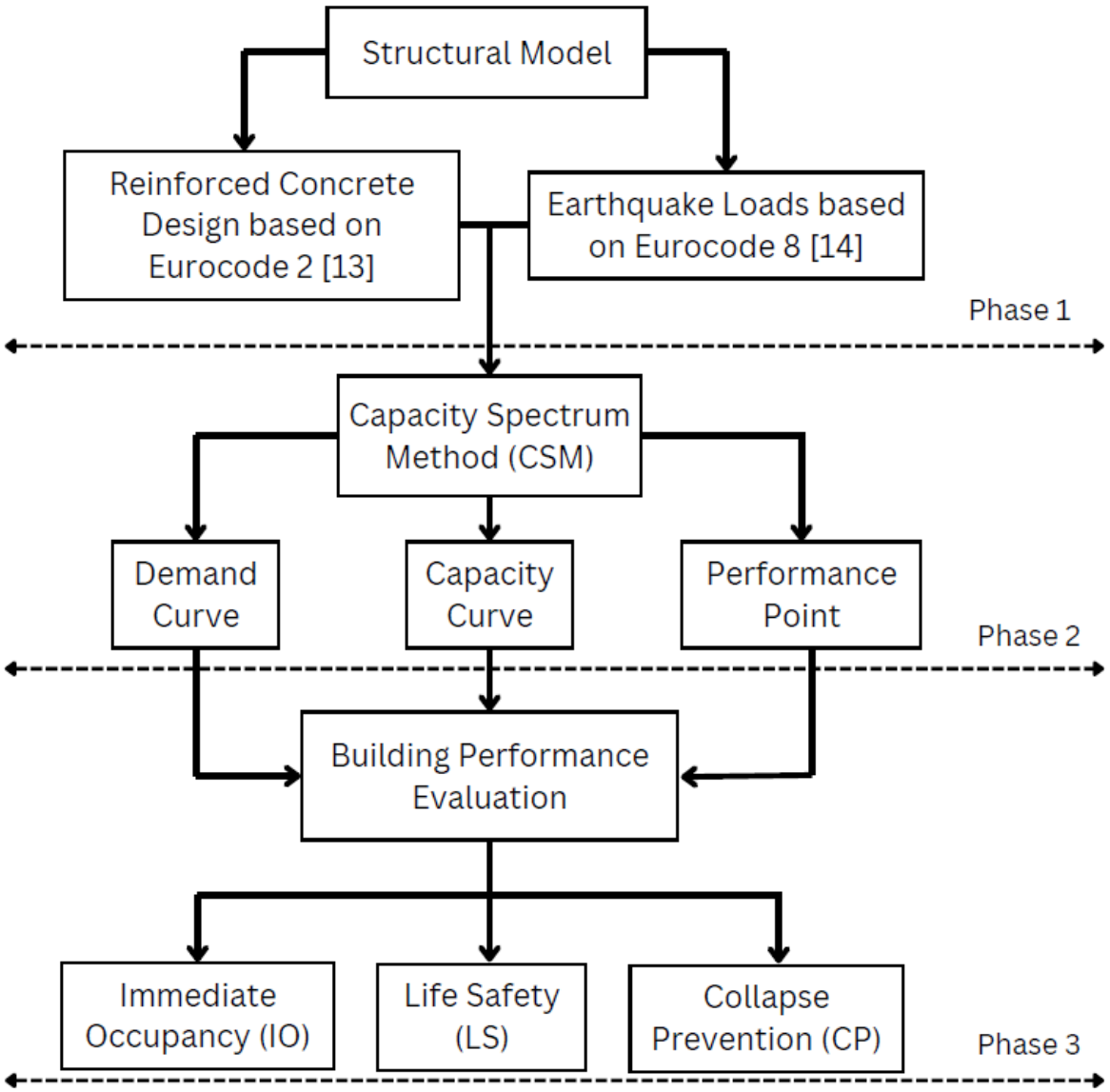

Figure 4. Flowchart of methodology.

2.1 Structural Model

The structural model of buildings represents a RC construction with brick infill masonry walls as shown in Figure 5-7. The structure is constructed using M20 concrete grade and designed according to Eurocode 2 [13] for RC and Eurocode 8 [14] for earthquake loads. Meanwhile, the dimensions of the building's structural members are shown in Table 1-3. The buildings were simulated with frame elements for beams and columns, while slabs were represented using shell elements. The pushover analysis of these buildings encompassed three distinct load scenarios which included different type of loads namely gravity loads which encompasses of dead and live loads, as well as lateral loads, including seismic forces, which collectively represent the forces acting on the structure, lateral loads in the X-X direction, and lateral loads in the Y-Y direction.

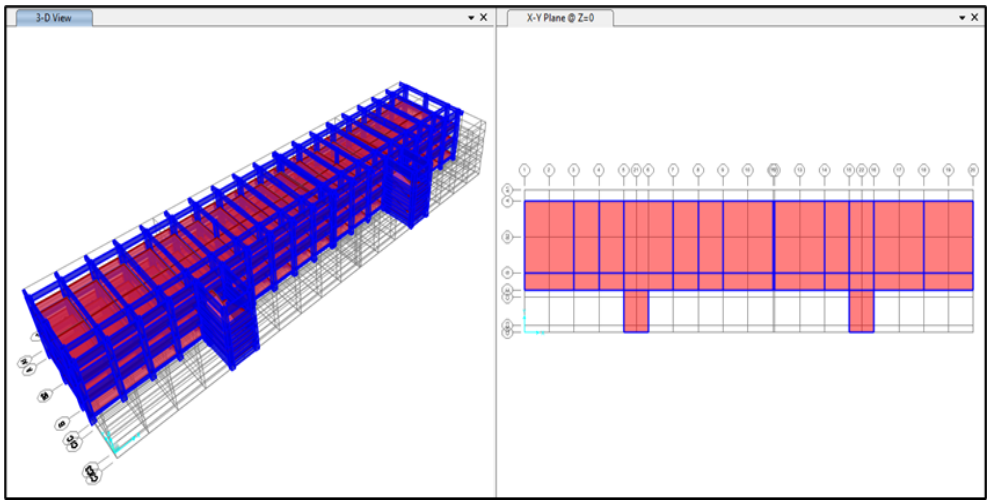

Figure 5. 3D view and typical floor plan of Building 1 (analysis taken from SAP2000 software).

Table 1. Dimension on the structural members of Building 1.

Structural Members	**Dimension (mm)**		
Beam	200 x 400	100 x 400	200 x 600
	200 x 500	100 x 1000	200 x 300
	100 x 1300	200 x 800	100 x 500
	100 x 300	100 x 600	400 x 600
Column	200 x 200	100 x 200	
Slab	100		

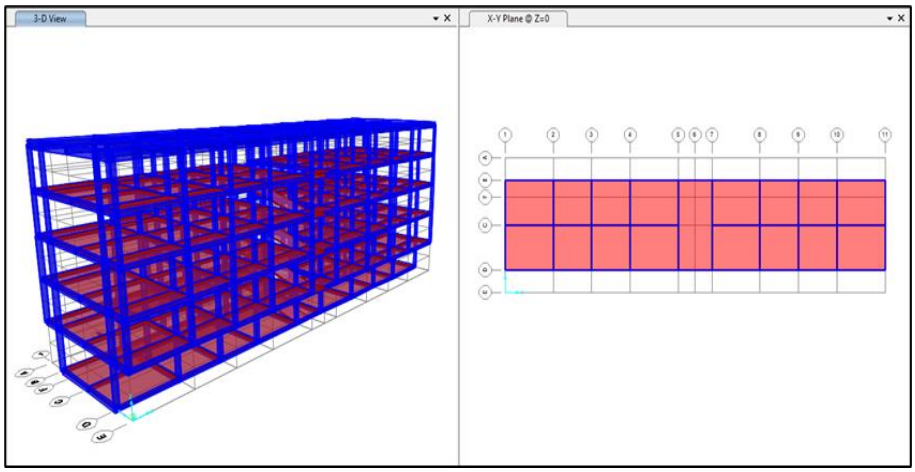

Figure 6. 3D view and typical floor plan of Building 2.

Table 2. Dimension on the structural members of Building 2.

Structural Members	Dimension (mm)		
Beam	200 x 300	200 x 400	200 x 500
	200 x 600		
Column	230 x 300	230 x 400	
Slab	135		

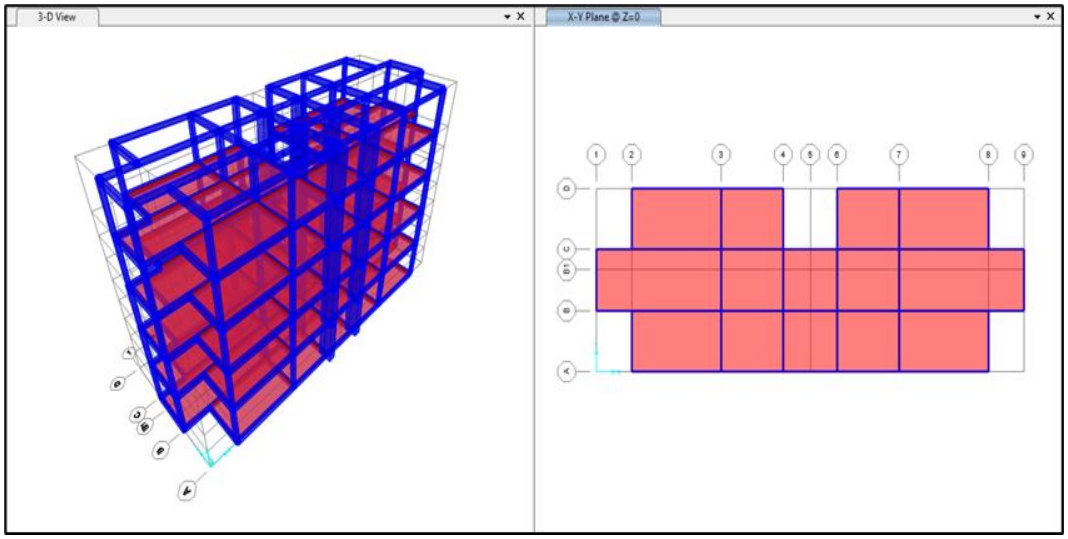

Figure 7. 3D view and typical floor plan of Building 3.

Table 3. Dimension on the structural members of Building 3.

Structural Members	Dimension (mm)		
Beam	200 x 350	200 x 400	150 x 300
	200 x 400		
Column	230 x 300	230 x 400	500 x 1000
Slab	135		

2.2 Capacity Spectrum Method (CSM)

Performance point analysis based on Capacity Spectrum Method (CSM) referring to ATC-40 [15] is a very useful tool in the evaluation design of existing concrete buildings. This method requires the determination of three crucial parameters such as the capacity curve, the demand curve, and the performance point under three different PGA. It provides a graphical representation of the structure's global force-displacement capacity curve and compares it with earthquake demand response spectra representations. CSM is beneficial because of its graphical nature, which allows for the visualization of the connection between demand and capacity when determining the point at which this capacity spectrum intersects with the earthquake demand. The capacity curve represented the ability of the structure to withstand the seismic demand while the demand curve represented the earthquake ground motion.

The demand and capacity curves will be plotted in terms of Acceleration Displacement Response Spectra (ADRS) format. This ADRS is a graph representation of spectral acceleration (Sa) in unit of m/s versus spectral displacement (Sd) in unit m. Demand curve expressed in terms of Sa and period, T based on the response spectrum in Eurocode 8 [14] with the conversion formula using Equation (1) as performed by Leslie and Naveen [9]. The

following equation defined as the spectral displacement ordinate (Sd), the corresponding period (T) and spectral acceleration ordinate (Sa).

$$Sd = \frac{T^2}{4\pi^2} Sa \quad (1)$$

2.3 Performance Point Evaluation

Once the capacity and demand curves are established, an evaluation of the expected performance level of the building can be carried out by comparing the estimated target displacement on the demand curve with the actual displacement on the capacity curve under three different PGA of 0.12g, 0.14g, and 0.16g. In this study, the building performance criteria, as suggested by Harith et al. [16], have been adapted to suit the assessment of expected performance levels based on the performance point. The performance point represents the intersection of the demand and capacity curves, indicating the actual displacement demand of a building. The performance level of the building at various stages can be expressed using performance following the guidelines outlined in ATC-40 [15], as shown in Figure 8 described by Abd-Elhamed and Mahmoud [17]. It is important to note that as the displacement of buildings increases, the extent of damage also increases.

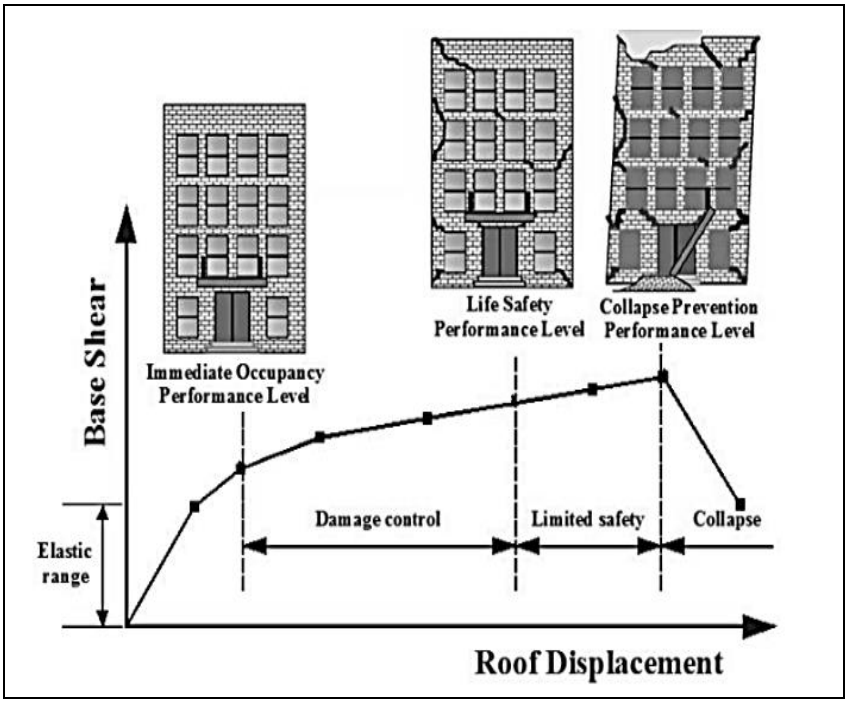

Figure 8. Illustration of building performance levels [15].

The previous study in Dya and Oretaa [18] mentioned that the different performance levels used in buildings describe the limiting damage state of a particular building. Immediate Occupancy (IO) represents a building condition in which the structure can withstand an earthquake without experiencing any structural or non-structural damage, but even if the building is affected by the earthquake, it remains recoverable. Life Safety (LS) signifies a condition where a building can endure an earthquake with minimal structural damage, ensuring the safety of people residing or present inside the building during the seismic event. Collapse Prevention (CP) pertains to a structural state in which a building sustains severe structural damage but does not collapse during an earthquake, thereby

preventing a complete structural failure. Furthermore, the performance point is the intersection between demand spectrum and capacity curve as illustrated and described in Wooi et al. [19] and Atul and Sekar [20].

3. Results and Discussion

The buildings were subjected to the seismic performance of pushover analysis for two different load cases, termed Push-X and Push-Y in both the x-direction and y-direction, respectively under the various PGA. This capacity-demand curve relationship enables a direct comparison between the capacity and demand curves, indicating the precise intersection point known as the performance point. Figure 9-10 illustrate the performance point for Push-X and Push-Y, respectively, under a Peak Ground Acceleration (PGA) of 0.12g. Similarly, Figure 11-12 represent the performance point for Push-X and Push-Y, respectively, at a PGA of 0.14g. Finally, Figure 13-14 display the performance point for Push-X and Push-Y, respectively, at a PGA of 0.16g. The comparison of performance point, it is evident that each intersection of the demand and capacity curves are between LS and CP signifies the buildings require to be retrofitted specifically at 0.14-0.16g.

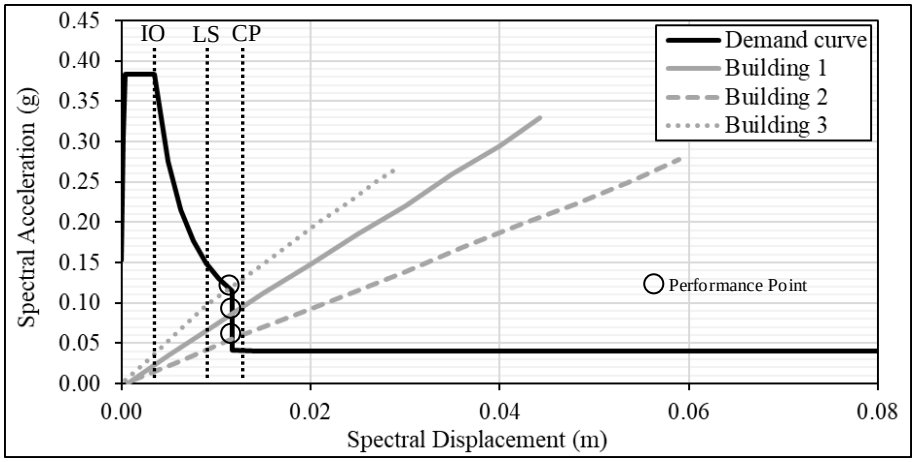

Figure 9. Performance point for Push-X under PGA of 0.12g.

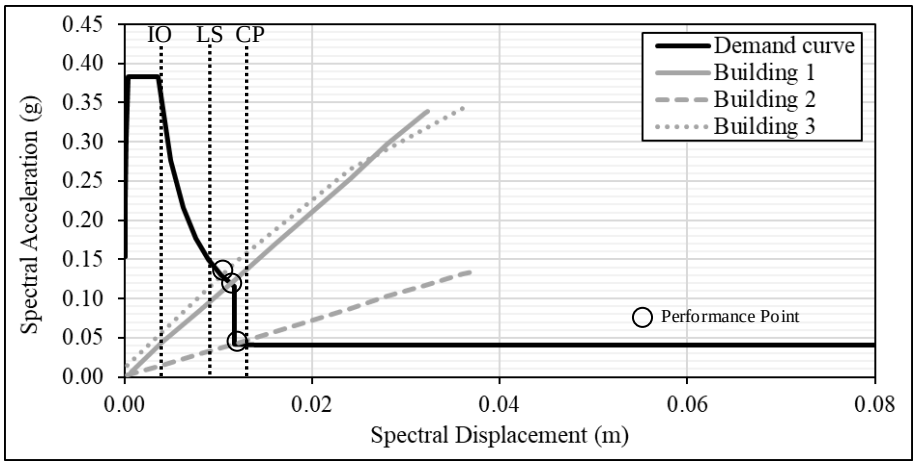

Figure 10. Performance point for Push-Y under PGA of 0.12g.

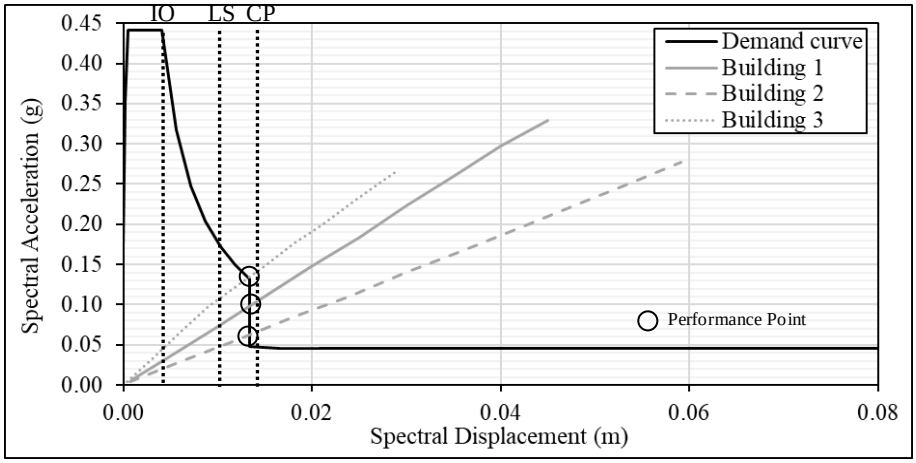

Figure 11. Performance point for Push-X under PGA of 0.14g.

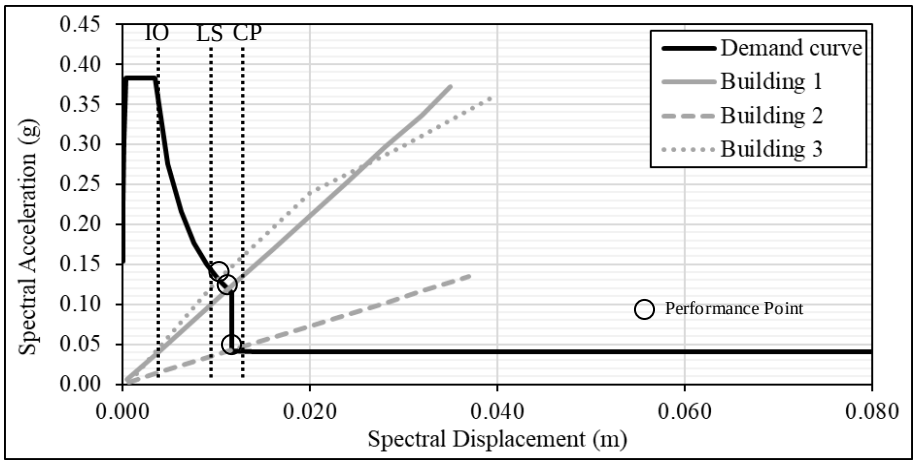

Figure 12. Performance point for Push-Y under PGA of 0.14g.

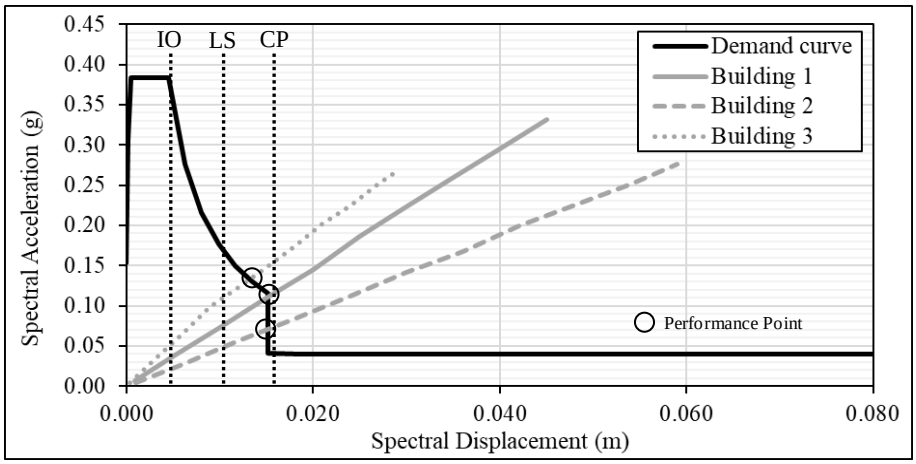

Figure 13. Performance point for Push-X under PGA of 0.16g.

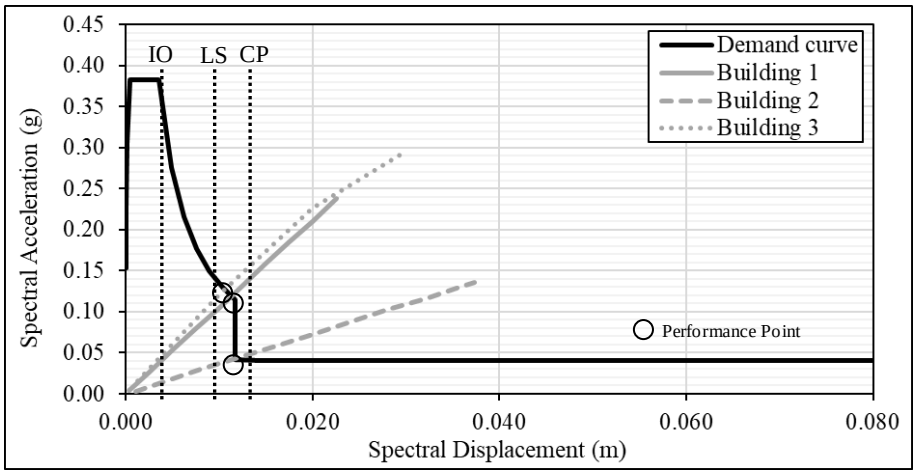

Figure 14. Performance point for Push-Y under PGA of 0.16g.

Table 4-5 present a tabulation of the roof displacements based on the performance point for each building, considering both Push-X and Push-Y directions across three distinct PGA values of 0.12g, 0.14g, and 0.14g, respectively. The correlation between displacement and PGA is a fundamental aspect when assessing the expected seismic performance level of buildings. Notably, as the PGA escalates, the displacement of buildings tends to escalate as well. This implies that more intense ground shaking or higher PGA levels can result in increased deformation and movement within the structure. A previous study conducted by Abd-Elhamed and Mahmoud [17] aligns with this notion, indicating that heightened seismic activity leads to greater building displacement. Their research concentrated on building evaluations subjected to 0.15g and 0.30g intensities, revealing that the building's performance point varies with the application of seismic forces in both the x-direction and y-direction.

Table 4. Expected displacement of buildings for Push-X under various PGA.

Building Name	**Peak Ground Acceleration (PGA)**			**Performance point**
	0.12 g	**0.14 g**	**0.16 g**	
Building 1	0.012 m	0.014 m	0.015 m	LS
Building 2	0.012 m	0.014 m	0.015 m	LS
Building 3	0.011 m	0.013 m	0.014 m	LS

Table 5. Expected displacement of buildings for Push-Y under various PGA.

Building Name	**Peak Ground Acceleration (PGA)**			**Performance point**
	0.12 g	**0.14 g**	**0.16 g**	
Building 1	0.011 m	0.011 m	0.012 m	LS
Building 2	0.012 m	0.012 m	0.012 m	LS
Building 3	0.010 m	0.010 m	0.011 m	LS

The performance point is linked to the inelastic roof displacement to assess how all buildings are expected to perform under varying PGA levels for both Push-X and Push-Y. It is evidence that the performance point in the elastic zone shows a good performance point. However, the performance point of buildings in the inelastic zones shows a poor performance point [21]. The inelastic zone is when buildings are subjected to dynamic loadings that exceed their elastic range and which damage will be permitted. A previous study conducted in Estêvão and Carvalho [7] proved that the performance point determined for RC buildings in the elastic zone is linked to no damage obtained grouped as the best-case scenario. Conversely, the performance point determined for RC buildings in the inelastic zone is categorized as the worst-case scenario. The overall buildings in Southeast Sabah show that they are prone to damage due to their performance point being associated to the inelastic roof displacement that occurs beyond the elastic range of deformation and is typically associated with the inelastic range.

In accordance with Maske et al. [22], if the performance point occurs with a minimal margin for strength and deformation capacity, it can be inferred that the buildings exhibited inadequate performance under the seismic forces applied and must undergo retrofitting to prevent significant future damage or structural failure. A level of damage that is considered tolerable for a particular building and a specific level of ground motion intensity is denoted as a performance level, particularly the state of Immediate Occupancy (IO), Life Safety (LS), and Collapse Prevention (CP). In Yadav et al. [23], the study concluded that the performance point considers both structural and non-structural performance criteria, incorporating aspects such as significant building damage, potential safety hazards, and the post-earthquake functionality of buildings. They identified the structural performance level which signifies a post-earthquake state where the building has undergone minimal structural damage.

A prior study by Ismaeil [24] found that buildings with performance levels that fell below a certain threshold after reaching the IO state were recommended to undergo retrofitting measures. The overall performance level of buildings in Southeast Sabah is categorized as LS state, thus the buildings may need to be retrofitted. In Mansor et al. [1], the authors recommended retrofitting existing buildings by incorporating steel diagonal braced frames with concrete frames as a highly effective technique for reinforcing the strength and stiffness of the structural system. This method allows for the enhancement of structural performance without significantly increasing the total weight of the building. There is considerable flexibility in the design process, with a multitude of configurations available for the diagonal braces, as well as the option to choose from various types of brace member sections. This adaptability in retrofit design ensures that the chosen approach can be tailored to the specific needs and requirements of the building, making it a versatile and efficient method for structural enhancement.

4. Conclusions

The seismic performance of three existing RC buildings was examined using pushover analysis as a relatively simple way to explore the non-linear behavior of buildings. This pushover analysis was employed to compare the performance levels of the buildings with the criteria outlined in ATC-40 [15], aiming to assess the extent of seismic damage

experienced by the structure. The relationship between PGA and the performance point related to the inelastic roof displacement of buildings shows that as PGA increases, the displacement experienced by the building tends to increase. The expected performance level evaluation exposes overall buildings in the LS state due to their performance point in the inelastic zone that needs retrofitting the addition of steel diagonal braced frames into an existing building.

Acknowledgments

This research has been supported by the Ministry of Higher Education (MoHE) Malaysia through the Fundamental Grant Scheme (FRGS), FRGS/1/2020/TK0/UMS/02/11 and Universiti Malaysia Sabah (UMS) through the Geran Bantuan Penyelidikan Pascasiswazah (UMSGreat)GUG0555-1/2022.

Conflicts of Interest

The authors declare no potential conflict of interest with respect to the research and publication of this article.

References

1. Mansor, M. N. A.; Siang, L. C.; Ahwang, A.; Saadun, M. A.; Dumatin, J. Vulnerability study of existing buildings due to seismic activities in Sabah. *International Journal of Civil Engineering and Geo-Environmental* **2017**, Special Publication for NCWE 2017.
2. Tongkul, F. Active tectonics in Sabah - seismicity and active faults. *Bulletin of the Geological Society of Malaysia* **2017**, *64*, 27-36. https://doi.org/10.7186/bgsm64201703
3. JMG, Seismic Hazard Map of Malaysia, Putrajaya, Malaysia: *Minerals and Geoscience Department*, **2018**.
4. Tongkul, F. An overview of earthquake science in Malaysia. *ASM Science Journal* **2021**, *14*, 1-12. https://doi.org/10.32802/asmscj.2020.440
5. Harith, N.S.H.; Tongkul F.; Adnan A. Seismic hazard curve as dynamic parameters in earthquake building design for Sabah, Malaysia, *Buildings* **2023**, *13(2)*, 318-334. https://doi.org/10.3390/buildings13020318
6. Tongkul, F. Earthquake science in Malaysia: Status, challenges and way forward. *Universiti Malaysia Sabah* **2020**.
7. Estêvão J. M.; Carvalho, A. The role of source and site effects on structural failures due to Azores earthquakes. *Engineering Failure Analysis* **2015**, *56*, 429-440. https://doi.org/10.1016/j.engfailanal.2014.12.010
8. Maio, R.; Estêvão, J. M.; Ferreira T. M.; Vicente, R. The seismic performance of stone masonry buildings in Faial Island and the relevance of implementing effective seismic strengthening policies. *Engineering Structures* **2017**, *141*, 41-58. https://doi.org/10.1016/j.engstruct.2017.03.009
9. Leslie, R.; Naveen, A. A study on pushover analysis using capacity spectrum method based on Eurocode 8, 16th World Conference on Earthquake Engineering, Chile, **2017**.
10. Douglas, J.; Seyedi, D. M.; Ulrich, T.; Modaressi, H.; Foerster, E.; Pitilakis, K.; Pitilakis, D.; Karatzetzou, A.; Gazetas, G.; Garini, E.; Loli, M. Evaluation of seismic hazard for the assessment of historical elements at risk: description of input and selection of intensity measures. *Bulletin of Earthquake Engineering* **2015**, *13*, 49-65. https://doi.org/10.1007/s10518-014-9606-0
11. MS EN 1998-1-1:2015, Malaysian National Annex to Eurocode 8: Design of structures for earthquake resistance Part 1: General rules, seismic actions, and rules for buildings, Kuala Lumpur, Malaysia: *Department of Standards Malaysia* **2017**; *1*.

12. Golutin, B. Seismic hazard map of Malaysia, Putrajaya, Malaysia: *Department of Mineral and Geoscience Malaysia*, **2017**.
13. EN 1992-1-1 (English): Eurocode 2: Design of concrete structures - Part 1-1: General rules and rules for buildings **2004**, 1-227.
14. EN 1998-1 (English): Eurocode 8: Design of structures for earthquake resistance – Part 1: General rules, seismic actions and rules for buildings **2004**, 1-231.
15. ATC-40, Seismic Evaluation and Retrofit of Concrete Buildings, Redwood, California: Applied Technology Council **1996**, *40*.
16. Harith, N. S. H.; Jainih, V.; Ladin, L. A.; Adiyanto, M. I. Assessing the vulnerability of Kota Kinabalu buildings, *Civil Engineering Architecture* **2021**, *9(5A)*, 68-77. https://doi.org/10.13189/cea.2021.091308
17. Abd-Elhamed, A.; Mahmoud, S. Nonlinear static analysis of reinforced concrete framed buildings - a case study on Cairo earthquake, *Journal of Engineering Research* **2016**, *4(4)*, 1-23.
18. Dya, A. F. C.; A. Oretaa, W. C. Seismic vulnerability assessment of soft story irregular buildings using pushover analysis. *Procedia Engineering* **2015**, *125*, 925-932. https://doi.org/10.1016/j.proeng.2015.11.103
19. Wooi Choi; Jae-Woo Park; Jinhwan Kim. Loss assessment of building and contents damage from the potential earthquake risk in Seoul, South Korea. *Natural Hazards and Earth System Sciences* **2019**, *19*, 985–997,
20. Atul; Sekar, S.K. Performance Based Design of Highrise Steel Structure Using Buckling Restrained Braces, International Conference on Sustainable Environment & Civil Engineering (ICSECE'19), Easwari Engineering College, Chennai, Tamilnadu-600 089, INDIA, 28-29 March **2019**, 173-181.
21. Alashker, Y.; Nazar, S.; Ismaiel, M. Effects of building configuration on seismic performance of RC buildings by pushover analysis. *Open Journal of Civil Engineering* **2015**, *5(2)*, 203-213. https://doi.org/10.4236/ojce.2015.52020
22. Maske, A. A.; Maske, N. A.; Shiras, P. P. Pushover analysis of reinforced concrete frame structures: a case study. *International Journal of Advanced Technology in Engineering and Science* **2014**, *2*, 118-128.
23. Yadav, R.; Gupta, T.; Sharma, R. K. Performance levels of RC structures by non-linear pushover analysis. *Journal of Engineering Research and Application* **2017**, *7(4)*, 1-8.
24. Ismaeil, M. Seismic capacity assessment of existing RC building by using pushover analysis. *Civil Engineering Journal* **2018**, *4(9)*, 2034-2043. https://doi.org/10.28991/cej-03091136

Sustainable Engineering

Review
Volume 1, Issue 1, 2024
https://doi.org/10.51200/susten.v1i1.5259

A Review on Utilising Combined Agricultural Waste Adsorbents for Ammonia Nitrogen Removal: Insights into Bamboo Biochar and Empty Fruit Bunch

Mariani Rajin*, Abu Zahrim Yaser and Dania Hazirah Rahman

Chemical Engineering Programme, Faculty of Engineering, Universiti Malaysia Sabah,
Jalan UMS, Kota Kinabalu, 88400, Malaysia.

*Correspondence: mariani@ums.edu.my *Scopus Author ID : 14034478400
Received: 15 July 2024, Accepted:03 September 2024

Abstract: This review highlights the effectiveness of bamboo biochar and empty fruit bunch (EFB) fibres as low-cost adsorbents for ammonia nitrogen removal from wastewater. Both materials are highlighted for their abundant availability and substantial adsorption capabilities. Bamboo biochar, derived from pyrolysed bamboo, benefits from its high surface area and porosity, enhanced further through chemical activation that increases its functional groups and pore structure. This modification significantly improves its efficiency in adsorbing ammonia nitrogen. Similarly, EFB, a by-product of palm oil production, is treated through carbonisation and activation, which enhances its adsorption properties. The review also discusses the potential for combining bamboo biochar and EFB, as their complementary properties could offer a more effective solution for wastewater treatment. The paper emphasises the advantages of these materials in addressing environmental challenges and highlights the need for further research into their combined use, as well as their potential for reuse and regeneration to promote sustainability. This review provides insights into optimising adsorbent modifications and exploring practical applications in wastewater treatment.

Keywords: Bamboo biochar; Modified empty fruit bunch; Combined adsorbent; Ammonia nitrogen Adsorption; Wastewater

1. Introduction

Wastewater is considered one of the primary contributors to water pollution. Human activities have led to the unavoidable production of waste, and a portion of this waste ends up as wastewater. The amount and type of waste produced vary depending on people's lifestyle, behaviour, and surrounding condition. The design of the sewer system plays a notable role in the composition of wastewater[1]. The urban drainage system is made up of a series of sewer networks that transport urban wastewater and rainwater to one or more terminal sites. Some of the wastewater discharged from the combined systems is released into local water bodies, sometimes without treatment [1]. Moreover, urbanization is rapidly increasing in many cities, leading to more frequent storm events due to climate change. Consequently, existing combined sewer systems in these cities are often unable to transport all rainwater and wastewater to treatment plants during periods of high-intensity rainfall. As a result, certain area experience flooding, and combined sewer overflows (CSOs) leak untreated water into the environment [2]. This has heightened societal concerned about environmental protection,

particularly water management in metropolitan areas, and growing the demand for access to clean drinking water [3-4].

There are many constituents that can be found in wastewater including debris, grease and grit, bacteria, nitrogen, ammonia, and metals [1]. When these contaminants are released into the environment through wastewater discharge, they can have harmful effects on both the environment and human health. Ammonia is an essential component in biological wastewater treatment because bacteria need it to create proteins, including enzymes for breaking down food and producing energy. However, in drainage system, the concentration of ammonia nitrogen should not be high due to various ecological problems [5]. Despite this, waste discharged from urban housing into urban drainage systems often contains high levels of ammonia, which is concerning as it can be released into rivers or other waterways. Excessive amount of ammonia nitrogen in water bodies can lead to environmental disruption, including the depletion of dissolved oxygen, eutrophication and toxicity to aquatic life [6]. Therefore, effective ways to remove ammonia nitrogen in water need to be developed, to improve the quality and sustainability of the environment.

Wastewater can be treated using various methods such as chemical precipitation, membrane filtration, reverse osmosis, ion exchange, and adsorption [7]. However, some of these approaches are considered limiting due to their significant capital and operational expenses, as well as the generation of secondary wastes that pose additional treatment challenges. Currently, researchers have studied several methods, both traditional and conventional, to remove ammonia nitrogen contamination from water, including chemical precipitation [8], biological treatment [9], air stripping [10-11], ion exchange [12-13], breakpoint chlorination [14], biological nitrification-denitrification [15-16] and adsorption [9]. Biological treatments are a classic way of eliminating ammonia from wastewater, but they have various drawbacks, such as being rapidly inhibited by toxic shock, pH shifts, low dissolved oxygen, and low temperature. Kinidi et al. (2018) reported that ammonia removal through air stripping can remove up to 95.4% of the ammonia from wastewater [17]. However, the ammonia stripping has several disadvantages, including high operating and maintenance costs, fouling issues, sludge generation, and the emission of ammonia gas into the environment. Viotti et al. (2015) reported that the stripper efficiency decreases from 98% to 80% over six months of usage [18]. Hence, among all the mentioned techniques, adsorption has been proven to be the best treatment method based on previous studies as it is cost-effective, simple to operate and eco-friendly. The adsorption process occurs when a solute in phase of gas or liquid accumulates on the surface of the adsorbent, forming an atomic or molecular film known as adsorbate. Purification, catalytic reaction and bulk separation processes benefit the most from adsorption due to its high efficiency of separation and mild operating conditions [19].

In adsorption, adsorbents are used to help remove the pollutants from wastewater. Many adsorbents effective in removing contaminants from wastewater system, including carbons, zeolites, aluminas, and silica gels [20]. However, the cost of these conventional absorbent is high, which limits the usage of adsorption in wastewater treatment applications. Consequently, research to identify effective and affordable adsorbents have been gradually increasing, as these are more economically feasible, readily available, and environmentally friendly (20-21). One alternative adsorbent that is gaining attention among researchers is the

use of agricultural waste and natural materials as adsorbents [22-23]. Ali et al. (2012) reported that the removal of various organic pollutants by the natural materials and agricultural waste as adsorbent ranges from 80% to 99.9% [24]. Bamboo charcoal, with its outstanding features such as high surface area, high porosity, and enriched surface functional groups, have shown enormous potential for various applications [25]. It also has considerable capability for removing pollutants from wastewater [26]. In addition, EFB fibres have been reported to be effective adsorbents for the removal of ammonia nitrogen, colour, and nutrients [6,27]. Demirak et al. (2015) observed that modifying agricultural waste can break the lignin structure, leading to increase in ammonia nitrogen removal [28]. A multi-adsorbent systems has also been gaining attention as it is reported to exhibit higher adsorption rates [29]. Based on previous research, no studies currently report that these systems have a lower adsorption rate compared to single adsorbent systems. The adsorbents in multi-adsorbent systems are either combined, mixed or hybridised, depending on the physical characteristics of the adsorbent used.

1.1 Types of adsorbent

Adsorbent are materials that adsorbs other substances through adsorption. There are two types of adsorbents: natural and synthetic [30]. Natural adsorbents are generally inexpensive, abundant, and offer great flexibility for modification and improvement to enhance their adsorption capabilities [31]. Synthetic adsorbents, on the other hand, are typically prepared from various types of waste materials [31]. Each adsorbent has unique characteristics that aid in removal of the contaminants. Adsorbents can also be derived from agricultural waste, including shells and stones of nuts and fruits, as well as waste from food industry processing, such as rice husks, sugarcane and bagasse [32-35]. In recent decades, agricultural waste has increasingly been used as an adsorbent in water treatment procedures, utilising materials like fruit shells and stones and waste from cereal production [36-39]. These materials can be used in their natural state or modified physically and chemically [40]. To enhance the adsorption effectiveness of adsorbates, these adsorbents can be blended, mixed, or hybridised.

Hammanini et al. (2007) reported that the physicochemical properties of adsorbents can be affected by the characteristics of the solution in which they are used [41]. Factors such as pH, concentration, ionic strength, the presence of anions, and other variables all play a role in the adsorption process [41-43]. Thus, this method is particularly convenient for immobilising ions in dilute solutions, such as wastewater [44]. Nevertheless, the most important property of an efficient adsorbent for pollutant removal is its porous structure. Good porous structure equates to high surface area, which results in high adsorption rate. Additionally, the time required to reach adsorption equilibrium should be as short as possible, allowing the adsorbent to remove contaminants quickly [45]. Furthermore, the capacity of the adsorbents to accumulate pollutants within the given time frame is also important.

Given the diverse range of adsorbents available, the cost-effectiveness and environmental impact of these materials are critical considerations. This has led to a growing interest in low-cost adsorbents derived from natural and waste materials, which offer a sustainable alternative for wastewater treatment.

https://doi.org/10.51200/susten.v1i1.5259

1.2 Low-cost adsorbent

As previously mentioned, the use of waste products as an adsorbent is gaining popularity, particularly in wastewater treatment, primarily due to their low cost. Natural materials such as wood or peat, wastes or by-products from the industrial, agricultural, or residential sectors, like bagasse and ash, can all be categorised as low-cost adsorbents, whether organic or inorganic in nature [44]. The availability, high efficiency, easy handling, and low cost of low-cost adsorbents make them ideal for use in large-scale industrial operations and farm waste management [46]. Many studies conducted over the last decade have found that many agricultural by-products and industrial wastes are low in price or have no economic value [44]. Waste such as rice husks, peanut skins, leaves, coffee and tea waste, onion and orange peels, and many other materials have shown potential as low-cost adsorbents [47-49]. Table 1 shows various studies and research on low-cost materials used as adsorbents, either in laboratory scale or in industry, for adsorbate removal. Most of these waste materials, which are rich in lignin, cellulose and tannin are produced in large volumes and face disposal problems. Hence, their abundance and availability make them a good source of raw material for producing activated carbon, a popular adsorbent for substance removal in wastewater treatment.

Table 1. Adsorption capacities of low-cost adsorbent from agricultural waste

Adsorbent material	Adsorbates	Adsorption / Removal capacity	Reference
Wheat bran	Cadmium	87.15%	[49]
Tea waste	Copper and lead	48 mg/g – 65 mg/g	[50]
Orange peels	Nickel	96%	[51]
Banana peel	Cadmium	35.53 mg/g	[52]
Banana peel	Cr(VI)	131.56 mg/g	[53]
Langsat Peel	Ammonia Nitrogen	28.67 %	[54]
Watermelon Rinds	Ammonia Nitrogen	4.62 mg/g	[20]
Banana Stalk	Pb (II)	13.53	[55]

While low-cost adsorbents provide an economical solution, their individual performance can sometimes be limited. To enhance their efficiency, researchers are increasingly exploring hybrid and combined adsorbent systems, which leverage the complementary properties of different materials to achieve superior adsorption results.

1.3 Hybrid and combined adsorbents in wastewater treatment

Numerous studies have focused on development and modification of adsorbents for wastewater treatment, particularly low-cost adsorbents. However, the application of mixed, combined or even hybrid forms of these low-cost adsorbents in a single system is still new and is growing among researches. This combined or hybrid adsorbent system is also known as the multi-system adsorbent, where different type of adsorbent materials are combined or hybridised to form a new class of adsorbent. The difference between hybrid and combined adsorbent is that hybrid adsorbent undergoes hybridisation where different adsorbent materials are merged into a single system, and once hybridised, the materials cannot return to

its original form. In contrast, combined adsorbent are materials that are simply combined into one system without the requirement of changing their chemical or physical originality. Hence, the materials can be easily recovered and recycled, as there is no chemical or physical attachment between them.

There are only few studies that research multi-adsorbent systems for the adsorption of pollutants and contaminants. Albadarin et al. (2014) used a mixture of tea waste and dolomite as an adsorbent to remove copper and methylene blue from aqueous solutions [56]. Tea waste (TW), dolomite (DO), and a mixture of TW-DO were used as adsorbents in six different sets of experiments. The purpose of the experiment was to see how contact time, pH, and the adsorption isotherms of the adsorbents influenced the outcomes. According to the findings, the highest adsorption capacity of tea waste with dolomite as an adsorbent was 150.4 mg/g. As a result, they discovered that tea waste and dolomite were both capable of extracting copper and methylene blue from aqueous solutions. On the other hand, Tuna et al. (2013) used hybrid apricot stone activated carbon with iron oxides to remove arsenic [58]. The hybrid was able to produce Iron-Activated Carbon (IAC) by precipitating iron salts with activated carbon [58-59]. The IAC adsorbent was then added at a mass ratio of 2:1 to a solution containing 0.3 M Fe^{3+} ($FeCl_3.6H_2O$) or Fe^{2+} ($FeCl_2.4H_2O$) ions. After some further mixing, washing, and drying, a hybrid IAC-Fe (II) or IAC-Fe (III) adsorbent emerged. The author highlighted in their study that hybrid adsorbents were able to achieve higher adsorption efficiency for the removal of arsenic compared to activated carbon [58].

Table 2 shows existing studies of combined or hybrid adsorbent from different agricultural wastes for the removal of different types of pollutants. It is concluded that multi-adsorbents may be more efficient at removing pollutants or contaminants from wastewater than using single adsorbents. Since bamboo biochar and modified EFB show effective removal rate, combining them may be more practical as an adsorbent in wastewater treatment. Apart from that, bamboo and EFB are abundant, grow abundantly and are relatively cheap. Moreover, both shows high carbon, lignin and cellulose content which makes them good choice of adsorbent. Furthermore, both adsorbent show effective adsorption for different types of adsorbates and modifications of both show increases in adsorption capacity [60-62].

https://doi.org/10.51200/susten.v1i1.5259

Table 2. Adsorption capacities of combined, mixed and hybrid adsorbents

Combined/Hybrid Adsorbents	Pollutants	Adsorption Capacity (mg/g)	Reference
Tea waste and dolomite	Copper and methylene blue	150.4	[56]
Coconut mesocarp, sawdust and termite nest	Cadmium and lead ions	138.9	[63]
Waste tea and coffee	Copper, zinc, cadmium and lead ions	0.528	[64]
Apricot stone and iron oxides	Arsenic	2.023 – 3.009	[57]
Dried pinecone and sodium alginate	Copper and nickel ions	112 – 156	[65]
Bamboo waste and iron	Arsenic	0.019 – 0.027	[66]
Mixed recyclable waste and ionic liquid	Mercury	124	[67]

While hybrid and combined adsorbent systems offer significant potential for improving wastewater treatment efficiency, the practical application of such systems can be further explored through specific materials. In this context, the potential of bamboo biochar and empty fruit bunches as effective adsorbents is presented in the following section, highlighting their unique properties and advantages in the combined adsorbent approach for ammonia nitrogen removal.

2. Potential of Bamboo Biochar and Empty Fruit Bunch as Materials for Combined Adsorbent

Both bamboo biochar and modified empty fruit bunch (EFB) are chosen as they have potential to be combined as an embedded multi adsorbent system. This is mainly due to their characteristics and ability to adsorb ammonia nitrogen especially as both are commonly used as adsorbents for ammonia nitrogen removal as shown in Table 3. On top of that, both of these materials are categorised as good sources of material to be chosen as adsorbents due to their unlimited supply, abundant growth and relatively low cost.

Biochar is a carbon-enriched substance that can be obtained from a combination of renewable and waste sources, such as trees and agricultural residue, industrial by-products and municipal solid waste under restricted oxygen conditions via pyrolysis [68-69]. Chemical activation is a key method used to improve its adsorption properties. For example, bamboo biochar is often treated with potassium hydroxide (KOH) or phosphoric acid (H_3PO_4) to increase its surface area and pore volume. These chemical treatments create additional porosity and introduce functional groups such as hydroxyl, carboxyl, and lactone groups on the biochar's surface. The increased surface area and additional functional groups enhance the material's capacity to interact with and adsorb ammonia nitrogen. The presence of these functional groups promotes better binding of ammonia through both physical adsorption and chemical interactions. Due to its outstanding features, including high surface area, high porosity, and enriched surface functional groups, biochar has shown enormous potential for a variety of applications [25].

Table 3. Adsorption studies of modified empty fruit bunch and bamboo biochar for ammonia nitrogen removal

Adsorbent	Adsorbate	Adsorption Capacity	Isotherm Model	Kinetic Model	Reference
Modified empty fruit bunch	Ammonia nitrogen	0.01 – 0.60 mg/g	n/a	n/a	[74]
Modified empty fruit bunch	Ammonia nitrogen	0.32 mg/g	n/a	n/a	[75]
Modified empty fruit bunch	Ammonia nitrogen	0.83 mg/g	n/a	n/a	[21]
Modified empty fruit bunch	Ammonia nitrogen	79.50 %	Langmuir	n/a	[27]
Modified empty fruit bunch	Ammonia nitrogen	0.56- 0.83 mg/g	Tempkin	Pseudo second order	[74]
Empty fruit bunch biochar	Ammonia nitrogen	0.46 – 2.49 mg/g	Freundlich	Pseudo second order	[76]
Unmodified empty fruit bunch	Ammonia nitrogen	n/a	Freundlich	Pseudo second order	[6]
Modified empty fruit bunch	Ammonia nitrogen	0.53 - 10.89 mg/g	n/a	N/a	[21]
Unmodified empty fruit bunch	Ammonia	n/a	Freundlich	Pseudo second order	[77]
Ball-milled bamboo biochar	Ammonia nitrogen	22.90 mg/g	Langmuir	Pseudo second order	[78]
Bamboo biochar	Ammonia nitrogen	7.00 mg/g	Langmuir	Pseudo second order	
Bamboo biochar	Ammonia nitrogen	6.38 mg/g	Freundlich	N/a	[79]
Hydrous bamboo biochar	Ammonia nitrogen	6.38 mg/g	Freundlich	Pseudo second order	[80]
Modified bamboo biochar	Ammonia nitrogen	12.60 mg/g	Langmuir	Pseudo second order	[81]
Unmodified bamboo biochar	Ammonia nitrogen	3.23 - 5.66 mg/g	Langmuir	Pseudo second order	
Unmodified bamboo charcoal	Ammonia	0.80 – 5.80 mg/g	n/a	n/a	[82]
Modified bamboo charcoal	Ammonia	0.90 - 9.50 mg/g	n/a	n/a	
Modified bamboo charcoal	Ammonia nitrogen	0.65 mg/g	Langmuir	n/a	[83]

In addition, empty fruit bunch (EFB) is also known as a carbon-rich substance that is produced during palm oil production. Previous research has found that the carbon content of EFB ranges from 40.93% to 68.3% [70-72]. As a result of its characteristics and availability, it is attracting research interest in adsorption investigations. However, the utilisation of EFB is a challenge as its processing cost is high and direct utilisation of raw EFB is time consuming at large scales [62]. Besides its high carbon content, the lignin and cellulose content of EFB also make it a good choice as an adsorbent. Furthermore, EFB's alkali nature allows it to adsorb cationic contaminants owing to electrostatic interaction [73]. Similarly, with bamboo, these characteristics of EFB make it a suitable adsorbent, and the effectiveness

of EFB also affected by its BET surface area, as high surface area corresponds to high adsorption capacities [62]. The authors also mention various research studies that reveal raw EFB's ability to remove dyes and heavy metals from aqueous solutions, as well as a limited investigation of EFB as an adsorbent, indicating a data gap in its potential.

Apart from that, both bamboo biochar and EFB have been proven to have good adsorption efficiency not only in ammonia removal but also for several other contaminants. Hence, the combination of these materials can be used universally to remove different types of contaminants instead of focusing only on ammonia nitrogen. For instance, several studies have shown that bamboo biochar can be used as an adsorbent to remove undesirable pollutants. Viglasova et al. (2020), for example, investigated the performance of biochar as a viable wastewater treatment option and linked nitrate sorption ability to the substance's features [81]. On top of that, Mohan et al. (2014), Tan et al. (2016) and Cha et al. (2016) in their past review articles have addressed and discussed the methods of decomposition and characterization of the biochar as well as its use in the removal of dye from different contaminants [84-86]. Another research by Wang et al. (2017) and Yang et al (2019) also suggested the pre-treatment and post-treatment properties of both feedstock and biochar respectively may also influence biochar properties [87-88]. Yang et al. (2004) used bamboo-derived biochar to examine the high potential of adsorption for the removal of metal-complex pigments in wastewater [71]. In the study, the equilibrium, kinetics and modelling of the artificial neural network were investigated using a biochar where it was generated by pyrolysis. Bamboo biochar is an efficient low-cost adsorbent for metal-complex removal from aqueous solutions, according to the findings. The adsorption capacity of the metal-complex, acid black 172, was unaffected by ionic strength throughout the experiment, and the kinetics investigation revealed that intraparticle transport was not the only rate-limiting phase. With a pH of 1.0, the adsorption capacity was found to be 401.88 mg/g [71].

Sajab et al. (2013) on the other hand, studied the ability of oil palm EFB to remove dyes from aqueous solution [89]. This study was conducted by pre-treating the EFB by sodium hydroxide (NaOH) first, and the pre-treatment EFB was modified by using citric acid (CA) (CA-EFB) and polyethylenimine (PEI) (PEI-EFB) to make it cationic and anionic adsorbent. The removal efficiency of CA-EFB and PEI-EFB was tested by using cationic methylene blue (MB) and anionic phenol red (PR) as adsorbate, at various pHs, temperatures and initial dye concentrations. The negative charges of CA-EFB increased with an increase in pH range from 3 to 7, meanwhile, the PEI-EFB was positive charge for the pH range. Thus, the different ion charges will attract one another, which suggests that MB and PR will attract to CA-EFB and PEI-EFB respectively. The study recorded that the maximum removal capacity of MB by using CA-EFB as adsorbent is 103.1 mg/g and 158.7 mg/g of maximum removal capacity of PR when using PEI-EFB adsorbent. The data of the experiment showed that the adsorption of MB onto CA-EFB and PR onto PEI-EFB fitted the Langmuir isotherm and Freundlich isotherm, respectively. This suggests different adsorption behaviours of dyes onto both adsorbents [89].

Most importantly, these materials have potential to be reused, recovered and regenerated. As the adsorbent used in this study are not physically or chemically combined, the chance for them to be reused again in the same form or regenerated and reused should be considered. On

top of that, both materials are commonly used as soil amendment or for potting media and for composting. Hence, this ability should not be taken for granted as it will help to reduce waste,promote circular economy, and introduce sustainability concepts. In addition, the concept of reuse, recovery and regeneration of waste have been gaining attention by researchers as it is a way of maintaining and sustaining our environment on top of growing our economy.

4. Conclusion and Future Perspectives

This review demonstrates that bamboo biochar and empty fruit bunch (EFB) fibres are promising, low-cost adsorbents for ammonia nitrogen removal from wastewater. Both materials exhibit significant adsorption capacities, which are notably enhanced through specific modifications. Combining these adsorbents could offer an even more effective solution, utilising their complementary properties to address ammonia nitrogen contamination more efficiently. Future research should focus on optimising these modifications to further enhance adsorption performance. Additionally, exploring the practical applications of combining bamboo biochar and EFB in wastewater treatment could yield valuable insights. The potential for reuse, recovery, and regeneration of these materials should be investigated to promote sustainability and circular economy practices. Addressing any limitations and understanding the interactions between different adsorbent materials will be crucial for developing effective and sustainable wastewater treatment solutions. Overall, the continued exploration of these materials holds promise for advancing environmental management and improving wastewater treatment technologies.

Acknowledgments

This project is financially supported by Skim Dana Inovasi (SGI0064-2018) from Universiti Malaysia Sabah (UMS).

References

1. Henze, M.; Comeau, Y. Wastewater Characterization. In Biological Wastewater Treatment: Principles, Modelling, and Design; Henze, M., van Loosdrecht, M. C. M., Lier, J. B. v., Ekama, G. A., Brdjanovic, D., Eds.; IWA Publishing: London, **2008**; pp 33–52.
2. Cembrano, G.; Quevedo, J.; Salamero, M.; Puig, V.; Figueras, J.; Martí, J. Optimal Control of Urban Drainage Systems: A Case Study. Control Engineering Practice 2004, 12(1), 1–9, https://doi.org/10.1016/S0967-0661(02)00280-0
3. Krebs, P.; Larsen, A. Guiding the Development of Urban Drainage Systems by Sustainability Criteria. *Water Sci. Technol*. **1997**, 35 (9), 89–98, https://doi.org/10.1016/S0273-1223(97)00187-X
4. Price, R. K. Hydroinformatics and Urban Drainage: An Agenda for the 21st Century. *J. Hydroinformatics* **2000**, 2 (2), 133–147, https://doi.org/10.2166/hydro.2000.0011
5. Seruga, P.; Krzywonos, M.; Pyżanowska, J.; Urbanowska, A.; Pawlak-Kruczek, H.; Niedźwiecki, Ł. Removal of Ammonia from Municipal Wastewater Treatment Effluents Using Natural Minerals. *Molecules* **2019**, 24 (20), 3633., https://doi.org/10.3390/molecules24203633
6. Zahrim, A. Y.; Asis, T.; Hashim, M. A.; Al-Mizi, T. M. T. M. A.; Ravindra, P. A Review on the Empty Fruit Bunch Composting: Life Cycle Analysis and the Effect of Amendment(s). In Advances in Bioprocess Technology; Springer: Cham, **2015**; pp 3–15, https://doi.org/10.1007/978-3-319-17915-5_1.
7. Obotey Ezugbe, E.; Rathilal, S. Membrane Technologies in Wastewater Treatment: A Review. *Membranes* **2020**, 10 (5), 89, https://doi.org/10.3390/membranes10050089
8. Taddeo, R.; Prajapati, S.; Lepisto, R. Optimizing ammonium removal by natural zeolite from wastewater with high loads of ammonium and solids. *J. Porous Mater.* **2017**, 24, 1545–1554, https://doi.org/10.1007/s10934-017-0394-1

9. Chen, P.; Xie, Q.; Addy, M.; Zhou, W.; Liu, Y.; Wang, Y.; Cheng, Y.; Li, K.; Ruan, R. utilisation of municipal solid and liquid wastes for bioenergy and bioproducts production. *Bioresour. Technol.* **2016**, 215, 163–172, https://doi.org/10.1016/j.biortech.2016.02.094
10. Limoli, A.; Langone, M.; Andreottola, G. Ammonia removal from raw manure digestate by means of a turbulent mixing stripping process. *J. Environ. Manag.* **2016**, 176, 1–10, https://doi.org/10.1016/j.jenvman.2016.03.007
11. Liu, L.; Pang, C.; Wu, S.; Dong, R. optimization and evaluation of an air-recirculated stripping for ammonia removal from the anaerobic digestate of pig manure. *Process Saf. Environ. Prot.* **2014**, 94, 350–357, https://doi.org/10.1016/j.psep.2014.08.006
12. Jorgensen, T.C.; Weatherley, L.R. Ammonia removal from wastewater by ion exchange in the presence of organic contaminants. *Water Res.* **2003**, 37, 1723–1728, https://doi.org/10.1016/S0043-1354(02)00571-7
13. Rahmani, A.R.; Mahvi, A.H.; Mesdaghinia, A.R.; Nasseri, S. Investigation of ammonia removal from polluted waters by Clinoptilolite zeolite. *Int. J. Environ. Sci. Technol.* **2004**, 1, 125–133, https://doi.org/10.1007/BF03325825
14. Zaghouane-Boudiaf, H.; Boutahala, M. Kinetic analysis of 2,4,5-trichlorophenol adsorption onto acid-activated montmorillonite from aqueous solution. *Int. J. Miner. Process.* **2011**, 100, 72–78, https://doi.org/10.1016/j.minpro.2011.04.011
15. Karadag, D.; Koc, Y.; Turan, M.; Armagan, B. Removal of ammonium ion from aqueous solution using natural Turkish clinoptilolite. *J. Hazard Mater.* **2006**, 136, 604–609, https://doi.org/10.1016/j.jhazmat.2005.12.042
16. Wu, Z.; An, Y.; Wang, Z.; Yang, S.; Chen, H.; Zhou, Z.; Mai, S. Study on zeolite enhanced contact–adsorption regeneration–stabilization process for nitrogen removal. *J. Hazard Mater.* **2008**, 156, 317–326, https://doi.org/10.1016/j.jhazmat.2007.12.029
17. Kinidi, L.; Lennevey, I. A. W.; Tan, N. B. A. W.; Tamrin, K. F. B.; Hipolito, C. N.; Salleh, S. F. Recent Development in Ammonia Stripping Process for Industrial Wastewater Treatment. *Int. J. Chem. Eng.* **2018**, Article 3181087, .https://doi.org/10.1155/2018/3181087
18. Viotti, P.; Gavasci, R. Scaling of Ammonia Stripping Towers in the Treatment of Groundwater Polluted by Municipal Solid Waste Landfill Leachate: Study of the Causes of Scaling and Its Effects on Stripping Performance. *Rev. Ambiente Água* **2015**, 10, 240–252. https://doi.org/10.4136/ambi-agua.1567
19. Bono, A.; Sarbatly, R.; Krishnaiah, D.; San, P. M.; Yan, F. Y. Effect of Ultrasound on Liquid Phase Adsorption of Azeotropic and Non-Azeotropic Mixtures. *Catal. Today* **2008**, 131, 472–476., https://doi.org/10.1016/j.cattod.2007.10.084
20. Zahrim, A. Y.; Ali, R. S.; Hilal, N.; Tamrin, K. F. Fruit Waste Adsorbent for Ammonia Nitrogen Removal from Synthetic Solution: Isotherms and Kinetics. *IOP Conf. Ser.: Earth Environ. Sci.* **2016**, 36, 012028, https://doi.org/10.1088/1755-1315/36/1/012028
21. Zahrim, A. Y.; Ricky, L. N. S.; Hilal, N.; Tamrin, K. F. Ammonia-Nitrogen Recovery from Synthetic Solution Using Agricultural Waste Fibres. *Indian J. Sci. Technol.* **2017**, 10, 1–5, https://doi.org/10.17485/ijst/2017/v10i6/111221
22. Chan, B. K. C.; Bouzalakos, S.; Dudeney, A. W. L. Integrated Waste and Water Management in Mining and Metallurgical Industries. Trans. Nonferrous Met. Soc. China **2008**, 18, 1497–1505, https://doi.org/10.1016/S1003-6326(09)60032-7
23. Singh, R. P.; Ibrahim, M. H.; Esa, N.; Iliyana, M. S. Composting of Waste from Palm Oil Mill: A Sustainable Waste Management Practice. *Rev. Environ. Sci. Bio/Technol.* **2010**, 9, 331–344. . https://doi.org/10.1007/s11157-010-9199-2
24. Ali, I.; Asim, M.; Khan, T. A. Low-Cost Adsorbents for the Removal of Organic Pollutants from Wastewater. *J. Environ. Manage.* **2012**, 113, 170–183, https://doi.org/10.1016/j.jenvman.2012.08.028
25. Li, Y.; Liu, Y.; Yang, W.; Liu, L.; Pan, J. Adsorption of Elemental Mercury in Flue Gas Using Biomass Porous Carbons Modified by Microwave/Hydrogen Peroxide. *Fuel* **2021**, 291, 120152, https://doi.org/10.1016/j.fuel.2021.120152
26. Wang, B. Q.; Peng, B.; Sun, J. F.; Wang, C.; Jiang, K.; Ma, J. H.; He, Y. C. Pretreatment of Bamboo Shoot Shell with Surfactant OP-10 in Acidified Media for Enhancing the Biosynthesis of Ethyl (S)-4-Chloro-3-Hydroxybutanoate. *Bioresour. Technol. Rep.* **2019**, 5, 74–79, https://doi.org/10.1016/j.biteb.2018.12.004
27. Nasir, N.; Daud, Z.; Awang, H.; Ab Aziz, N. A.; Ahmad, B.; Ridzuan, M. B.; et al. Utilisation of Empty Fruit Bunch Fibre as Potential Adsorbent for Ammonia Nitrogen Removal in Natural Rubber Wastewater. *Int. J. Integr. Eng.* **2018**, 10 (8), 27–32, https://doi.org/10.30880/ijie.2018.10.08.009
28. Demirak, A.; Keskin, F.; Şahin, Y.; Kalemci, V. Mugla *J. Sci. Technol.* **2015**, 5, 5–12., https://doi.org/10.22531/muglajsci.209992

29. Safie, N. N.; Zahrim, Y. A.; Hilal, N. Ammonium Ion Removal Using Activated Zeolite and Chitosan. *Asia-Pac. J. Chem. Eng.* **2020**, 15, e2448, https://doi.org/10.1002/apj.2448
30. De Gisi, S.; Lofrano, G.; Grassi, M.; Notarnicola, M. Characteristics and Adsorption Capacities of Low-Cost Sorbents for Wastewater Treatment: A Review. Sustainable *Mater. Technol.* **2016**, 9, 10–40, https://doi.org/10.1016/j.susmat.2016.06.002
31. Rashed, M. N. Adsorption Technique for the Removal of Organic Pollutants from Water and Wastewater. Organic Pollutants: Monitoring, Risk and Treatment 2013, 7, 167–194, https://doi.org/10.5772/54048
32. Bandura, L.; Woszuk, A.; Kołodyńska, D.; Franus, W. Application of Mineral Sorbents for Removal of Petroleum Substances: A Review. *Minerals* **2017**, 7 (3), 37, https://doi.org/10.3390/min7030037
33. Crini, G.; Lichtfouse, E.; Wilson, L. D.; Morin-Crini, N. Adsorption-Oriented Processes Using Conventional and Non-Conventional Adsorbents for Wastewater Treatment. In Green Adsorbents for Pollutant Removal; Lichtfouse, E.; Crini, G., Eds.; Springer: Cham, **2018**; pp 23–71, https://doi.org/10.1007/978-3-319-92111-2_2
34. Crini, G.; Lichtfouse, E., Eds. Sustainable Agriculture Reviews 36: Chitin and Chitosan: Applications in Food, Agriculture, Pharmacy, Medicine and Wastewater Treatment; Vol. 36; Springer: Cham, **2019**.
35. Ahmadpour, A.; Do, D. D. The Preparation of Activated Carbon from Macadamia Nutshell by Chemical Activation. *Carbon* **1997**, 35, 1723–1732, https://doi.org/10.1016/S0008-6223(97)00127-9
36. Tsai, W. T.; Chang, C. Y.; Lee, S. L. A Low Cost Adsorbent from Agricultural Waste Corn Cob by Zinc Chloride Activation. *Bioresource Technology* **1998**, *64*, 211-217, https://doi.org/10.1016/S0960-8524(97)00168-5
37. Nyazi, K.; Yaacoubi, A.; Baçaoui, A.; Bennouna, C.; Dahbi, A.; Rivera-Utrilla, J.; Moreno-Castilla, C. Preparation and Characterization of New Adsorbent Materials from the Olive Wastes. In Journal de Physique IV (Proceedings); EDP Sciences: **2005**; Vol. 123, pp 121–124, https://doi.org/10.1051/jp4:2005123020
38. Namasivayam, C.; Sangeetha, D. Recycling of Agricultural Solid Waste, Coir Pith: Removal of Anions, Heavy Metals, Organics, and Dyes from Water by Adsorption onto ZnCl2 Activated Coir Pith Carbon. *Journal of Hazardous Materials* **2006**, 135, 449–452, https://doi.org/10.1016/j.jhazmat.2005.11.066
39. Elizalde-González, M. P.; Mattusch, J.; Wennrich, R. Chemically Modified Maize Cobs Waste with Enhanced Adsorption Properties upon Methyl Orange and Arsenic. *Bioresource Technology* **2008**, 99, 5134-5139, https://doi.org/10.1016/j.biortech.2007.09.023
40. Bhatnagar, A.; Sillanpää, M. Utilisation of Agro-Industrial and Municipal Waste Materials as Potential Adsorbents for Water Treatment-A Review. *Chemical Engineering Journal* **2010**, 157, 277–296, https://doi.org/10.1016/j.cej.2010.01.007
41. Hammanini, A.; Gonzaliz, A. F.; Ballester, A.; Bakzaquez, M. L.; Muniz, J. A. Bioadsorption of Heavy Metals by Activated Sludge and Their Desorption Characteristics. *J Environ Manage.* **2007,** 84, 419- 426, https://doi.org/10.1016/j.jenvman.2006.06.015
42. Schiewer, S.; Volesky, B. Ionic Strength and Electrostatic Effects in Biosorption of Divalent Metal Ions and Protons. *Environ. Sci. Technol.* **1997**, *31*, 2478-2485, https://doi.org/10.1021/es960751u
43. Pagnanelli, F.; Petrangeli Papini, M.; Toro, L.; Trifoni, M.; Veglio, F. Biosorption of Metal Ions on Arthrobacter sp.: Biomass Characterization and Biosorption Modeling. *Environ. Sci. Technol.* **2000**, 34, 2773-2778, https://doi.org/10.1021/es991271g
44. Božić, D.; Stanković, V.; Gorgievski, M.; Bogdanović, G.; Kovačević, R. Adsorption of Heavy Metal Ions by Sawdust of Deciduous Trees. *J. Hazard. Mater.* **2009**, 171, 684-692, https://doi.org/10.1016/j.jhazmat.2009.06.055
45. Gupta, V. K.; Jain, R.; Shrivastava, M.; Nayak, A. Equilibrium and Thermodynamic Studies on the Adsorption of the Dye Tartrazine onto Waste "Coconut Husks" Carbon and Activated Carbon. *J. Chem. Eng. Data* **2010**, 55,5083-5090, https://doi.org/10.1021/je100649h
46. Mata, Y. N.; Blázquez, M. L.; Ballester, A.; González, F.; Muñoz, J. A. Sugar-Beet Pulp Pectin Gels as Biosorbent for Heavy Metals: Preparation and Determination of Biosorption and Desorption Characteristics. *Chem. Eng. J.* **2009**, 150, 289-301, https://doi.org/10.1016/j.cej.2009.01.001
47. Gaballah, I.; Kilbertus, G. Recovery of Heavy Metal Ions through Decontamination of Synthetic Solutions and Industrial Effluents Using Modified Barks. *J. Geochem. Explor.* **1998**, 62, 241-286, https://doi.org/10.1016/S0375-6742(97)00068-X
48. Febrianto, J.; Kosasih, A. N.; Sunarso, J.; Ju, Y. H.; Indraswati, N.; Ismadji, S. Equilibrium and Kinetic Studies in Adsorption of Heavy Metals Using Biosorbent: A Summary of Recent Studies. *J. Hazard. Mater.* **2009**,*162*, 616-645, https://doi.org/10.1016/j.jhazmat.2008.06.042
49. Singh, K. K.; Singh, A. K.; Hasan, S. H. Low Cost Bio-Sorbent 'Wheat Bran' for the Removal of Cadmium from Wastewater: Kinetic and Equilibrium Studies. *Bioresour. Technol.* **2006**, *97*, 994-1001, https://doi.org/10.1016/j.biortech.2005.04.043

50. Amarasinghe, B. M. W. P. K.; Williams, R. A. Tea Waste as a Low Cost Adsorbent for the Removal of Cu and Pb from Wastewater. *Chem. Eng. J.* **2007**, 132, : 299-309, https://doi.org/10.1016/j.cej.2007.01.016
51. Ajmal, M.; Rao, R. A. K.; Ahmad, R.; Ahmad, J. Adsorption Studies on Citrus reticulata (Fruit Peel of Orange): Removal and Recovery of Ni(II) from Electroplating Wastewater. *J. Hazard. Mater*. **2000**, 79, 117-131, https://doi.org/10.1016/S0304-3894(00)00234-X
52. Memon, S. Q.; Memon, J. R.; Bhanger, M. I.; Khuhawar, M. Y. Banana Peel: A Green and Economical Sorbent for Cr(III) Removal. *Pakistan J. Anal. Environ. Chem.* **2008**, 9,1-6
53. Memon, J. R.; Memon, S. Q.; Bhanger, M. I.; El-Turki, A.; Hallam, K. R.; Allen, G. C. Banana Peel: A Green and Economical Sorbent for the Selective Removal of Cr(VI) from Industrial Wastewater. *Colloids Surf. B: Biointerfaces* **2009**,70, 232-237, https://doi.org/10.1016/j.colsurfb.2008.12.032
54. Azreen, I.; Lija, Y.; Zahrim, A. Y. Ammonia Nitrogen Removal from Aqueous Solution by Local Agricultural Wastes. *IOP Conf. Ser.: Mater. Sci. Eng.* **2017**, 206, 012077. https://doi.org/10.1088/1757-899X/206/1/012077
55. Ogunleye, O. O.; Ajala, M. A.; Agarry, S. E. Evaluation of Biosorptive Capacity of Banana (Musa paradisiaca) Stalk for Lead (II) Removal from Aqueous Solution. *J. Environ. Prot.* **2014**,5, 1451-1465, https://doi.org/10.4236/jep.2014.515138
56. Albadarin, A. B.; Mo, J.; Glocheux, Y.; Allen, S.; Walker, G.; Mangwandi, C. Preliminary Investigation of Mixed Adsorbents for the Removal of Copper and Methylene Blue from Aqueous Solutions. *Chem. Eng. J.* **2014**, 255, 525-534, https://doi.org/10.1016/j.cej.2014.06.029
57. Tuna, A. Ö. A.; Özdemir, E.; Bilgin Simsek, E.; Beker, U. Optimization of Process Parameters for Removal of Arsenic Using Activated Carbon-Based Iron-Containing Adsorbents by Response Surface Methodology. *Water, Air, Soil Pollut.* **2013**, 224, 1-15, https://doi.org/10.1007/s11270-013-1685-z
58. Zhang, Q. L.; Gao, N. Y.; Lin, Y. C.; Xu, B.; Le, L. S. Removal of Arsenic (V) from Aqueous Solutions Using Iron-Oxide-Coated Modified Activated Carbon. *Water Environ. Res.* **2007**, 79 (8), 931-936, https://doi.org/10.2175/106143007X156727
59. Joshi, S.; Sharma, M.; Kumari, A.; Shrestha, S.; Shrestha, B. Arsenic Removal from Water by Adsorption onto Iron Oxide/Nano-Porous Carbon Magnetic Composite. *Appl. Sci.* **2019**, 9, 3732. https://doi.org/10.3390/app9183732
60. Liu, Q. S.; Zheng, T.; Wang, P.; Guo, L. Preparation and Characterization of Activated Carbon from Bamboo by Microwave-Induced Phosphoric Acid Activation. *Ind. Crops Prod*. **2010**, 31, 233-238, https://doi.org/10.1016/j.indcrop.2009.10.011
61. Mahanim, S. M. A.; Wan Asma, I.; Rafidah, J.; Puad, E.; Shaharuddin, H. Production of Activated Carbon from Industrial Bamboo Wastes. *J. Trop. For. Sci.* **2011**,4, 417-424.
62. Thoe, J. M. L.; Surugau, N.; Chong, H. L. Application of Oil Palm Empty Fruit Bunch as Adsorbent: A Review. *Trans. Sci. Technol.* **2019**, 6, 9-26.
63. Cunha, S.; Costa Rodrigues, M.; Reis Mattos, R.; Sena Gomes Teixeira, L.; Oliveira Santos, A.; Santos, E. V.; Souza, R. S.; dos Santos Andrade, G.; De Paula, R.; de Jesus, D. S. Avocado, Spent Coffee Grounds, Licuri and Coconut Milk for Oil Extraction, Biodiesel Production, and Spectral Analysis. *Quim. Nova* **2018**, 41, 691-698, https://doi.org/10.21577/0100-4042.20170213
64. Utomo, H. D.; Hunter, K. A. Adsorption of Divalent Copper, Zinc, Cadmium and Lead Ions from Aqueous Solution by Waste Tea and Coffee Adsorbents. *Environ. Technol.* **2006**, 27 (1), 25-32, https://doi.org/10.1080/09593332708618619
65. Biswas, S.; Siddiqi, H.; Meikap, B. C.; Sen, T. K.; Khiadani, M. Preparation and Characterization of Raw and Inorganic Acid-Activated Pine Cone Biochar and Its Application in the Removal of Aqueous-Phase Pb^{2+} Metal Ions by Adsorption. *Water Air Soil Pollut.* **2020**, 231, 1-17, https://doi.org/10.1007/s11270-019-4375-7
66. Moreno-Piraján, J.; Giraldo, L. Activated Carbon from Bamboo Waste Modified with Iron and Its Application in the Study of the Adsorption of Arsenite and Arsenate. *Open Chem.* **2013**, 11 (2), 160-170., https://doi.org/10.2478/s11532-012-0138-7
67. Habila, M. A.; AlOthman, Z. A.; Ghfar, A. A.; Al-Zaben, M. I.; Alothman, A. A. S.; Abdeltawab, A. A.; El-Marghany, A.; Sheikh, M. Phosphonium-Based Ionic Liquid Modified Activated Carbon from Mixed Recyclable Waste for Mercury (II) Uptake. *Molecules* **2019**, 24 (3), 570, https://doi.org/10.3390/molecules24030570
68. Zubair, M.; Ramzani, P. M. A.; Rasool, B.; Khan, M. A.; Akhtar, I.; Turan, V.; Tauqeer, H. M. Efficacy of Chitosan-Coated Textile Waste Biochar Applied to Cd-Polluted Soil for Reducing Cd Mobility in Soil and Its Distribution in Moringa (Moringa oleifera L.). *J. Environ. Manage.* **2021**, 284, 112047, https://doi.org/10.1016/j.jenvman.2021.112047

69. Wang, R. Z.; Huang, D. L.; Liu, Y. G.; Zhang, C.; Lai, C.; Zeng, G. M.; Cheng, M.; Gong, X. M.; Wan, J.; Luo, H. Investigating the Adsorption Behavior and the Relative Distribution of Cd^{2+} Sorption Mechanisms on Biochars by Different Feedstock. *Bioresour. Technol.* **2018**, 261, 265-271, https://doi.org/10.1016/j.biortech.2018.04.032
70. Idris, S. S.; Abd Rahman, N.; Ismail, K.; Alias, A. B.; Abd Rashid, Z.; Aris, M. J. Investigation on Thermochemical Behaviour of Low Rank Malaysian Coal, Oil Palm Biomass and Their Blends During Pyrolysis via Thermogravimetric Analysis (TGA). *Bioresour. Technol.* **2010**, 101, 4584-4592, https://doi.org/10.1016/j.biortech.2010.01.059
71. Yang, H.; Yan, R.; Chin, T.; Liang, D. T.; Chen, H.; Zheng, C. Thermogravimetric Analysis− Fourier Transform Infrared Analysis of Palm Oil Waste Pyrolysis. *Energy Fuels* **2004**, 18, 1814-1821. https://doi.org/10.1021/ef030193m
72. Nasir, N. H. M.; Ahmad Zaini, M. A.; Mohd Setapar, S. H.; Hassan, H. Removal of Methylene Blue and Copper (II) by Oil Palm Empty Fruit Bunch Sorbents. *J. Teknol.* **2015**, 74, https://doi.org/10.11113/jt.v74.4707
73. Arshadi, M.; Amiri, M. J.; Mousavi, S. Kinetic, Equilibrium and Thermodynamic Investigations of Ni (II), Cd (II), Cu (II) and Co (II) Adsorption on Barley Straw Ash. *Water Resour. Ind.* **2014**, 6, 1-17. https://doi.org/10.1016/j.wri.2014.06.001
74. Ricky, L. N. S.; Shahril, Y.; Nurmin, B.; Zahrim, A. Y. Ammonia-Nitrogen Removal from Urban Drainage Using Modified Fresh Empty Fruit Bunches: A Case Study in Kota Kinabalu, Sabah. *IOP Conf. Ser.: Earth Environ. Sci.* **2016**, 36, 012055. https://doi.org/10.1088/1755-1315/36/1/012055
75. Safie, N. N., Zahrim, A. Y., Rajin, M., Ismail, N. M., Saalah, S., Anisuzzaman, S. M., ... & Calvin, T. T. H. (2019, August). Adsorption of ammonium ion using zeolite, chitosan, bleached fibre and activated carbon. In IOP Conference Series: Materials Science and Engineering (Vol. 606, No. 1, p. 012003). IOP Publishing. https://doi.org/10.1088/1757-899X/606/1/012003
76. Ahmad, R.; Sohaimi, K. S. A.; Mohamed, A. R.; Zailani, S. N.; Salleh, N. H. M.; Azizan, N. H. Kinetic and Isotherm Studies of Empty Fruit Bunch Biochar on Ammonium Adsorption. IOP Conf. Ser.: Earth Environ. Sci. 2021, 646 (1), 012052, https://doi.org/10.1088/1755-1315/646/1/012052
77. Zahrim, A. Y.; Ricky, L. N. S.; Shahril, Y.; Rosalam, S.; Nurmin, B.; Harun, A. M.; Azreen, I. Partly Decomposed Empty Fruit Bunch Fiber as a Potential Adsorbent for Ammonia-Nitrogen from Urban Drainage Water. In InCIEC 2014; Springer: Singapore, **2015**; pp 989-1001, https://doi.org/10.1007/978-981-287-290-6_86
78. Qin, Y.; Zhu, X.; Su, Q.; Anumah, A.; Gao, B.; Lyu, W.; Zhou, X.; Xing, Y.; Wang, B. Enhanced Removal of Ammonium from Water by Ball-Milled Biochar. *Environ. Geochem. Health* **2020**, 42 (6), 1579-1587, https://doi.org/10.1007/s10653-019-00474-5
79. Fan, R.; Chen, C.; Lin, J.; Tzeng, J.; Huang, C.; Dong, C.; Huang, C. Adsorption Characteristics of Ammonium Ion onto Hydrous Biochars in Dilute Aqueous Solutions. *Bioresour. Technol.* **2019**, 272, 465-472, https://doi.org/10.1016/j.biortech.2018.10.064
80. Fan, R. Biochars for Removal of Ammonium, Phosphate, and Hydrogen Peroxide from Aqueous Solutions: Potential Applications in Agricultural and Semiconductor Industrial Waters. Ph.D. Dissertation, University of Delaware, **2018**.
81. Viglašová, E.; Galamboš, M.; Diviš, D.; Danková, Z.; Daňo, M.; Krivosudský, L.; Lengauer, C. L.; Matik, M.; Briančin, J.; Soja, G. Engineered Biochar as a Tool for Nitrogen Pollutants Removal: Preparation, Characterization and Sorption Study. *Desalin. Water Treat.* **2020**, 191, 318-331, https://doi.org/10.5004/dwt.2020.25750
82. Asada, T.; Ohkubo, T.; Kawata, K.; Oikawa, K. Ammonia Adsorption on Bamboo Charcoal with Acid Treatment. *J. Health Sci.* **2006**, 52, 585-589, https://doi.org/10.1248/jhs.52.585
83. Li, C.-Y.; Li, W.-G.; Wei, L. Research on Absorption of Ammonia by Nitric Acid-Modified Bamboo Charcoal at Low Temperature. *Desalin. Water Treat.* **2012**, 47 (1-3), 3-10, https://doi.org/10.1080/19443994.2012.696365
84. Mohan, D.; Sarswat, A.; Ok, Y. S.; Pittman, C. U., Jr. Organic and Inorganic Contaminants Removal from Water with Biochar, a Renewable, Low Cost and Sustainable Adsorbent–A Critical Review. *Bioresour. Technol.* **2014**, 160, 191-202, https://doi.org/10.1016/j.biortech.2014.01.120
85. Tan, X.; Liu, Y.; Gu, Y.; Xu, Y.; Zeng, G.; Hu, X.; Liu, S.; Wang, X.; Liu, S.; Li, J. Biochar-Based Nano-Composites for the Decontamination of Wastewater: A Review. *Bioresour. Technol.* **2016**, 212, 318-333, https://doi.org/10.1016/j.biortech.2016.04.093
86. Cha, J. S.; Park, S. H.; Jung, S.-C.; Ryu, C.; Jeon, J.-K.; Shin, M.-C.; Park, Y.-K. Production and Utilisation of Biochar: A Review. *J. Ind. Eng. Chem.* **2016**, 40, 1-15, https://doi.org/10.1016/j.jiec.2016.06.002

87. Wang, B.; Gao, B.; Fang, J. Recent Advances in Engineered Biochar Productions and Applications. *Crit. Rev. Environ. Sci. Technol.* **2017**, 47, 2158-2207, https://doi.org/10.1080/10643389.2017.1418580
88. Yang, F.; Zhang, S.; Sun, Y.; Du, Q.; Song, J.; Tsang, D. C. W. A Novel Electrochemical Modification Combined with One-Step Pyrolysis for Preparation of Sustainable Thorn-Like Iron-Based Biochar Composites. *Bioresour. Technol.* **2019**, 274, 379-385, https://doi.org/10.1016/j.biortech.2018.10.042
89. Sajab, M. S.; Chia, C. H.; Zakaria, S.; Khiew, P. S. Cationic and Anionic Modifications of Oil Palm Empty Fruit Bunch Fibres for the Removal of Dyes from Aqueous Solutions. *Bioresour. Technol.* **2013**, 128, 571-577, https://doi.org/10.1016/j.biortech.2012.11.010

Sustainable Engineering

Review Paper
Volume 1, Issue 1, 2024
https://doi.org/10.51200/susten.v1i1.5219

A Review of Artificial Neural Networks (ANNs) as a Potential Predictive Tool for the Performance of Scissor-Type Deployable Bridges

John Robert D. Gabriel [1,*], Orlean G. Dela Cruz [2,*]

[1] Instructor 1, Department of Civil Engineering, Don Honorio Ventura State University, Bacolor, Pampanga, Philippines
[2] Graduate School, Polytechnic University of the Philippines, Philippines

*Correspondence: jrdgabriel@dhvsu.edu.ph, ogdelacruz@pup.edu.ph *Scopus Author ID 58654317200
Received: 1 July 2024, Accepted: 3 September 2024

Abstract: After a severe disaster, some places may be unreachable for rescue operations due to bridge destruction. A scissor-type deployable bridge is a novel rescue technology that enables a lifeline to be quickly recovered during a catastrophic event. Several structural analysis approaches have been used to predict the structural behavior of deployable bridges, yet none of the prior studies have used Artificial Neural Networks (ANNs) to predict the structural behavior of scissor-type deployable bridges. This research explores the potential of ANNs to predict the performance of a scissor-type deployable bridge. The study aims to leverage the capabilities of ANNs in modeling complex relationships to forecast key parameters related to the bridge's functionality. ANNs can assist engineers in optimizing the design parameters of scissor-type deployable bridges by predicting how different configurations affect total deformation and stress levels. The analysis involves training the neural network with relevant data to learn and generalize patterns, enabling more informed predictions for diverse scenarios. Lastly, the application of ANNs in simulating bridge behavior contributes to advancing research in structural engineering, particularly in the field of deployable structures, by providing insights into complex structural responses that are challenging to model analytically.

Keywords: Deployable Bridge, Mobile Bridge, Scissor-Type Bridge, Aluminum Alloy, Artificial Neural Networks (ANNs), MATLAB

1. Introduction

One of the most important aspects contributing to nations' quick growth and stability is the development of their transportation infrastructure networks. Bridges are the primary components of the infrastructure transportation network, and they are frequently regarded as lifelines for connecting communities and regions [1]. Natural and human-caused calamities, including tsunamis, hurricanes, earthquakes, floods, and inadequate designs, have seriously threatened bridge infrastructure safety in recent decades. Statistical studies predict a five-times rise in severe natural disasters over the next 50 years [2]. For example, Typhoon Morakot in 2009 triggered 88 floods in Taiwan, damaging over 200 bridges and destroying over 100 [3]. In the Philippines, the October 2013 earthquake in Bohol is regarded as the strongest and most catastrophic natural event to hit the nation, costing over Php 2 billion in infrastructure losses [4] and resulting in 41 bridges being reported destroyed.

To survive calamities like these, we need to create a new rescue structure. We must examine how to repair a damaged structure or establish a new sort of rescue system as quickly as possible after a disaster because time is of the essence when trying to save lives. A temporary or mobile bridge is a structure that allows a lifeline to be quickly recovered after a tragedy [5]. The mobility, adaptability, and standard of a mobile bridge are more demanding than those of a regular bridge, and the bridge must be delivered and erected quickly. In addition, a bridge must be built to support the weight applied across its width.

The design and production of emergency bridges began in the 1940s. The Bailey Bridge, which is made up of modular panels and was created by British engineer Donald Sie Bailey, is the most noteworthy. It is still in use in many places of the world and is particularly significant due to its military tactical status and performance [6]. As technology evolves, emergency response bridges are foldable and may expand to a fixed size; the extended construction is strong enough to withstand loads [7]. One of the notable research that focuses on the Mobile Bridge (MB), a specific type of emergency response bridge, explored its design and application for natural disaster response. A scissor-type mechanism is the fundamental component of the bridge's design that enables rapid deployment. Many test MBs of different sizes were constructed and evaluated. The moveable bridge was successfully deployed over the real river in less than an hour, with no technical problems, and the simulation results demonstrated that it was operational and could be utilized by vehicles [8]. Moreover, a study on deployable scissor-type bridges used numerical models based on Finite Element (FE) analysis to approach a simpler design. The experimental strain variations are found to be compatible with the FE numerical model, with deviations of less than 5% on the safe side. The method is considered reliable [9]. Furthermore, influence line diagrams and equilibrium equations were used in another study to provide a unique design approach for scissor-type bridges. By examining changes in the live load distribution on the structure, the suggested methods could precisely calculate each member's size and provide the minimum and maximum values of the influence line border when carrying light vehicles [10]. However, no research has examined using Artificial Neural Networks (ANNs) for predicting scissor-type deployable bridge performance through structural analysis. ANNs can assist engineers in optimizing the design parameters of scissor-type deployable bridges by predicting how different configurations affect total deformation and stress levels.

ANNs have been applied in structural engineering to address diverse issues and provide novel solutions. One related research conducted is the structural reliability assessment of steel four-bolt unstiffened extended end plate connections using ANNs [11]. Another study utilized an ANN as the basis for creating a prediction capacity model and seismic fragility estimation for reinforced concrete (RC) bridges. The capability measures were trained, validated, and tested using an ANN model, yielding an excellent agreement between experimental data and predicted results, as demonstrated by the high correlation [12]. Hence, this proves that ANNs could serve as a better alternative in structural analysis, as they are more convenient to design and implement with enough training data.

2. Materials and Methods

This research will review the potentiality and reliability of Artificial Neural Network (ANN) to predict the performance of scissor-type deployable bridges. The datasets needed for training the ANN model will be based on the chosen reference scissor-type deployable bridge from recent studies. The deployable bridge model will be then subjected to Finite Element Analysis (FEA) using ANSYS static structural function. The numerical results gathered from FEA will be utilized for the development of ANN. Accordingly, the datasets will be trained using a back-propagation algorithm in a feed-forward architecture. The design of the ANN architecture will define the number of inputs, outputs, neurons, and hidden layers. The input datasets include the length, width, height, deck thickness, Gross Vehicle Weight Rating (GVWR), modulus of elasticity, density, Poisson's ratio, yield strength, and ultimate tensile strength, whereas, the output datasets are the maximum deformation and maximum stresses.

The design and training of the ANN for the scissor-type deployable bridge will be done using the Neural Network Fitting Tool in MATLAB. In the field of neural network modeling, the Neural Network Fitting Tool in MATLAB, known as the "nftool" is a valuable resource for beginners and professionals, providing an extensive range of functionalities for the design, training, and validation of neural networks for data fitting applications. During the training process of the network, the Levenberg-Marquardt Algorithm (LMA) will be implemented. When solving non-linear least squares problems, the LMA, sometimes referred to as the Damped Least-Squares (DLS) approach, is an effective numerical optimization technique. It works especially well for fitting least squares curves, where the objective is to determine a model curve's parameters that minimize the sum of the squares of the discrepancies between the observed data points and the model predictions. If the error percentage of the trained ANN is not acceptable, the trained ANN will be optimized and retrained, continuing in a loop until the least possible error percentage is achieved. Mean Squared Error (MSE) will be used to check how close estimates or forecasts are to actual values. The value ranges from 0 or greater, with lower values indicating higher model accuracy. Finally, the coefficient of determination, often known as R-squared, quantifies the fraction of the variance in the dependent variable that can be explained by the independent variable. It quantifies the extent of diversity within the provided dataset, with R-squared values ranging from 0 to 1, indicating the extent to which the dependent variable can be predictable.

After developing and training the ANN model, the final phase is the prediction of the outcome based on the input datasets. The model will continuously carry out iterative procedures until the ANN gives the predicted output, which includes the maximum deformation and maximum stresses. These output parameters are essential for evaluating the safety and structural performance of the scissor-type deployable bridge, which helps engineers make well-informed decisions for optimization and improvement. Subsequently, the effectiveness of the developed ANN model is examined by comparing the model's predicted outputs with the outcomes derived from FEA.

The proposed methodological process in this study is presented in Figure 1.

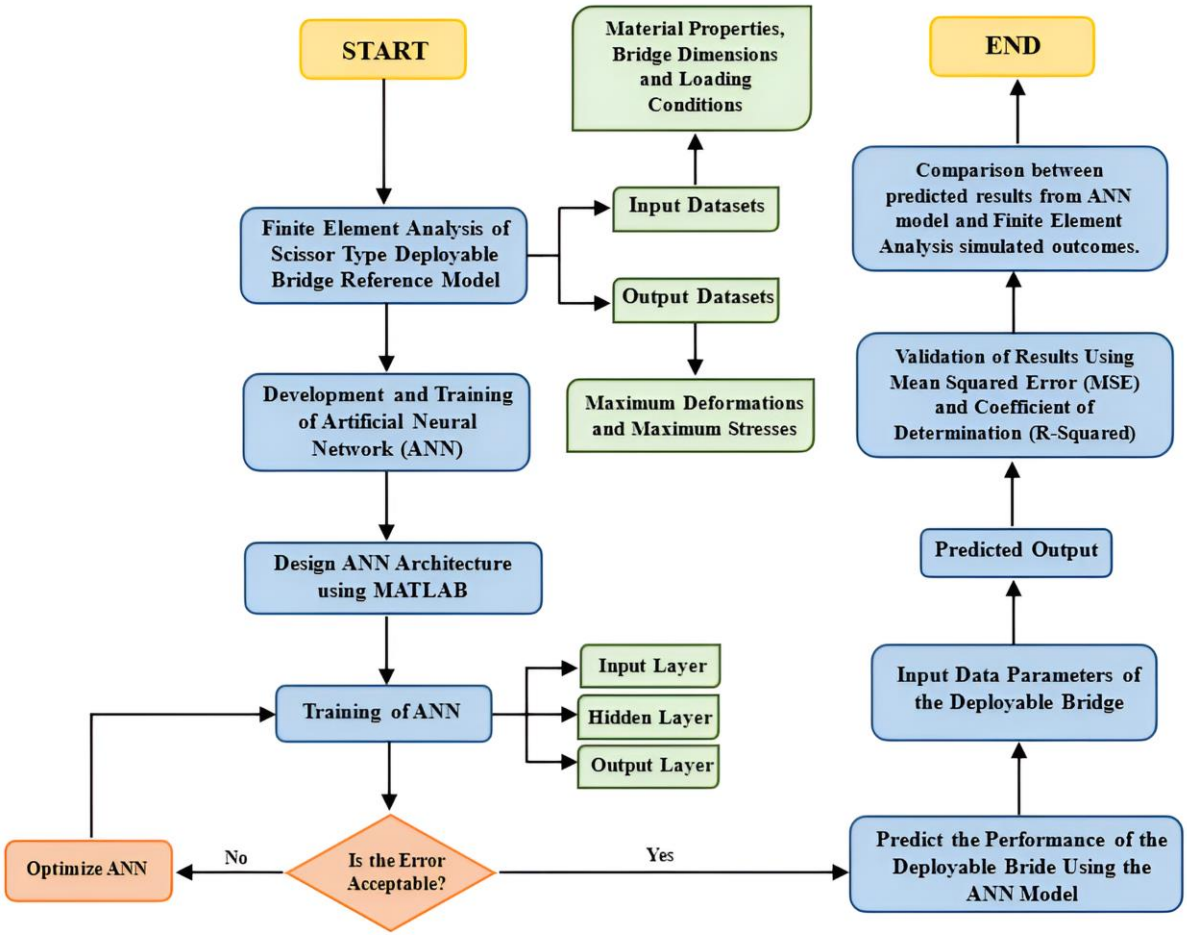

Figure 1. Flowchart of Artificial Neural Network (ANN) as a Predictive Tool in the Performance of Scissor Type Deployable Bridge

3. Results and Discussion

This section of the research paper gives a summary of previous research and literature that is pertinent to concerns about disaster operations by developing a rescue system in the form of deployable bridges as a solution. This paper will address several kinds of deployable emergency response bridges and their uses, materials for scissor-type bridges, and the use of Artificial Neural Networks (ANNs) for predictive modeling in structural analysis of bridges.

3.1 Structural Forms of Deployable Bridges.

Modern post-disaster rescue equipment, such as emergency deployable bridges, makes it possible to access the disaster site, which will facilitate rescue efforts and resulting in the saving of more lives [14]. A deployable structure's ability to exist in two distinct stable states—the fully folded state and the fully unfolded one—is its most distinctive characteristic. The deployable structure is smaller and convenient to transport and store when it is fully folded. The structure is durable and capable of supporting weights when completely extended [15]. Likewise, to facilitate launching, retracting, transporting, and storing, a lightweight bridging system is required [16].

3.1.1 Arch Type Deployable Bridge.

In the course of the deployment procedure, deployable structures show inconsistencies in the member lengths at intermediate geometric configurations. The corresponding snap-through event "locks" the structures in their deployed position by generating second-order strains and stresses. To take on this limitation, a geometric design approach that takes into consideration the discrete joint size and is suitable for deployable arches with any curvature has been proposed. The semi-elliptical arch's geometric design has been successfully implemented using this type of approach. A preliminary structural design shows that the “arch” is generally feasible for light loads and short to medium-span structures [17]. Recent studies demonstrate the advantages of deployable arch bridges, such as it is built with a simple configuration and may be deployed quickly. The deployable arch bridge has good adaptability; depending on the need, the number of bridge span modules can be increased or decreased to fulfill the needs of crossing various obstacles. It is very convenient to transport and unfold the arch bridge design [15]. However, the increased number of joints may increase the amount of maintenance required. Long vehicles with low clearances (such as tractor-trailers) may be unable to cross due to the arch's curvature, which might be solved by constructing ramps to lessen the slope at the extremities. Finally, when the arch's height is combined with significant wind loads, the arch may overturn in the transverse direction [18].

3.1.2 Scissor Type Deployable Bridge.

The scissor mechanisms are most commonly used in the field of temporary dome architecture. Organizing the scissor units as a geodesic grid or maximizing the scissor components' sectional area improves their strength and stability. To enable safe passage for people and vehicles, an emergency bridge's design must ensure construction speed and structural strength [19].

The idea of multi-folding microstructures and earlier research on deployable structures have led to the proposal of a novel kind of emergency bridge known as a Mobile Bridge (MB) [20]. Although the upper and lower chords are the primary elements that resist sectional stresses in a typical truss bridge, the MB lacks chords but can be carried and built rapidly utilizing a scissor mechanism [21]. In its most basic form, the scissors mechanism is made up of two straight linear elements. A pivot connects the pieces at their centers, forming a hinge connection. The two members are in the shape of the character “X” in the fully deployed state. As seen in Figure 2, two hinges connect one unit to the next. The structure can be deployed and has a big length-to-width ratio from the expanded to the folded state. There are two types of compacts: non-deployed and deployed. In its current state, the construction is easily transportable and may be kept for future use. In this way, this method is particularly effective for systems that need to be moved and kept in a small amount of space at a time [8].

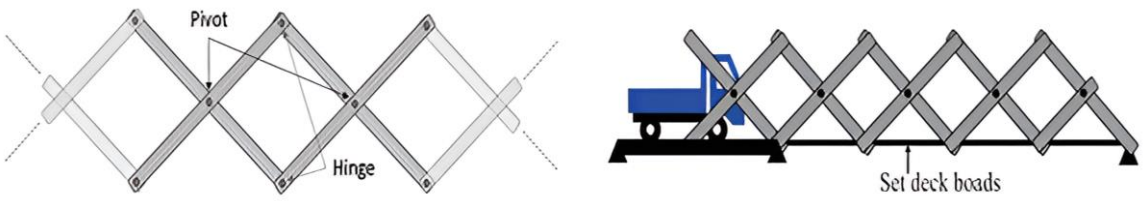

Figure 2. Basic Concept of Scissor-Type Bridge

When the scissors mechanism is successfully applied to the bridge structure, the structure should have the following features: it should be easier to deploy and fold with just one control force, have a shorter transport time than a more conventional temporary bridge, and be more efficient in terms of size when comparing its deployed and folded states. The scissor-type mobile bridge has a smaller live load capacity and span than other bridge types due to the lack of upper and lower chord elements, which, when present, resist bending forces. As a result, the lighter bridge may be erected more rapidly and its components carried in a light vehicle [9]. Although it offers several advantages, research studies have identified drawbacks with the scissor-type bridge mechanism. Due to the coupled stiffness of these bridges, the vibration of scissors-type movable bridges is more sensitive in the horizontal rather than vertical direction [22].

3.2 Materials Used in a Scissor-Type Deployable Bridge.

The selection of materials for the building of scissor bridges is a complex procedure that involves considering several elements, such as the length of the span, environmental circumstances, load-bearing capacity of the bridge, and financial limitations. Pursuing ideal materials has emerged as a catalyst for innovation in scissor bridge building, as engineers and researchers persistently explore novel design possibilities.

3.2.1 Structural Steel.

The selection of structural steel for bridges should take into account the required material attributes or stress state, the construction site's environmental factors, the corrosion protection system, and the building method [23]. The fundamental factors involved in designing and constructing steel bridges are the physical attributes of structural steel, which include strength, ductility, toughness, weldability, weather resistance, chemical composition, shape, size, and surface features [24]. One of the research studies explores the use of A36 structural steel as the main material for scissor-type deployable bridges. The deployable bridge is designed to fit in the trunk of a 4 × 4 pick-up truck; therefore, its overall dimensions are 2.2 m (width), 2 m (height), and 14m (length). Stress analysis is simulated using ANSYS Workbench's static structural function. It was discovered that one of the limitations of the steel deployable bridge design is the overall weight of the bridge. An emergency deployable bridge should be as lightweight as possible without losing strength to be easily transported and deployed during a natural disaster. Therefore, research and analysis on bridge weight reduction techniques involving the use of lightweight materials may take into consideration the significance of material selection in further studies [25].

3.2.2 Fiber Reinforced Polymer (FRP).

Although composite materials are less ductile than traditional materials like structural steel in applications, they have several advantages, such as high specific stiffness and strength, lightweight material, excellent corrosion resistance, and low maintenance costs, which make them very appealing for use in the construction industry in certain circumstances. These benefits have prompted the examination of Fiber Reinforced Polymer (FRP) as a bridge-building option. The following applications have been taken under consideration thus far: (a) bridge component repair and upgrade retrofitting schemes; (b) design of replacement bridge components; and (c) design and construction of new bridge structures for pedestrian or highway use [26]. However, the disadvantages of using FRP in a composite bridge

application are as follows: (a) a large deflection of the structure caused by the low modulus of materials (compared to steel) and low stiffness of the FRP components; (b) the need to simplify the joints and connections; and (c) the high cost of composite materials necessitates the solution of cost-effective problems [3].

In general, carbon fiber is the most desirable reinforcing due to its extremely high strength compared to other fibers. Due to its high modulus of elasticity, carbon fiber reinforced polymer (CFRP) is the material most suitable for deployable bridges. The less material deflects, the higher the modulus of elasticity. This attribute is necessary to guarantee that the bridge will not deflect excessively. Fiber-reinforced composite (FRP) is highly beneficial for building deployable bridges [27]. A study was conducted to analyze the mechanical properties of a lightweight FRP scissor-type bridge using the finite element method to identify its strength and durability [28]. The findings indicate that FRP scissor bridges can be designed to withstand the same loads as traditional steel scissor bridges. The results suggest that FRP composites are a better choice for bridge construction than traditional materials [29].

3.2.3 Aluminum Alloy.

As a lightweight material, aluminum alloy provides an alternative for deployable bridges. Additionally, experiments conducted in a research laboratory have shown that aluminum alloy has superior corrosion resistance, eliminating the need for any protective coating [30]. According to theoretical and practical research, it was reported that aluminum alloy has the best mechanical and anticorrosive qualities. This might be very advantageous for applications involving bridges, such as the restoration of bridge decks, deployable bridges, and military bridges [31].

According to a current study, a scissor-type Mobile Bridge (MB 4.0) made of aluminum alloy with improved mobility, functionality, and a lighter weight was created. Consequently, the MB4.0 is now more easily transportable and can be set up at temporary construction sites without requiring heavy machinery or foundation work. It is therefore also far more economical [8]. However, experimental findings reveal that vibrations in the horizontal direction are significantly more pronounced than those in the vertical direction. Reinforcing elements added to the bridge's upper level resulted in higher horizontal and vertical eigenvalue frequencies compared to the unreinforced bridge. This suggests that reinforcing components enhance the stiffness of the MB4.0 bridge, thereby reducing the influence of bending moments on the primary structural members. The application of appropriate reinforcement can improve both the bridge's stability and safety [32].

3.3 The Artificial Neural Networks (ANNs) Capabilities

Artificial Neural networks (ANNs) are capable of producing extremely accurate predictions when provided with a substantial quantity of training data. Neural networks can be emulated in digital systems, even though they are more frequently connected to analog computers. They use a series of algorithms that are inspired by the structure of the human brain [33]. These algorithms involve an array of numerical learning methods and consist of a large number of nonlinear computational units, known as network nodes, which are interconnected by weighted links. ANNs can effectively solve a wide range of complex problems, from

small to large scale. This is due to their massively parallel distributed structure, which allows them to learn and generalize. Additionally, they can produce reasonably accurate outputs for inputs not used during the learning phase, also known as “training” [34].

ANNs are used to predict how materials with similar properties will perform under different testing scenarios, based on experimental data. They are used as predictive tools, forecasting certain outputs based on input values. Engineering predictions are the main use for the backpropagation network model. One or more continuously valued outputs and several continuous-valued inputs can be connected through this efficient method to create nonlinear transfer functions. The network is named for the way it handles mistakes during training and essentially employs a multi-layer perception architecture [35].

Feed Forward Neural Networks (FFNN) are the most widely utilized artificial neural network technique for dealing with various engineering limitations. A layer in the FFNN technique is entirely linked to the layer before it by weights [36]. The typical three-layer feed-forward type of an ANN is shown in Figure 3. Currently, this backpropagation architecture-based interactive network has gained popularity, value, and ease of learning, especially for complex models like multi-layered networks. The ability of ANNs to handle nonlinear solutions to indefinite problems is their greatest strength. There are three layers in the professional backpropagation network: input, output, and at least one hidden layer [37].

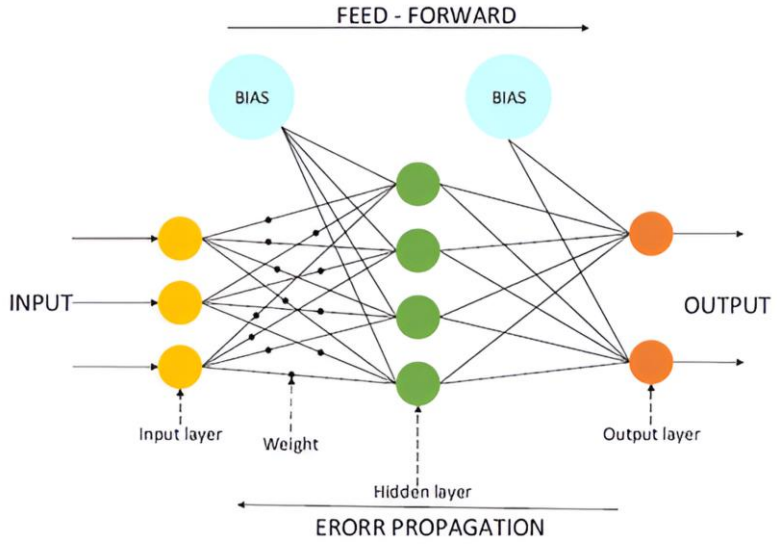

Figure 3. Three-layer Feed Forward Artificial Neural Network Schematic Representation [37]

Nowadays, ANNs have garnered growing interest in civil engineering. They have been used to address numerous structural analysis and design problems. These types of problems are most suited for ANN applications: the problem domain is rich in examples or historical data; the data set is incomplete or contains errors; the function to find solutions is unknown; and applications are data-intensive and dependent on numerous criteria. The amount of research being done on using ANNs to solve civil engineering problems is expanding quickly. The application of ANNs in structural engineering has developed as a new paradigm for computing, despite its continued extreme limitations. It has been used in a variety of

applications, including finite element analysis, structural design, material behavior modeling, damage assessment, and structural analysis [38].

3.3.1 Application of Artificial Neural Networks (ANNs)on Bridge Performance.

Artificial Neural Networks (ANNs) have been applied in structural engineering to address diverse issues and provide novel solutions [39]. The following applications of ANNs in structural analysis and design could be emphasized: topology optimization (based on the removal of ineffective structural members), joint location, size optimization of structural members, shape optimization of structural types (e.g., truss geometry), structural analysis of systems with large degrees of freedom, and maximum stress identification and location [40]. From past studies, numerous research findings confirmed the efficiency and accuracy of the proposed ANN models as a successful predictive modeling technique for assessing the structural behavior of structures, especially bridges.

Table 1. Application of Artificial Neural Networks (ANNs) on Bridge Behaviour

Application of ANNs on Bridges	Research Methods and Findings	Reference
Estimation on Dynamic Displacements due to Dynamic Loads on Bridges	- This study made recommendations on how to make perception of the limited data on individual girder points to understand the overall behavior of bridges. - To replicate real-world traffic scenarios, dynamic vehicle load assumptions using the Pearson Type III distribution of traffic theory were created. - Ultimately, the ANN allowed us to reasonably precisely estimate the vertical dynamic displacement, which had been influenced by FEM results from loads based on actual conditions.	[41]
Bridge Damage Identification	- An ANN-based bridge behavior model was formed. By using this technique for damage identification and localization, bridge performance trends may be obtained, early inspections can be triggered, and inspectors can be directed toward the regions of the bridge that are most likely to sustain damage. - The study's initial findings show that engineers may find it useful in the future to quickly ascertain a bridge's baseline performance and obtain automated weekly updates on the bridge's condition.	[42]
Developing Bridge Deterioration Models	- ANN models with diversified configurations were developed and used to provide predictions on the degradation of the superstructure, substructure, and bridge deck. - The National Bridge Inventory (NBI) database provided the information needed to create the deterioration models for bridge structures. - As a result of this study, a bridge deterioration model was created using the proposed ANN models to predict deterioration in all bridge systems.	[43]
Identification of Flexural Structural Damage in the Girders of a Vehicle Bridge	- A Neural Network (NN) based model was created, performed, and assessed to identify flexural structural damage in the girders of a vehicle bridge. - Based on the findings of this study, it can be concluded that NN models trained using modal strain energy differences can be used to accurately determine the position and extent of damage in a bridge's girders.	[44]

3.3.2 Training of Artificial Neural Network (ANN).

Artificial Neural Networks (ANNs) can be worked with a variety of software programs. One of these is TensorFlow, a comprehensive open-source machine-learning platform that offers an extensive set of customizable tools, libraries, and community offerings [45]. When it comes to ANN software, one of the best in Neural Designer, a desktop tool for data mining that employs neural networks, a key machine learning paradigm; however, one of the drawbacks is its high cost [46]. The Neural Lab is another software used to construct models, which allows for the creation of custom ANN-based application by combining the C++ classes within its object-oriented implementation. This modeling tool was created and implemented using a variety of optimization methodologies. The model supports multi-layer feed-forward networks, as well as probabilistic neural networks, and it has been used in previous research due to its user-friendly coding and versatility [46]. Lastly, MATLAB is a program that gives an interactive environment where users may collaborate and visualize ideas in a variety of domains, including computational finance, communications, control systems, signal and image processing, and computational imaging. A collection of tools and applications for building, training, and modeling neural networks can be found in MATLAB's Neural Network Toolbox. Neural network development for tasks like clustering, pattern recognition, and data-fitting (including time-series data) is made simple by the software [47]. When using MATLAB to solve a problem, prototype solutions are typically produced more quickly than when employing other programming languages [48].

4. Conclusions

Scissor-type deployable bridges are ideal for disaster operations due to their rapid deployment capabilities and simplified assembly processes, which require fewer personnel. Various structural analysis methods have been utilized to forecast the structural behavior of deployable bridges. These are the Coefficient Technique, Kutzbach Equation, ANSYS Workbench, well-known Finite Element Analysis (FEA), and Influence-Line based design. However, none of the previous studies utilized Artificial Neural Networks (ANNs) to predict the structural behavior of scissor-type deployable bridges. This technique has the potential to be a highly effective tool in predicting the structural behavior of scissor-type bridges. When dealing with complicated structures like scissor-type bridges, ANNs shine because of their ability to detect patterns and trends in data. ANNs can learn from new data and adapt as needed. This means that the ANN model can be updated and improved as additional information about the efficiency of scissor-type bridges becomes available. ANN has been applied to several bridge applications, such as the detection of bridge damage, flexural behavior, as well as deterioration. ANNs can assist engineers in optimizing the design parameters of scissor-type deployable bridges by predicting how different configurations affect total deformation and stress levels. Overall, leveraging ANNs for simulating deformation and stresses in scissor-type deployable bridges enhances both the understanding and management of their structural performance, leading to safer, more cost-effective, and resilient infrastructure solutions.

Acknowledgments

The authors would like to express their deepest gratitude to the Polytechnic University of the Philippines (PUP) Graduate School for its unwavering support throughout this research.

Conflicts of Interest

The authors declare no conflict of interest.

References

1. Alhassan M.; Baily J.; Hoffman J.; Brown J.; Amaireh L. Shear Behavior of NWC and LWC Beams Comprising Structural Synthetic Fibers. *Proc. of ICIMART'16*. 109-119, **2016**.
2. Kumar, A.; Latif, Y.; Daver, F. Developing Forecasting Tool for Humanitarian Relief Organizations in Emergency Logistics Planning. *International Journal of Economics and Management Engineering* **2012**, 6(11), 3194 - 3200.
3. Yeh F. Y.; Chang K. C.; Sung Y. C.; Hung H. H.; Chou C. C. A Novel Composite Bridge for Emergency Disaster Relief: Concept and Verification. *Composite Structure* **2015**, 127, 199–210. https://doi.org/10.1016/j.compstruct.2015.03.012
4. Tomaneng S. D. G.; Docdoc J. A. P.; Hierl S. A.; Cerna P. D. Towards the Development a Cost-effective Earthquake Monitoring System and Vibration Detector with SMS Notification Using IOT. *International Journal of Engineering and Manufacturing* **2022**, 12(6), 22–31, https://doi.org/10.5815/ijem.2022.06.03
5. Ario I.; Nakazawa M.; Tanaka Y.; Tanikura I.; Ono S. Development of a Prototype Deployable Bridge Based on Origami Skill. *Automation in Construction* **2013**, 32, 104-111, https://doi.org/10.1016/j.autcon.2013.01.012
6. Joiner C. J. H. The Story of the Bailey Bridge. *Proc. of the Inst. of Civ. Engineers – Eng. History & Heritage* **2011**, 164(2), 65–72, https://doi.org/10.1680/ehah.10.00002
7. Liang J.; Zhang Y.; Hou S.; Shen P. Emergency Deployable Bridge Development Process and Prospect. *Journal of Civil Engineering and Urban Planning* **2022**, 4(3), 1–7, https://dx.doi.org/10.23977/jceup.2022.040301
8. Chikahiro Y.; Ario I.; Pawlowski P.; Graczykowski C; Nakazawa M.; Holnicki-Szulc J.; Ono S. Dynamics of the Scissors-type Mobile Bridge. *Procedia Engineering* **2017**, 199, 2919–2924, https://doi.org/10.1016/j.proeng.2017.09.339
9. Chikahiro Y.; Ario I.; Nakazawa M.; Ono S; Holnicki-Szulc J.; Pawlowski P.; Graczykowski C; Watson A. Experimental and Numerical Study of Full-scale Scissor Type Bridge. *Automation in Construction* **2016**, 71(2), 171–180, https://doi.org/10.1016/j.autcon.2016.05.007
10. Ario I.; Hama Y.; Chanthamanivong K.; Chikahiro Y.; Fujiwara A.; Ma H. Influence Line-Based Design of Scissors-Type Bridge. *Appl. Sci.* **2022**, 12(23), https://doi.org/10.3390/app122312170
11. Abbasianjahromi H; Shojaeikhah S. Structural Reliability Assessment of Steel Four-Bolt Unstiffened Extended End-Plate Connections Using Monte Carlo Simulation and Artificial Neural Networks. *Iranian Journal of Science and Technology-Transactions of Civil Engineering* **2021**, 45(1), 111-123, https://doi.org/10.1007/s40996-020-00480-z

12. Huang C.; Huang S. Predicting Capacity Model and Seismic Fragility Estimation for RC Bridge based on Artificial Neural Network. *Structures* **2020**, 27, 1930–1939, https://doi.org/10.1016/j.istruc.2020.07.063
13. Choy H. Y.; Tan A. A. Design and Analysis of Emergency Deployable Bridge. *International Journal of Mechanical Engineering and Robotics Research* **2020**, 9(10), 1393-1399, https://doi.org/10.18178/ijmerr.9.10.1393-1399
14. Hanus J. P.; Ray J. C.; Bank L. C.; Velazquez G. I. Optimized Design and Testing of a Prototype Military Bridge System for Rapid In-Theater Construction. *Proc. of 25th Army Science Conference – Transformational Army Science and Technology* **2006**.
15. Li Q.; Yuan J.; Sun H.; Zhou S.; Peng Y. Design of a New Type of Deployable Bridge. *IOP Conference Series: Materials Science and Engineering* **2020**, https://doi.org/10.1088/1757-899X/926/1/012026
16. Agusril S. T.; Nor N. M.; Zhao Z. J. Failure Analysis of Carbon Fiber Reinforced Polymer (CFRP) Bridge Using Composite Material Failure Theories. *Advanced Materials Research* **2012**, 488–489, 525-529, https://doi.org/10.4028/www.scientific.net/AMR.488-489.525
17. Gantes C. J.; Konitopoulou E. Geometric Design of Arbitrarily Curved Bi-stable Deployable Arches with Discrete Joint Size. *International Journal of Solids and Structures* **2004**, 41(20), 5517–5540, https://doi.org/10.1016/j.ijsolstr.2004.04.030
18. Lederman G.; You Z.; Glišić B. A Novel Deployable Tied Arch Bridge. *Engineering Structures* **2014**, 70, 1–10, https://doi.org/10.1016/j.engstruct.2014.03.015
19. Chikahiro Y.; Ario I.; Holnicki-szulc J.; Pawlowski P.; Graczykowski C. A Study on Optimal Reinforcement of Scissor Type of Bridge with Additional Strut Members. *International Conference on Civil and Environmental Engineering* **2016**.
20. Hunt G. W.; Ario I. Twist Buckling and the Foldable Cylinder: An Exercise in Origami," *International Journal of Non-Linear Mechanics* **2005**, 40(6), 833–843 https://doi.org/10.1016/j.ijnonlinmec.2004.08.011
21. Chikahiro Y.; Ario I.; Nakazawa M. Theory and Design Study of a Full-Scale Scissors-Type Bridge. *Journal of Bridge Engineering* **2016**, 21(9), https://doi.org/10.1061/(ASCE)BE.1943-5592.0000913
22. Chanthamanivong K.; Ario I.; Chikahiro Y. Smart Design of Coupling Scissors-type Bridge. *Structures* **2021**, 30, 206–216, https://doi.org/10.1016/j.istruc.2020.12.044
23. Kreislova K.; Geiplova H. Evaluation of Corrosion Protection of Steel Bridges. *Procedia Engineering* **2012**, 40, 229–234, https://doi.org/10.1016/j.proeng.2012.07.085
24. Lin W.; Yoda T. Steel Bridges. In Bridge Engineering: Classifications, Design Loading, and Analysis Methods; Lin W., Yoda T., Eds.; Butterworth-Heinemann: Cambridge, United States. **2017**. 111-136. https://doi.org/10.1016/B978-0-12-804432-2.00007-4
25. Biro M. N. A.; Abu Bakar N. Z. Design and Analysis of Collapsible Scissor Bridge. *MATEC Web Conf.* **2018**, 152, https://doi.org/10.1051/matecconf/201815202013
26. Kostopoulos V.; Markopoulos Y. P.; Vlachos D. E.; Katerelos D.; Galiotis C.; Tsiknias T.; Zacharopoulos D.; Karalekas D.; Chronis P.; Kalomallos D. Design and Construction of a Vehicular Bridge Made of Glass/Polyester Pultruded Box Beams. *Plastics, Rubber and Composites* **2005**, 34(4), 201-207, https://doi.org/10.1179/174328905X55641
27. Nor N. M.; Devarase V.; Yahya M. A.; Sojipto S.; Osmi S. K. C. Fiber Reinforced Polymer (FRP) Portable Bridge: Modeling and Simulation. *European Journal of Scientific Research* **2010**, 44(3), 437-448.

28. Agneloni E.; Casadei P. Case Studies on Advanced Composite Materials for Civil Engineering and Architectural Applications. *Structural Engineering International* **2011**, 21(3), 271–278, https://doi.org/10.2749/101686611X13049248220005
29. Agarwal P.; Pal P.; Mehta P. K. Finite Element Analysis of Reinforced Concrete Curved Box-Girder Bridges. *Advances in Bridge Engineering* **2023**, 4. https://doi.org/10.1186/s43251-023-00080-7
30. Saleem M. A.; Mirmiran A.; Xia J.; Mackie K. Experimental Evaluation of Aluminum Bridge Deck System. *Journal of Bridge Engineering* **2010**, 17(1), 97-106, https://doi.org/10.1061/(ASCE)BE.1943-5592.0000204
31. Höglund T.; Nilsson L. Aluminium in Bridge Decks and in a New Military Bridge in Sweden. *Structural Engineering International* **2006**, 16(4), 348-351, https://doi.org/10.2749/101686606778995100
32. Chikahiro Y.; Ario I.; Adachi K.; Shimizu S.; Zenza S.; Pawlowski P.; Graczykowski C.; Holnicki-Szulc J. Fundamental Study on Dynamic Property of Scissoring Bridge For Disaster Relief. *Environmental Science Engineering* **2017**.
33. Islam M.; Chen G.; Jin S. An Overview of Neural Network. *American Journal of Neural Networks and Applications* **2019**, 5(1), 7-11, https://doi.org/10.11648/j.ajnna.20190501.12
34. Abambres M.; Marcy M.; Doz G. Potential of Neural Networks for Structural Damage Localization. *The IUP Journal of Structural Engineering* **2019**, 12(4), 38-71, https://dx.doi.org/10.2139/ssrn.3368672
35. Shokri M.; Tavakoli K. A Review on the Artificial Neural Network Approach to Analysis and Prediction of Seismic Damage in Infrastructure. *International Journal of Hydromechatronics* **2019**, 2(4), 178-196, https://dx.doi.org/10.1504/IJHM.2019.104386
36. Chojaczyk A. A.; Teixeira A. P.; Neves L. C.; Cardoso J. B.; Guedes Soares C. Review and Application of Artificial Neural Networks Models in Reliability Analysis of Steel Structures. *Structural Safety* **2015**, 52(A), 78-89, https://doi.org/10.1016/j.strusafe.2014.09.002
37. Padil K. H.; Bakhary N.; Hao H. The Use of a Non-Probabilistic Artificial Neural Network to Consider Uncertainties in Vibration-Based-Damage Detection. *Mechanical Systems and Signal Processing* **2017**, 83, 194–209, https://doi.org/10.1016/j.ymssp.2016.06.007
38. Berrais A. Artificial Neural Networks in Structural Engineering: Concept and Applications. *Engineering Sciences Journal* **1999**, 12(1), 53-67.
39. Abiodun O. I.; Jantan A.; Omolara A. E.; Dada K. V.; Mohamed N. A. E.; Arshad H. State-of-the-Art in Artificial Neural Network Applications: A Survey. *Heliyon* **2018**, 4(11), https://doi.org/10.1016/j.heliyon.2018.e00938
40. Navarro-Rubio J.; Pineda P.; Navarro-Rubio R. Efficient Structural Design of a Prefab Concrete Connection by Using Artificial Neural Networks. *Sustainability* **2020**, 12(19), https://doi.org/10.3390/su12198226
41. Ok S.; Son W.; Lim Y. M. A Study of the Use of Artificial Neural Networks to Estimate Dynamic Displacements due to Dynamic Loads in Bridges. *Journal of Physics: Conference Series* **2012**, 382(1), https://doi.org/10.1088/1742-6596/382/1/012032
42. Weinstein J. C.; Sanayei M.; Brenner B. R. Bridge Damage Identification Using Artificial Neural Networks. *Journal of Bridge Engineering* **2018**, 23(11), https://doi.org/10.1061/(ASCE)BE.1943-5592.0001302

43. Althaqafi E.; Chou E. Developing Bridge Deterioration Models Using an Artificial Neural Network. *Infrastructures* **2022**, 7(8), https://doi.org/10.3390/infrastructures7080101
44. González-Pérez C.; Valdés-González J. Identification of Structural Damage in a Vehicular Bridge using Artificial Neural Networks. *Structural Health Monitoring* **2011**, 10(1), 33–48, https://doi.org/10.1177/1475921710365416
45. Ali S. M.; Krishna V. D. S.; Srinivas S. Overview on Open Source Machine Learning Platforms- Tensorflow. *Journal for Innovative Development in Pharmaceutical and Technical Science* **2020**, 3(11), 11-14, https://doi.org/10.1016/j.matpr.2020.09.625
46. Pradel M.; Chandra S. Neural Software Analysis. *Communications ACM* **2022**, 65(1), 86–96, https://doi.org/10.1145/3460348
47. Verma S.; Gupta V.; Kamboj D. A Comparative Study of Training Algorithms of Artificial Neural Network using MATLAB. *Proc. of Technical Symposium on Emerging Technologies in Computer Science* **2016**, 13–19.
48. Moustafa A. A.; Alqadi Z. A.; Shahroury E. A. Performance Evaluation of Artificial Neural Networks for Spatial Data Analysis. *WSEAS Transactions on Comput*ers **2011**, 10(4), 115–124.

Sustainable Engineering

Review paper
Volume 1, Issue 1, 2024
https://doi.org/10.51200/susten.v1i1.5218

Review of cost estimation practices for building projects using BIM

Tushar Jadhav [1,*]

[1] School of Project Management, NICMAR University Pune 411045, India

*Correspondence: tjadhav@nicmar.ac.in; *Scopus Author ID 57189632224
Received: 22 Jun 2024, Accepted: 3 September 2024

Abstract: Cost management remains one of the key challenges in architectural, engineering, and construction (AEC) projects. Building Information Modeling (BIM) has gained popularity among AEC industry professionals due to its better visualization and clash detection abilities. The present study, therefore, attempts to review the cost estimation practices for building projects using BIM. The objective of the present study is to find answers to the research questions viz., 1) What are the various methodologies adopted for estimating building cost using BIM? and 2) Is BIM popular tool among cost management professionals? The literature review is divided into four parts. The first part of the literature review deals with general observations addressing issues and challenges of using BIM for cost estimation. The second part of the literature review covers different types of models and frameworks developed by researchers for estimating the cost of building projects using BIM. The third part of the review investigates key observations by various associated stakeholders on the usage of BIM for estimating building cost. The interpretation through various case studies is discussed in the last part of the literature review.

Keywords: Cost estimation; Cost management; BIM

1. Introduction

Project cost management and project schedule management remain some of the most challenging tasks for engineers and project managers associated with engineering projects. The activities associated with these two knowledge areas often go in integrated manner to ensure that there are minimal cost and schedule overruns. The application of Building Information Modeling (BIM) for estimating cost of buildings has gained popularity among cost management professionals in recent years. One of the biggest advantages of using BIM for cost estimation lies in the faster quantification of data and its analysis compared to the traditional method. The increasing use of technologies to perform automatic quantity takeoff has helped quantity surveyors achieve sustainable development throughout the building life cycle [1].

2. Research Objective and Methodology

The main aim of this study is to review the cost estimation practices for building projects using BIM. The objective is to review the various studies done by past researchers on integrating BIM for estimating cost of buildings. The rationale behind selecting this topic is to conduct a literature review and investigate the answers to the two research questions:

1. What are the various methodologies adopted for estimating building cost using BIM?
2. Is BIM a popular tool among cost management professionals?

The above research objectives are investigated by referring to the secondary data in form of research publications and case studies.

3. Literature Review

An exhaustive review of literature was performed by searching in high-quality journals and using one or combination of keywords such as "cost," "cost estimation," "BIM", and "buildings". Out of 48 articles that were reviewed, 37 articles (77 %) were shortlisted, aligning with the research objectives for this study.

The literature review is divided into four parts. The first part of the literature review deals with general observations addressing issues and challenges of using BIM for cost estimation. The second part covers different types of models and frameworks developed by researchers for estimating the cost of building projects using BIM. The third part investigates the key observations by various associated stakeholders on the usage of BIM for estimating building cost. The interpretation through various case studies is discussed in the last part of the literature review.

3.1. BIM for cost estimation

Ma & Liu (2014) presented an approach to collect the necessary construction information for automatic cost estimation of building projects based on BIM designs [2]. Data exchange remains one of the key challenges in the architectural, engineering, and construction (AEC) industry. BIM provides the necessary assistance in sharing the required information systematically and accurately amongst the AEC stakeholders. The traditional costing methodology is mostly text-oriented, whereas BIM provides visual data management that helps in the clear understanding of building projects. This minimizes the chances of errors and avoids the wrong interpretation of data [3]. BIM provides a good alternative to quantity surveyors for cost estimation. However, Wu et al. (2014) observed that the quantity surveyors are unable to take the maximum benefit of BIM due to several limitations, such as low-quality BIM models, inconsistency in level of design information, data exchange issues, and inconsistent formats, among others [4]. The authors reviewed the capabilities of four BIM software for estimation. The software reviewed were Solibri Model Checker 8, Autodesk QTO 2012, CostX 3.5 and BIM Measure 16.4. Seven criteria (exchange, visualization, quantification, reliability, customization, change, and report) were selected for reviewing the mentioned software. The findings suggested that each of this software had its own unique capabilities to assist the quantity surveyors. However, the authors highlighted the need for some additional work in BIM software to take maximum benefit of BIM technology, especially for projects in United Kingdom (UK). In another investigation Sunil et al. (2015) reviewed the importance of BIM for cost management in UK construction sector [5].

Plebankiewicz et al. (2015) developed a costing system, BIMestiMate, which allows direct estimation of cost from BIM model for the Poland region [6]. Azhar et al. (2008) analyzed the benefits, risks and challenges of using BIM for AEC industry [7]. The authors highlighted the need for standardization of the BIM process and defining relevant guidelines for its implementation. The study conducted by Bryde et al. (2013) indicated that BIM has a noteworthy contribution in managing construction projects effectively [8]. The authors

reviewed that cost is one of the most significant components that has been positively impacted by implementation of BIM. The perspective of cost consultants on the usability and impact of BIM was investigated by Goucher & Thurairajah (2012). The authors have documented the potential advantages as well as the challenges for cost consultants using BIM [9]. Khaddaj & Srour (2016) reviewed the literature covering BIM and sustainability [10]. The authors proposed a research agenda to increase the applicability of BIM for building retrofit projects. To perform the life cycle assessment (LCA) of buildings, one of the significant challenges is the data exchange between BIM and LCA [11].

3.2. Framework and cost estimation models

Cheung et al. (2012) developed a multi-level cost estimation BIM tool to analyze the building design aspects at its early stage [12]. The authors proposed Low Impact Design Explorer (LIDX) as the knowledge-based tool for the assessment of design using Google SketchUp environment. The tool can make profile-driven estimates, which can be revised in real-time. Elbeltagi et al. (2014) developed a comprehensive cost estimation and monitoring model [13]. The model can be integrated with BIM and enables the user to visualize actual costs spent and compare them with the budgeted cost. The study deals with integration between project cost estimation, monitoring, and control techniques with BIM. Lee et al. (2014) proposed an ontological approach to overcome the subjectivity of cost estimators [14]. The study developed a work condition ontology comprising of determinants to select work items, work item ontology, and semantic reasoning rules. This methodology can automatically determine the most appropriate work item based on the work conditions through the use of semantic technology. Choi et al. (2015) proposed an open BIM-based quantity takeoff process for schematic estimation. It comprises four steps: BIM modeling for schematic estimation, physical quantity verification to increase accuracy, verification of property (data quality), and quantity takeoff [15].

Abanda et al. (2017) developed and demonstrated use of ontology for cost estimation using BIM [16]. The ontology was developed based on New Rules of Measurement (NRM) for cost estimation. BIM-based construction cost estimation needs effective communication between BIM authoring software and specialized cost estimating software. The study demonstrated the use of ontologies in reasoning and performing quantity takeoffs, which can subsequently be used for cost estimation. Whole building development needs methods, workflows, and tools to implement integration of LCA with BIM [17]. The authors proposed a methodology for companies working in Switzerland to perform LCA using well-established BIM structure. Fazeli et al. (2020) successfully demonstrated the linkage between Iran's cost estimation standard (FehrestBaha) and the CSI standards of UniFormat and MasterFormat [18]. The authors developed a BIM-based extension in Autodesk Revit with five primary functions using C# programming. This enabled the automation of cost estimation process and also ensured that the cost estimation standard of Iran became compatible with the BIM environment. Errors in BIM models can cause deviations in the quantity takeoff, especially for compound building elements such as walls and floors. Therefore, to address this issue, Khosakitchalert et al. (2019) proposed a methodology, 'BIM-based compound element quantity takeoff improvement (BCEQTI)' [19]. The study also validated the implementation of BCEQTI through a few case studies. The methodology is based on integrating the concept of BIM-based clash detection to support the BIM-based quantity takeoff process. The authors

highlighted that BCEQTI is based on the general concept of calculation algorithm and can be used with any BIM software.

3.3. Surveys and Interviews

This section documents the experiences of various cost management professionals on the use of BIM for cost estimation.

The application of BIM by construction companies in the United States (US) was investigated by Sattineni & Bradford (2011) [20]. The authors used a web-based survey to understand the viewpoints of various respondents, including owners, vice presidents, BIM managers, BIM engineers, estimators, and architects. The most common application of BIM was for visualization. A majority of the respondents highlighted the use of BIM for cost estimation. The respondents also indicated that BIM improved the quality of cost estimation and reduced the overall time needed for cost estimation. Smith (2014) studied issues related to implementation of BIM by project management professionals in the construction industry [21]. Interviews were conducted with three medium-sized firms (10–20 employees) and three large firms (20-plus employees) in Australia. The issues highlighted by the respondents included: the quality of BIM models, documentation accuracy, lack of standards, and legal/contractual issues, among others. Aibinu & Venkatesh (2014) investigated the BIM experience of quantity surveying firms and cost consultants in Australia [22]. The data collection included forty responses and two in-depth interviews. CostX and Buildsoft estimating software were among the commonly used BIM software reported in this study. Time savings was the most important advantage of using BIM, as observed in the study. The most challenging task reported by respondents was automation of quantity takeoff through the BIM model, followed by scarcity of skilled employee using BIM.

Harrison & Thurnell (2015) investigated the benefits and barriers of 5D BIM implementation through survey and interviews within a single large multinational consultancy in New Zealand [23]. Though the respondents were only five in number, they were all experienced and qualified quantity surveyors. The benefits of BIM reported by the respondents included: enhanced visualization, efficient data extraction for estimation at both the preliminary and detailed stages, efficient data extraction for preparing schedule of quantities, rapid identification of design changes, and improved coordination, among others. The barriers to using 5D BIM, summarized by the respondents, included: software inter-operability issues, incompatibility with quantity surveying formats, lack of industry standards/protocols to facilitate design embedment, and lack of context for construction methods, among others. Taihairan & Ismail (2015) analyzed the use of BIM among the quantity surveyors working with consultancy firms and government agencies in Malaysia [24]. Twenty-five respondents participated in the questionnaire study, followed by semi-structured interviews with five respondents. The dominant factors of using BIM for cost estimation reported were: more value-added activities during estimation and better visualization. The study also identified collaboration and information sharing between project teams and software investment as important barrier to BIM implementation.

The survey conducted by Franco et al. (2015) highlighted accuracy and precise takeoff with the help of BIM [25]. The study also highlighted the need of proper mechanism of BIM adoption amongst subcontractors. BIM has certainly gained popularity in past few years in terms of quantity takeoff and cost estimation. Olsen & Taylor (2017) performed a

questionnaire survey (14 respondents), followed by interviews with four respondents [26]. The respondents were working either as estimators or virtual design and coordination (VDC) coordinators in the southeastern US. Autodesk Revit, Bentley, Vico, Assemble and Autodesk Navisworks were among the popular BIM software identified in this study. The majority of the respondents in the survey preferred Assemble, followed by Autodesk Revit for quantity takeoff. Visualization and speed were the common advantages of using BIM for cost estimation, whereas BIM models with incorrect data and software complexity were some of the limitations reported in this study. Mayouf et al. (2019) conducted semi-structured interviews (20 respondents) to investigate the role of quantity surveyors within the BIM process [27]. The first group (10 respondents) had a research and academic background, while the remaining group were quantity surveying practitioners (most of these practitioners used CostX tool for 5D BIM). The respondents from academia followed an information-driven approach, whereas practitioners adopted a process-change approach when working with BIM. The authors highlighted the need for more collaboration between academia and industry for the effective teaching of BIM. The study revealed a lack of understanding of the BIM workflow and the identification of missing information from the BIM model as some of the challenges for implementing 5D BIM. Babatunde et al. (2019) analyzed the use of BIM for detailed cost estimation and the drivers for BIM adoption [28]. The study included survey of 37 quantity surveying firms (13 BIM users and 24 non-BIM users) from Nigeria. It was found that Microsoft Excel is more often used along with 3D BIM. The commonly used BIM software for detailed cost estimation were Autodesk QTO, Navisworks, Innovaya composer and CostX. The major drivers for BIM adoption were quantity automation, time savings in quantity preparation, enhance decision-making quality, data coordination, and improvements in design quality.

3.4. Case analysis

This section covers the findings of three case studies in which researchers have demonstrated the benefits of BIM for cost estimation across different project phases.

3.4.1. Quantitative evaluation of the BIM-assisted construction detailed cost estimates

Shen & Issa (2010) evaluated the effectiveness of BIM-assisted detailed estimating (BADE) tools in generating detailed construction cost estimates [29]. The evaluation was done based on four parameters: generality, flexibility, efficiency, and accuracy. Entry-level users found BADE tools to perform better compared to traditional estimating methods. The authors also presented a simple case of brick veneer quantities to highlight the effect of construction methods and trade knowledge on detailed quantity breakdowns. Following were the key findings through this case study:

1. Detailed cost estimation involves calculation of product/procurement quantities (PPQ) as well as estimating process quantities (PCQ).
2. The variation in PPQ is negligible, but PCQ will vary significantly from one contractor to another. PCQ will depend on several factors such as construction process/methods and job-specific conditions.
3. Even though BADE tools are available, the estimator's manual interpretation and analysis are still critical for extracting correct PCQs from the BIM model.

3.4.2. Project-based quantification of BIM Benefits

In this case study Li et al. (2014) revealed the BIM benefits in resource management and real-time costs control [30]. The authors documented the lessons learnt from the project 'Shanghai Disaster Recovery Centre'. The case study was analyzed in three areas: BIM in MEP design review, 4D simulation of construction scheme, and BIM-based materials management and control. Following were the key findings through this case study:

1. The use of BIM helped in resolving MEP design issues before and during construction. This resulted in total savings of approximately 66 days of schedule and 3% of the total MEP construction cost.
2. The pre-discussions and real-time coordination using BIM shortened the construction schedule by three months.
3. BIM can help project managers in procurement audit and achieve cost savings by increasing the efficiency of the procurement process.

3.4.3. Cost comparison of a building project

Haider et al. (2020) performed a comparative cost analysis between traditional method and BIM for a building project [31]. The following were the key findings from this case study:

1. The cost comparison was conducted for activities comprising brick work, RCC slab, plaster work, PCC for flooring, floor tile work, skirting, paint work, false ceiling, doors, and aluminum work.
2. The total cost difference between manual and BIM estimation method was approximately 5%. The authors observed that BIM-assisted estimates have better performance compared to the traditional (manual) method.

Table 1 summarizes a few additional case studies on cost estimation using BIM.

4. Conclusions

The present study attempted to find answers to the research questions viz., 1) What are the various methodologies adopted for estimating building cost using BIM? and 2) Is BIM a popular tool among cost management professionals? A systematic literature review conducted provides the requisite findings to the research questions. The BIM approach provides an acceptable range of cost estimation for various design scenarios [18]. However, there is a need to integrate relevant standards to develop a comprehensive bill of quantities [27].

It is revealed through the present investigation that BIM is becoming a more popular tool among cost management professionals due to better visualization, reliability, and documentation, among other factors. The various BIM software mentioned in this study have their own unique characteristics to support quantity surveyors. Expert opinion is necessary along with the use of BIM software. Revisions in the construction methods and technological advancement is necessary depending upon the nature of work item [14]. Barlish & Sullivan (2012) argued that the success of BIM depends on the project and the organization [37]. The present study provides significant insights to the associated stakeholders from AEC industry on the use of BIM for cost estimation of building projects.

Table 1. Additional case studies on BIM

Authors / Year	Topic	Observations
Azhar et al. (2008) [7]	"Building information modeling (BIM): benefits, risks and challenges"	The case deals with hotel project. The use of BIM had a cost benefit of $600,000 due to removal of clashes and 1143 hours of savings in the scheduling.
Naneva et al. (2020) [17]	"Integrated BIM-based LCA for the entire building process using an existing structure for cost estimation in the Swiss context"	Developed a methodology to integrate life cycle assessment (LCA) with BIM. The methodology helps to minimize the rework of data entry and also helps in decision making.
Jalaei & Jrade (2014) [32]	"Integrating BIM with green building certification system, energy analysis, and cost estimating tools to conceptually design sustainable buildings"	Proposed an integrated method that helps for green building certification.
Wasmi & Castro-Lacouture (2016) [33]	"Potential impacts of BIM-based cost estimating in conceptual building design: a university building renovation case study"	Analyzed the impact of building design modifications on cost using BIM tools.
Forgues et al. (2012) [34]	"Rethinking the cost estimating process through 5D BIM: A case study"	Investigated the advantages and challenges of cost estimation using BIM.
Franco et al. (2015) [25]	"Using building information modeling (BIM) for estimating and scheduling, adoption barriers"	Demonstrated use of BIM through a case study.
Le et al. (2021) [35]	"A BIM-database-integrated system for construction cost estimation"	Developed a workflow for automatic quantity takeoff and cost calculation using Dynamo and Python.
Fazeli et al. (2020) [18]	"An integrated BIM-based approach for cost estimation in construction projects"	Applied the proposed BIM-based approach for estimating the architectural cost of a residential complex in Iran.
Pandit et al. (2018) [36]	"Operational Feasibility of BIM Applications in Indian Construction Projects"	Performed cost analysis for a residential building using Autodesk Revit and Navisworks. Also made a comparative analysis between traditional and BIM estimate.

References

1. Matipa W. M.; Kelliher D.; Keane M. How a quantity surveyor can ease cost management at the design stage using a building product model. *Construction Innovation* **2008**, 8(3), 164-181, https://doi.org/10.1108/14714170810888949
2. Ma Z.; Liu Z. BIM-based intelligent acquisition of construction information for cost estimation of building projects. *Procedia Engineering* **2014**, 85, 358-367, https://doi.org/10.1016/j.proeng.2014.10.561
3. Sabol L. (2008). Challenges in cost estimating with Building Information Modeling. *IFMA World Workplace*, 1, 1-16.
4. Wu S.; Wood G.; Ginige K.; Jong S. W. A technical review of BIM based cost estimating in UK quantity surveying practice, standards and tools. *Journal of Information Technology in Construction* **2014**, 19, 534-562.
5. Sunil K.; Pathirage C.; Underwood J. The importance of integrating cost management with building information modeling (BIM). *12th International Postgraduate Research Conference (IPGRC 2015)* **2015**.
6. Plebankiewicz E.; Zima K.; Skibniewski M. Analysis of the first Polish BIM-Based cost estimation application. *Procedia Engineering* **2015**, 123, 405-414, https://doi.org/10.1016/j.proeng.2015.10.064
7. Azhar S.; Hein M.; Sketo B. Building information modeling (BIM): benefits, risks and challenges. In *Proceedings of the 44th ASC Annual Conference* **2008**, 2-5.
8. Bryde D.; Broquetas M.; Volm J. M. The project benefits of building information modelling (BIM). *International Journal of Project Management* **2013**, 31(7), 971-980, https://doi.org/10.1016/j.ijproman.2012.12.001
9. Goucher D.; Thurairajah N. Usability and impact of BIM on early estimation practices: Cost consultant's perspective. In *Proc. of Joint CIB International Symposium MCrp, Management of Construction: Research to Practice* **2012**, 2, 555-569.
10. Khaddaj M.; Srour I. Using BIM to retrofit existing buildings. *Procedia Engineering* **2016**, 145, 1526-1533, https://doi.org/10.1016/j.proeng.2016.04.192
11. Soust-Verdaguer B.; Llatas C.; García-Martínez A. Critical review of bim-based LCA method to buildings. *Energy and Buildings* **2017**, 136, 110-120, https://doi.org/10.1016/j.enbuild.2016.12.009
12. Cheung F. K.; Rihan J.; Tah J.; Duce D.; Kurul, E. Early stage multi-level cost estimation for schematic BIM models. Automation in Construction **2012**, 27, 67-77, https://doi.org/10.1016/j.autcon.2012.05.008
13. Elbeltagi E.; Hosny O.; Dawood M.; Elhakeem A. BIM-based cost estimation/monitoring for building construction. *International Journal of Engineering Research and Applications* **2014**, 4(7), 56-66.
14. Lee S. K.; Kim K. R.; Yu J. H. BIM and ontology-based approach for building cost estimation. *Automation in Construction* **2014**, 41, 96-105, https://doi.org/10.1016/j.autcon.2013.10.020
15. Choi J.; Kim H.; Kim I. Open BIM-based quantity take-off system for schematic estimation of building frame in early design stage. *Journal of Computational Design and Engineering* **2015**, 2(1), 16-25, https://doi.org/10.1016/j.jcde.2014.11.002

16. Abanda F. H.; Kamsu-Foguem B.; Tah J. H. M. BIM-New rules of measurement ontology for construction cost estimation. *Engineering Science and Technology, an International Journal* **2017**, 20(2), 443-459, https://doi.org/10.1016/j.jestch.2017.01.007
17. Naneva A.; Bonanomi M.; Hollberg A.; Habert G.; Hall, D. Integrated BIM-based LCA for the entire building process using an existing structure for cost estimation in the Swiss context. *Sustainability* **2020**, 12(9), 3748, https://doi.org/10.3390/su12093748
18. Fazeli A.; Dashti M. S.; Jalaei F.; Khanzadi M. An integrated BIM-based approach for cost estimation in construction projects. Engineering, Construction and Architectural Management **2020**, 28(9), 2828-2854, https://doi.org/10.1108/ECAM-01-2020-0027
19. Khosakitchalert C.; Yabuki N.; Fukuda T. Improving the accuracy of BIM-based quantity takeoff for compound elements. Automation in Construction **2019**, 106, 102891, https://doi.org/10.1016/j.autcon.2019.102891
20. Sattineni A.; Bradford R. H. (2011). Estimating with BIM: A survey of US construction companies. In *Proceedings of the 28th ISARC, Seoul, Korea,* 2011, 564-569, https://doi.org/10.22260/ISARC2011/0103
21. Smith P. BIM & the 5D project cost manager. *Procedia-Social and Behavioral Sciences* **2014**, 119, 475-484, https://doi.org/10.1016/j.sbspro.2014.03.053
22. Aibinu A.; Venkatesh S. Status of BIM adoption and the BIM experience of cost consultants in Australia. *Journal of Professional Issues in Engineering Education and Practice* **2014**, 140(3), 04013021, https://doi.org/10.1061/(ASCE)EI.1943-5541.0000193
23. Harrison C.; Thurnell D. BIM implementation in a New Zealand consulting quantity surveying practice. *International Journal of Construction Supply Chain Management* **2015**, 5(1), 1-15.
24. Taihairan R. B. R.; Ismail Z. BIM: Integrating cost estimates at initial/design stage. *International Journal of Sustainable Construction Engineering and Technology* **2015**, 6(1), 62-74.
25. Franco J.; Mahdi F.; Abaza H. Using building information modeling (BIM) for estimating and scheduling, adoption barriers. *Universal Journal of Management* **2015**, 3(9), 376-384, https://doi.org/10.13189/ujm.2015.030905
26. Olsen D.; Taylor J. M. Quantity take-off using building information modeling (BIM), and its limiting factors. *Procedia Engineering* **2017**, 196, 1098-1105, https://doi.org/10.1016/j.proeng.2017.08.067
27. Mayouf M.; Gerges M.; Cox, S. 5D BIM: An investigation into the integration of quantity surveyors within the BIM process. *Journal of Engineering, Design and Technology* **2019**, 17(3), 537-553, https://doi.org/10.1108/JEDT-05-2018-0080
28. Babatunde S. O.; Perera S.; Ekundayo D.; Adeleye T. E. An investigation into BIM-based detailed cost estimating and drivers to the adoption of BIM in quantity surveying practices. *Journal of Financial Management of Property and Construction* **2019**, 25(1), 61-81, https://doi.org/10.1108/JFMPC-05-2019-0042
29. Shen Z.; Issa R. R. Quantitative evaluation of the BIM-assisted construction detailed cost estimates. *Journal of Information Technology in Construction* **2010**, 15, 234-257.
30. Li J.; Hou L.; Wang X.; Wang J.; Guo J.; Zhang S.; Jiao Y. A project-based quantification of BIM benefits. *International Journal of Advanced Robotic Systems* **2014**, 11(8), https://doi.org/10.5772/58448

31. Haider U.; Khan U.; Nazir A.; Humayon M. Cost Comparison of a Building Project by Manual and BIM. *Civil Engineering Journal* **2020**, 6(1), 34-49, https://doi.org/10.28991/cej-2020-03091451
32. Jalaei F.; Jrade A. Integrating BIM with green building certification system, energy analysis, and cost estimating tools to conceptually design sustainable buildings. In *Construction Research Congress 2014: Construction in a Global Network*, 2014, 140-149, https://doi.org/10.1061/9780784413517.015
33. Wasmi H. A.; Castro-Lacouture D. Potential impacts of BIM-based cost estimating in conceptual building design: a university building renovation case study. In *Construction Research Congress*, 2016, pp. 408-417, https://doi.org/10.1061/9780784479827.042
34. Forgues D.; Iordanova I.; Valdivesio F.; Staub-French S. Rethinking the cost estimating process through 5D BIM: A case study. In *Construction Research Congress 2012: Construction Challenges in a Flat World*, 2012, 778-786, https://doi.org/10.1061/9780784412329.079
35. Le H. T. T.; Likhitruangsilp V.; Yabuki N. A BIM-database-integrated system for construction cost estimation. *ASEAN Engineering Journal* **2021**, 11(1), 45-59, https://doi.org/10.11113/aej.v11.16666
36. Pandit S.; Kaur B.; Goel A. Operational Feasibility of BIM Applications in Indian Construction Projects. *Indian Journal of Science and Technology* **2018**, 11(29), 1-13, https://dx.doi.org/10.17485/ijst/2018/v11i29/127830
37. Barlish K.; Sullivan K. How to measure the benefits of BIM – A case study approach. *Automation in Construction* **2012**, 24, 149-159, https://doi.org/10.1016/j.autcon.2012.02.008